STUDY ON THE GROWTH OF ZnO THIN FILMS AND THEIR APPLICATIONS(Dissertation_全文)

AUTHOR(S):

Shimizu, Masaru

STUDY ON THE GROWTH OF ZnO THIN FILMS AND THEIR APPLICATIONS

MASARU SHIMIZU

September 1989

Department of Electronics
Kyoto University

STUDY ON THE GROWTH OF ZnO THIN FILMS AND THEIR APPLICATIONS

MASARU SHIMIZU

September 1989

Department of Electronics
Kyoto University

PREFACE

Remarkable advances have been made in recent years in the science and technology of thin film processes for deposition because of their potential technical value and scientific curiosity in the properties of a two dimensional solid. Many fabrication techniques to obtain metal, insulater, amorphous material and semiconductor films in the production of VLSI and many electro-optic devices have been reported. Numerious important process for film deposition, such as thermal evaporation, sputtering, ion-plating, ionized-cluster-beam(ICB)deposition, chemical vapor deposition(CVD), plasma CVD, metalorganic CVD and photo-CVD have been studied.

Recently ZnO thin film has much attention for applications such as surface acoustic wave (SAW) devices, integrated optic devices, heterojunction solar cell devices and transparent electrodes, because of its large piezoelectricity, large optical refractive indices, large acousto-optical, electro-optical and nonlinear-optical coefficients, and high optical transparency in the visible region. Therefore many fabrication techniques for growing ZnO film have been developed. However it has been very difficult to obtain high quality ZnO films at low substrate temperatures because of its high melting points. If new techniques for growing ZnO film with good crystalline quality can be developed, many applications will have great possibility.

This thethis describes the growth and properties of ZnO thin films prepared by some techniques. The development of new fabri-

cation techniques using plasma and photon energy for obtaining ZnO film at low substrate temperatures are also described.

This thesis consists of 8 chapters. In chapter I, the basic properties of ZnO and a brief historical sketch are introduced. In chapter II and IV, the growth and properties of ZnO film by chemical vapor deposition method are described. Chapter III describes the optical waveguide properties and three dimensional optical waveguide utilizing the selective film growth technique. In chapter V and VI, new techniques for growing ZnO film with high crystalline quality at low substrate temperatures using plasma technology are investigated. Photo-MOCVD technique and the effect of UV light irradiation on the growth are explained in detail in chapter VII. Chapter VIII summerizes the conclusions of the present investigation.

Masaru Shimizu

ACKNOWLEDGEMENTS

I want to express my deep appreciation to Professor Akira Kawabata for his invaluable guidance and supervision throughout this work. I am grateful to Assistant Professor Tadashi Shiosaki for his continuing guidance and encouragement. I am grateful to Professor Hiroyuki Matsunami for his encouragements and suggestions. Appreciations are also due to Professor Shigeo Fujita for his helpful advices and discussions. I am indebted to Dr.Masatoshi Adachi and Dr.Susumu Fukuda for frequent and helpful discussion and experimental facilities. I wish to thank the former and present members of Professor Kawabata's laboratory group, Dr.Takashi Yamamoto, Messers.Yuukichi Murakami, Sakae Wada, Yutaka Kakuno, Tadashi Horii, Tastushi Yamamoto, Youjiro Mastueda, Hidenori Kamei, Motoaki Tanizawa, Hidenori Nakahata, Akira Monma and Takuma Katayama for their help in the experiments. Thanks are also due to Dr.Yuji Yamamoto for helpful discussions and his help in the experiments. I would like to express my thanks to Miss.Kaoru Nakamura for her helpful in typing.

CONTENTS

CHAPTER I. INTRODUCTION

Zinc Oxide (ZnO) is one of II-VI compounds and has the wurtzite structure with the lattice parameter a=3.24Å and c=5.19Å [1]. It melts at temperatures higher than 1800°C and the density is 5.6g/cm^3 [1].

Zinc Oxide is an n-type semiconductor and the band gap of this oxide is 3.2ev at room temperature. Its conductivity is due to the non-stoichiometry consisting in the excess of zinc.

The growth of single crystal ZnO presents a difficult problem. Experimental difficulties arise first of all from the relatively high melting temperature. In addition, it shows a tendency to deviate from stoichiometry, particularly at high temperatures, which necessities a strict control of the conditions of crystal growth.

Many methods of crystal growth have been adopted and improved in order to prepare single ZnO crystals of high purity and perfect structure. However, no attempt has yet been made to pull crystals from the melt because the vapor pressure of ZnO is too high. Therefore, crystals of ZnO have been grown by the hydrothermal method [2-4], by the traveling solvent zone technique [5] and from vapor phase reaction [6-9].

In the hydrothermal method, large(10 to 20g) macroscopically sound ZnO crystals suitable for preliminary transducer use have been grown at rates of from 10 to 15mm/day [3].

Growth of ZnO single crystals by the travelling solvent zone technique was carried out by G.A. Walff and H.E. LaBella [5]. In this

method, PbF_2 was used as a solvent, and the temperature of the hot zone was about 900°C. The rate of passing the system downwards was 3.5mm/day [5].

The vapor growth techniques have also been applied to the growth of ZnO single crystals by a number of investigations [6-10]. Both needles and platelets of single crystal ZnO were obtained by this method at temperatures between 1050 and 1325°C.

Many growth techniques to obtain bulk ZnO crystals as mentioned above have been developed. However current trends show the more extensive applications of ZnO thin films. For example, ZnO piezoelectric films have been applied to ultrsonic devices for bulk acoustic waves as well as surface acoustic waves, because ZnO has a low dielectric constant and a high electromechanical coupling factor. Therefore, an improvement in the method of preparing thin films, a more fundamental interest in the character of these films, and controlling the properties of films are required.

Preparation of thin ZnO films has been described by many researchers. Numerous processes, such as sputtering [11-17], ion-plating [18], ionized-cluster beam deposition [19,20], spray pyrolysis [21,22], chemical vapor deposition (CVD) [23-29], and metalorganic chemical vapor deposition (MO-CVD) [30-36], have been carried out. Among these deposition methods, the most frequently employed technique was sputtering, and many sputtering techniques have been developed to grow ZnO films with high quality for various applications.

The sputtering methods are classified into the dc sputtering

and rf sputtering methods. In the dc sputtering method, diode sputtering [11,37,38] and triode sputtering methods [15,39-41] have been carried out to obtain piezoelectric ZnO films. ZnO films with high resistivity have also been prepared by many rf sputtering techniques [11-14,16].

ZnO thin films obtained by these sputtering techniques have been applied to ultrasonic transducers, composit resonator, SAW filters, SAW amplifires, integrated optic devices and transparent electrodes.

The sputtering method is very useful and convenient in preparing ZnO thin films at considerably low substrate temperatures. However, the sputtering method has some disadvantages ; 1)the growth rate is not very high, 2)the composition of a sputtered film is not the same as that of target (the deviation from a stoichiometry), 3)a sputtered film surface is bombarded by energetic particles.

Thus the development of new techniques with high controllability for obtaining high quality ZnO thin films is required. This thesis includes the research on some new developments in ZnO thin film growth technology, explains the properties of these newly obtained films, and illustrates various applications.

References

[1] M.Neuberger, in: II-VI Semiconducting Compounds Data Tables(E.P.I.C., Culver City, California, 1969).

[2] R.A.Laudise and A.A.Ballman, J.Phys.Chem. 64(1960)688.

[3] R.A.Laudise, E.D.Kalf and A.J.Caporaso, J.Amer.Ceram.Soc. 47(1964)9.

[4] E.D.Kalf and R.A.Laudise, J.Amer.Ceram.Soc. 48(1965)342.

[5] G.A.Wolf and H.E.LaBelle,Jr., J.Amer.Ceram.Soc. 48(1965)441.

[6] E.M.Dodson and J.A.Savage, J.Materials Sci. 3(1968)19.

[7] J.A.Savage and E.M.Dodson, J.Materials Sci. 4(1969)809.

[8] I.Kubo, Japn.J.Appl.Phys. 4(1965)225.

[9] E.A.Weaver, J.Cryst.Growth, 1(1967)320.

[10] T.Takahashi, A.Ebina and A.Kamiyama, Japn.J.Appl.Phys. 5(1966)560.

[11] D.L.Raimondi and E.Kay, J.Vacuum Sci.Technol. 7(1970)96.

[12] B.T.Khuri-Yakub, G.S.Kino and P.Galle, J.Appl.Phys. 46(1975)3266.

[13] T.Shiosaki, S.Ohnishi, Y.Murakami and A.Kawabata, J.Cryst.Growth, 45(1978)346.

[14] K.Ohji, T.Tohda, K.Wasa and S.Hayakawa, J.Appl.Phys. 47(1976)1726.

[15] F.S.Hickernell, in: Proc. 1980 IEEE Ultrasonics Symp. (1980)p.785.

[16] T.Yamamoto, T.Shiosaki and A.Kawabata, J.Appl.Phys. 51(1980)3113.

[17] M.Matsoka, Y.Hoshi and M.Noe, J.Appl.Phys. 63(1988)2098.

[18] M.Machida, M.Shibutani, Y.Murayama and M.Matsumoto, Trans. IECE.Japan, 562-C(1979)358(in Japanese).

[19] T.Takagi, I.Yamada, K.Matsubara and H.Takaoka, J.Cryst.growth 45(1978)318.

[20] T.Takagi, K.Matsubara, H.Takaoka and I.Yamada, Thin Solid Films 63(1979)41.

[21] J.Aranovich, A.Orliiz and R.H.Bube, J.Vacuum Sci.Technol. 16(1979)994.

[22] J.Aranovich, P.Golwayo, A.L.Fuhrenbruch and R.H.Bube, J.Appl.Phys. 51(1980)4260.

[23] R.F.Belt and G.C.Florio, J.Appl.Phys. 39(1968)5215.

[24] G.Galli and J.E.Coker, Appl.Phys.Letters 39(1968)439.

[25] S.Ohnishi, Y.Hirikawa, T.Shiosaki and A.Kawabata, Japn.J.Appl.Phys. 17(1978)773.

[26] A.Reisman, M.Berkenblit, S.A.Chan and J.Angilello, J.Electron.Mater. 2(1973)177.

[27] M.Aoki, K.Tada, T.Murai and T.Inoue, Thin Solid Films 83(1981)283.

[28] Shimizu, T.Shiosaki and A.Kawabata, J.Cryst.Growth 57(1982)94.

[29] M.Kasuga and M.Mochizuki, J.Cryst.Growth 54(1981)185.

[30] C.K.Law, S.K.Tiku and K.M.Lakin, J.Electrochemi.Soc. 127(1980)1845.

[31] S.K.Ghandhi, R.J.Field and J.R.Shealy, Appl.Phys.Letters 37(1980)449.

[32] J.R.Shealy, B.J.Baliga, R.J.Fiield and S.K.Ghandhi, J.Electrochem.Soc. 128(1981)449.

[33] A.P.Roth and D.F.Williams, J.Electrochem.Soc. 128(1981)2684.

[34] A.P.Roth and D.F.Williams, J.Appl.Phys. 52(1981)6685.

[35] F.T.J.Smith, Appl.Phys.Letters 43(1983)1108.

[36] P.J.Wright, R.J.M.Griffiths and B.Cockayne, J.Cryst.Growth 66(1984)26.

[37] R.A.Mickelsen and W.D.Kingery, J.Appl.Phys. 37(1966)3541.

[38] R.Wagers, G.Kino, P.Galle and D.Winslow, Proc. IEEE Ultrasonics Symp. (1972)p.194.

[39] N.F.Foster, J.Appl.Phys. 40(1969)4203.

[40] F.S.Hickernell and J.W.Brewer, Appl.Phys.Letters 21(1972)389.

[41] F.S.Hickernell, J.Appl.Phys. 44(1973)1061.

CHAPTER II. GROWTH AND PROPERTIES OF ZnO FILMS ON SAPPHIRE SUBSTRATES BY CHEMICAL VAPOR DEPOSITION

2-1. Introduction

A ZnO thin film is one of the most promising materials for devices utilizing their piezoelectrical and optical properties as mentioned in Chapter I. Many studies on applications of ZnO to surface acoustic wave, acoust-optic and optical waveguiding devices have been made. Recently, applications to light emitting diode, a solar cell and a transparent electrode have been reported. Several fabrication techniques of ZnO thin films, such as sputtering, ion-plating, ionized-cluster-beam deposition, spray pyrolysis, chemical vapor deposition (CVD) and metalorganic chemical vapor deposition (MOCVD), have been investigated for these purposes. Among these growth techniques, sputtering has been most widely applied to the growth of ZnO films. However, ZnO films obtained by this technique are polycrystalline, and it is very difficult to obtain single crystal films.

Recently, the growth of ZnO thin films by chemical vapor deposition has become one of the most important methods of single crystal ZnO film formation. Chemical vapor deposition can be defined as a material synthesis method in which the constituents of vapor phase react to form a solid film at some surface, and CVD is versatile and flexible technique in producing deposits of pure semiconductors. Thus many researches on CVD of ZnO have been carried out. Single crystal ZnO can be prepared by any of the following CVD techniques:

1) chemical reactions of zinc-halide

ZnO single crystals were obtained by chemical reactions as follows:

$$2ZnX_2 + O_2 \rightarrow 2ZnO + 2X_2 \qquad (2\text{-}1)$$

Needle-like ZnO single crystals were obtained by chemical reaction of zinc-fluoride (ZnF_2) with air at 950°C by I.Kubo [1]. Takahashi et al. described the growth of plate-like zinc oxide single crystals by using zinc-cloride ($ZnCl_2$) as the starting material, and in their method $ZnCl_2$ and H_2O vapors were introduced by carrier gas N_2 and O_2, respectively to obtain ZnO crystals [2].

2) chemical reactions of zinc sulfide or zinc selenide

Single crystal of ZnO have been grown by sublimating both ZnS and ZnSe, and by reacting them with oxygen in an argon gas flow. Using ZnS as the starting material, both platelet- and prism-type ZnO crystals were grown. When ZnSe was used as the starting material, hollow-type prisms and plates were the general formes [3]. The oxidation and hydrolysis of ZnS was used to obtain ZnO ribbon crystals by Iwanaga et al. [4].

3) chemical reaction of zinc oxide

The reduction of ZnO by H_2, or H_2 and Ar, or NH_3 was a widely used method to obtain ZnO. In this method, Zn vapor produced by the reduction of ZnO at high temperature was trnsported to a lower temperature region and reduced again to form ZnO. When hydrogen is used reduction gas, the reaction is

$$ZnO(s) + H_2(g) \rightleftarrows Zn(g) + H_2O(g) \qquad (2\text{-}2)$$

$$K = P_{Zn} \cdot P_{H_2O} / P_{H_2} \qquad (2\text{-}3)$$

Where (s) and (g) designate solid and gaseous species, respectively. K is equilibrium constant. The crystal grown by this method has advantage concerning to impurity content compared with the one grown by the other method because the starting material with high purity can be prepared easily. By using close space vapor transport method as mentioned above, epitaxial ZnO films were obtained on sapphire substrate at source temperatures of 650-825°C and at substrate temperatures of 550-775°C by G. Galli [5], K.A. Rabadanov [6], F. Pizzallo [7] and J.M. Hammer [8]. Hammer and coworkers measured the optical waveguide properties of single crystal ZnO films epitaxially deposited on sapphire substrates. They concluded that epitaxial ZnO films grown on sapphire might provide a useful medium for many integrated optic applications. The vapor transport using open tube method has been also employed in the epitaxial growth of ZnO by M. Kasuga et al. [9].

Aoki and his coworkers have described an other method to obtain single crystal films, in which the gas used for reducing the ZnO source was ammonia instead of the more conventional hydrogen [10]. The growth reaction can be represented by

$$3ZnO(s) + 2NH_3 \rightarrow 3Zn(g) + N_2 + 3H_2O \quad \text{(at the source)} \quad (2\text{-}4)$$

$$Zn(g) + H_2O \rightarrow ZnO + H_2 \quad \text{(at the substrate)} \quad (2\text{-}5)$$

In the chemical vapor deposition methods as mentioned above, single crystal ZnO films are epitaxially deposited on sapphire substrates. However single crystal ZnO films with good surface flatness has not been obtained uniformly over wide area by using these CVD techniques. In order to obtain single crystal ZnO films with mirror like surface and wide area, a new CVD technique

have carried out. In this chapter, the new CVD technique utilizing $ZnO-H_2-H_2O-O_2$ system is described.

2-2. Experimental Procedure

At first stage of our study, the following chemical reaction was carried out:

$$ZnO + Br_2 \rightleftarrows ZnBr_2 + O_2 \qquad (2\text{-}6)$$

In this case, ZnO film was not grown on a sapphire substrate, nevertheless the film deposition was carried out for ninety hours, and only the polycrystalline grains grew.

The chemical vapor reaction using zinc-cloride as the starting materials was also used to obtain single crystal ZnO films. The grain growth was observed and thin films with smooth surface were not grown on supphire. This method has small supersaturation ratio which relates to generation probability of critical nucleus at an early stage of crystal growth. The adoption of new chemical reaction system which has high supersaturation ratio can increase the generation probability and give high nucleation density which has possibility of growth of uniform thin film. Therefore, $ZnO-H_2-H_2O-O_2$ system was adopted. However, attempts to grow ZnO thin film with large uniformity by using this chemical reaction system was unsuccessful. Even if ZnO films were grown, they had rough surfaces. This unsuccess of thin film growth may be caused by low density and non uniformity of crystal nuclei on substrate surface in heterogeneous nucleation. In this heterogeneous nucleation, the generation rate of critical nucleus is dependent on distribution of

preferential point of crystal nuclei, such as dust, impurity and kink of substrate. If these preferential points of crystal nuclei do not distribute uniformly, thin film which has high crystalline quality and good uniformity can not be obtained. The difference of lattice constant between substrate and grown layer is also important factor in the crystal growth. In the present study, sputter-deposited ZnO layer was used as a high density of nuclei, and buffer layer for difference of lattice constant and of thermal expansion coefficience between substrate and grown layer. At succeeding process, a $ZnO-H_2-H_2O-O_2$ chemical reaction system was carried out. The intimate procedures used in the present study are described in next section.

2-3. Film Growth

At the first step of the film growth, an intermediate layer was deposited on a sapphire substrate by a planar magnetron sputtering system (Nichiden ANELVA: SPF-210H). This sputtering equipment was composed of a vacuum chamber consisting of coaxial planer magnet under the target holder and a substrate heating system, an rf power supply and a pumping system as shown in Fig.2.1. The substrate holder was positioned above and parallel to the target and could change a space from 2.5 to 5cm. The substrate was held with metal clamps on the substrate holder and was heated by the heating system, which was placed behind the substrate holder. The substrate temperature was controllable from 150 to 400^{o}C. The substrate temperature was measured with a thermocouple and depended both on applied rf power and on the

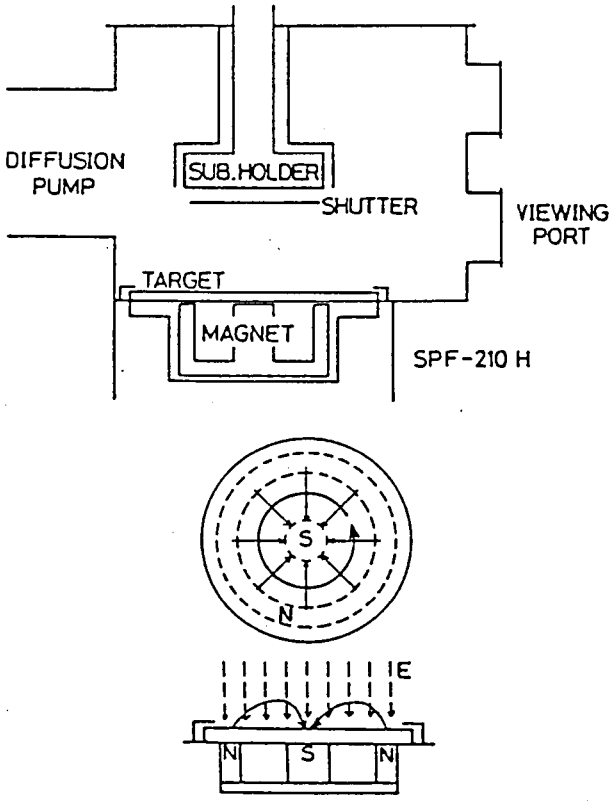

Fig.2.1. Sputtering chamber and magnetron cathode.

Table 2-1. Sputtering conditions of ZnO.

Sputtering gas	O_2+Ar (1 : 1)
Gas pressure	$3\times10^{-3}\sim3\times10^{-2}$Torr
Substrate temperature	Above 300°C
Target	ZnO ceramic (Li dope) Zn metal (99.9%)
Size of target	Diameter 100 mm Thickness 6 mm
Target to substrate	40 mm
Input power	50~400 W
Film thickness	3000 Å~48 μm
Deposition rate	Max 9.8 μ/hr

substrate heater current. The pumping system had a 300 l/min oil diffusion pump and a trap cooled by liquid nitrogen, and gave a pressure of about 5×10^{-7} Torr. Sputtering was performed in argon(50%)/oxygen(50%) premixed gas. The pressure in the sputtering chamber was 3×10^{-3}-5×10^{-2} Torr during sputtering and was continuously pumped. The ZnO ceramic target used in our experiment was prepared by sintering a pressed ZnO powder cake. The diameter of the ZnO target was 10cm.

Table 2-1 shows the sputtering conditions used in this study. Figure 2.2 shows the evaluation of crystallographic quality for sputtered films by X-ray diffraction (using C_u-K_α radiation) patterns and X-ray rocking curves, where σ is the standerd deviation angle of the rocking curve when Gaussian distribution is assumed. The value of σ for the high quality regions of $(11\bar{2}0)$ and (0001) ZnO films obtained by sputtering were less than 0.5° and 0.7°, respectively. Intermediate sputtered layers were deposited under the conditions correspondening to the "excellent" region in Fig 2.2. The film thickness of the intermediate ZnO layers was 200-400Å for deposition on the $(01\bar{1}2)$ sapphire substrate and 2000-3000Å for deposition on the (0001) sapphire substrate.

After the intermediate layer mentioned above had been deposited on sapphire substrates, the CVD growth using the ZnO-H_2-H_2O-O_2 system was carried out, as shown in Fig.2.3. The schematic diagram of the reactor for the chemical vapor deposition and its temperature profile are shown in Fig.2.4.. The quartz reaction tubes had an internal diameter of 30 and 84mm, respectively. The

small and large tubes were 100 and 145cm long respectively. Sintered pieces of ZnO(5N) and substrate were placed in the inner tube. The temperature profile which did not have temperature gradient was mainly used in the present study. The substrate was a sapphire with or without a ZnO sputtered layer. A mixture of H_2, H_2O and N_2 gases was introduced into the inner tube. Nitrogen gas was used as a carrier gas. The deoxidation reaction took place at the source, according to the next reaction:

$$ZnO(s)+H_2 \rightleftarrows Zn(g)+H_2O \qquad (2\text{-}7)$$

On the oter hand, a mixture gas of O_2 and N_2 was introduced into the outer tube and the oxidation reactions might take place at substrates, following the equation:

$$2Zn(g)+O_2 \rightleftarrows 2ZnO(s) \qquad (2\text{-}8)$$

$$Zn(g)+H_2O \rightleftarrows ZnO(s)+H_2 \qquad (2\text{-}9)$$

$$2H_2+O_2 \rightleftarrows 2H_2O \qquad (2\text{-}10)$$

ZnO was formed on the substrate by the chemical reaction according to the above equations. The optimum growth conditions in this CVD system is shown in Table 2-2.

When chemical vapor deposition of a ZnO film was tried on a sapphire substrate without a sputtered ZnO layer, ZnO film was not grown. Even if a film was deposited, it had a very rough surfase. On the other hand, ZnO films were reproducibly obtained on a sapphire substrate with the intermediately-sputterd ZnO thin layer. The deposition rate, crystalographic properties and surface morphology were dependent on the flow rates of N_2, H_2, O_2 and H_2O gases.

The typical X-ray diffraction patterns of ZnO film deposited

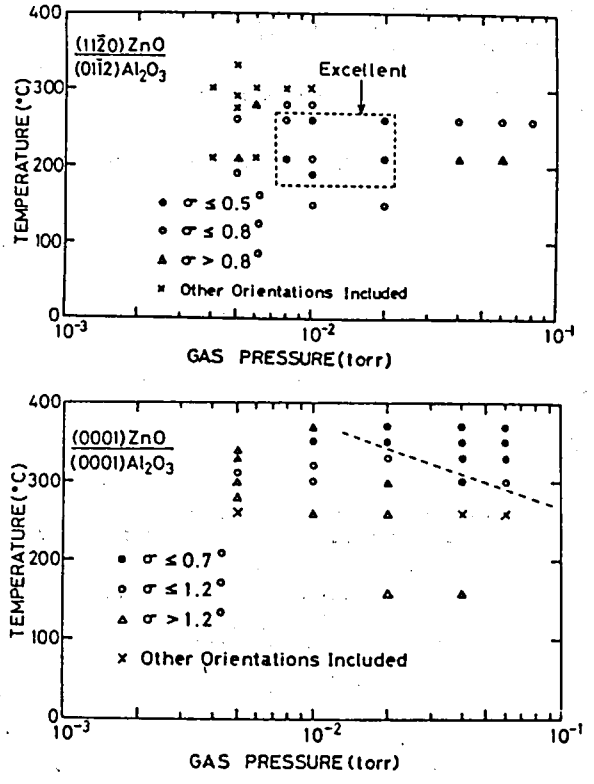

Fig.2.2. Diagram of film quality evaluated by x-ray diffraction patterns and x-ray rocking curves.

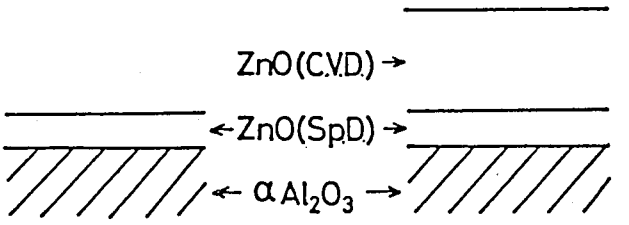

Fig.2.3. CVD process.

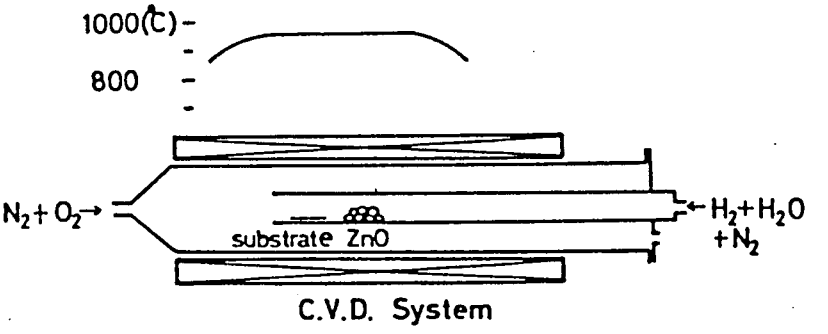

Fig.2.4. Schematic diagram of the CVD system.

Table 2-2. Growth conditions for epitaxial ZnO.

ZnO source	H_2	: 30 ml/min
	H_2O	: 7.5 gr/hr
	N_2	: 270 ml/min
substrate	O_2	: 13 ml/min
	N_2	: 210 ml/min

on $(01\bar{1}2)$ and (0001) sapphire substrate are shown in Fig.2.5.. Only the $(11\bar{2}0)$ and (0002) peaks were observed and the half width of these peaks were very small. Moreover, the $(11\bar{2}0)$ and (0002) peaks produced by the Cu-K_{α_1} lines were clealy separated from those by the Cu-K_{α_2} lines. Figure 2.6 shows the X-ray rocking curve of ZnO film on $(01\bar{1}2)$ sapphire substrate. The standerd deviation angle a was 0.11^{o}. These evaluation from X-ray diffraction indicated ZnO films were single crystalline.

The crystallographic quality of the obtained ZnO films were also evaluated by the Laue back-reflection and the reflection high energy electron diffraction (RHEED) technique. The Laue back-reflection pattern is shown in Fig.2.7 , where the spots can be seen correspondingly to single crystalline film. Figure 2.8 shows the typical RHEED patterns of ZnO films grown by CVD on $(01\bar{1}2)$ and (0001) sapphire sustrates. These patterns showed distinct spots and the different spot pattern appeared periodically by changing an incident angle of electron beam. These results means that the chemical vapor deposited ZnO films were single crystalline and are supported by the X-ray evaluation technique. The surface of film obtained by the CVD method was so smooth that they were used as optical waveguides without polishing surfaces. Figure 2.9 shows the SEM photographs of the film surfaces obtained by the sputtering method and by the CVD method.

As mentioned above, attempts to grow single crystal ZnO film directly on bare sapphire substrates in the $ZnO-H_2-H_2O-O_2$ system under various conditions were unsuccessful. This means that in

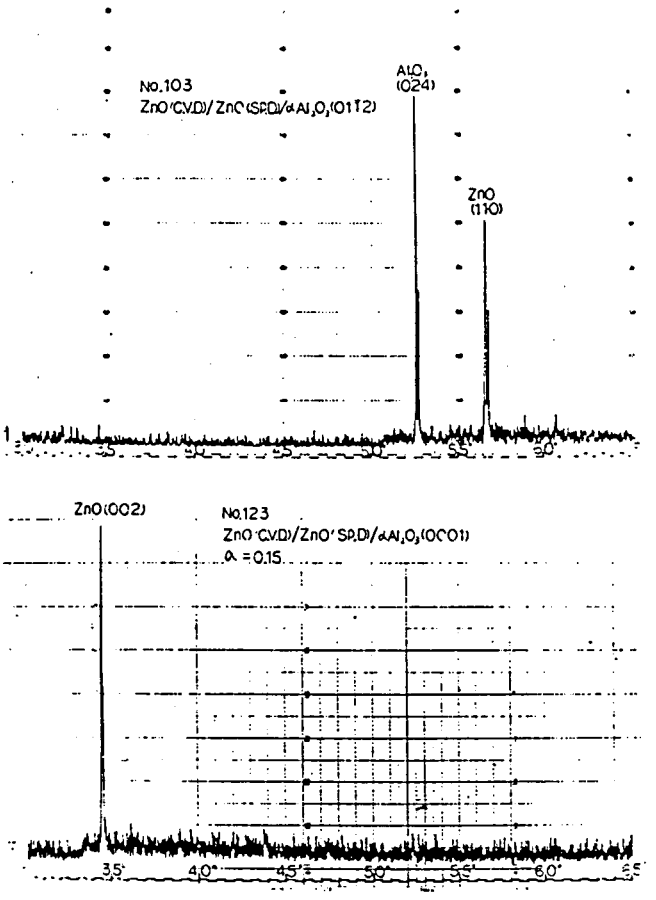

Fig.2.5. X-ray diffraction patterns of ZnO films on: (a) (01$\bar{1}$2) sapphire, (b) (0001) sapphire.

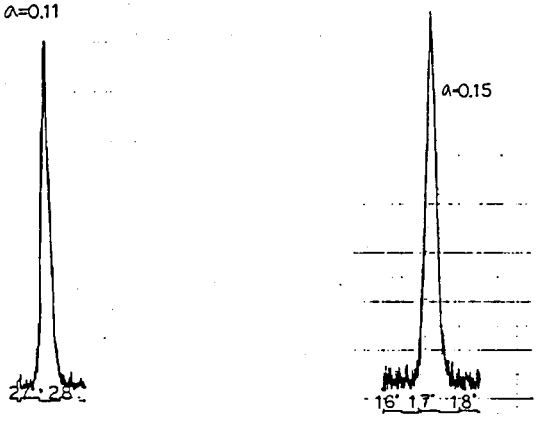

Fig.2.6. X-ray rocking curves of ZnO films on: (a) (01$\bar{1}$2) sapphire, (b) (0001) sapphire.

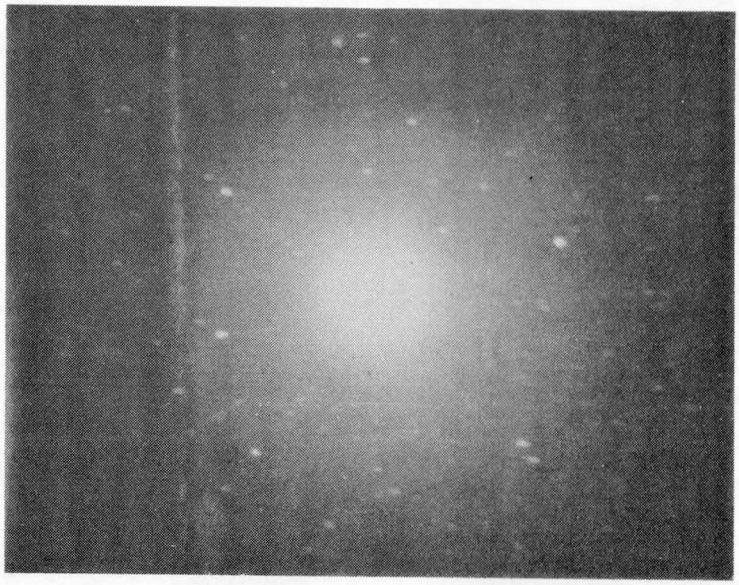

Fig.2.7. X-ray Laue back reflection pattern of $(11\bar{2}0)$ ZnO and $(01\bar{1}2)$ sapphire.

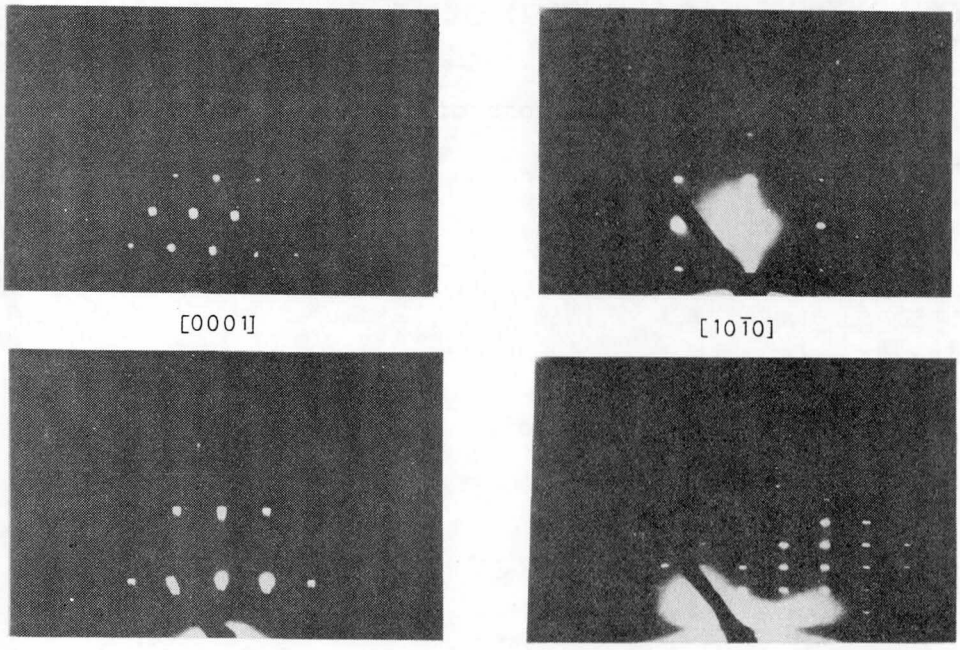

(a) ZnO$(11\bar{2}0)$ / $Al_2O_3(01\bar{1}2)$

(b) ZnO(0001) / Al_2O_3(0001)

Fig.2.8. RHEED patterns of epitaxial ZnO films.

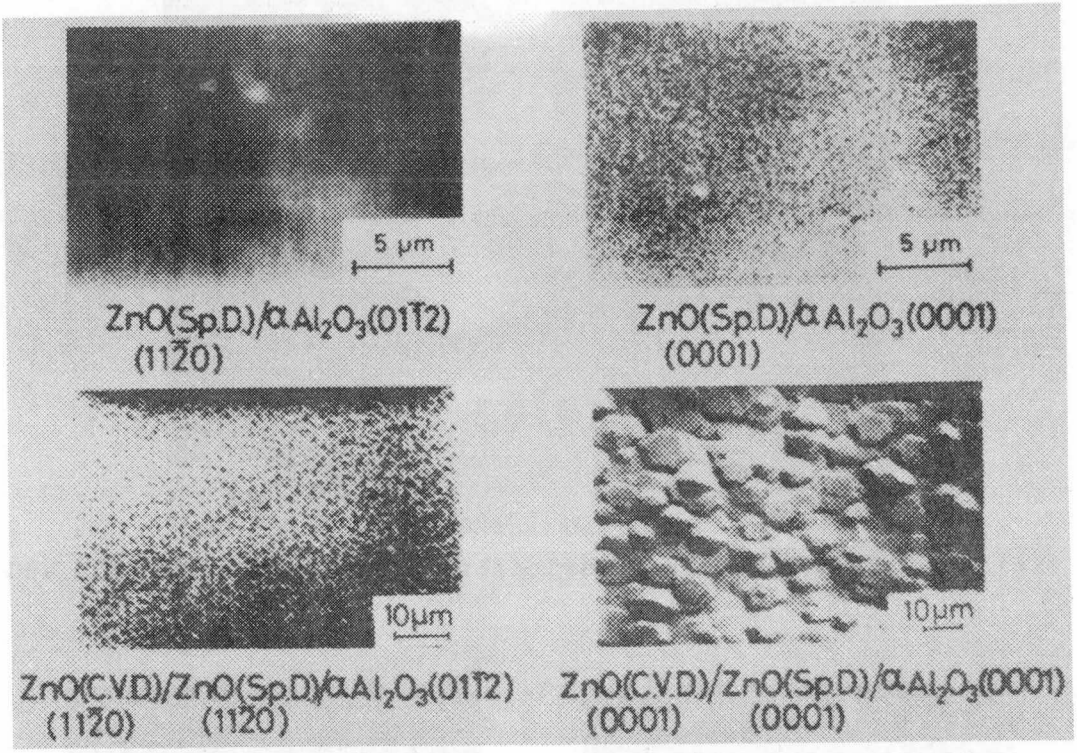

Fig.2.9. SEM photographs of epitaxial ZnO films.

this CVD method the intermediately sputterd ZnO thin layer plays an important role in growth process. In order to investigate the effect of intermediate sputterd ZnO layer on the CVD growth, two kind of substrates with different intermediately sputtered layers in thickness were used in growth. In one sample, the intermediately sputtered layer was 25nm in thickness. Another sample had 250nm intermediate layer.

X-ray diffraction patterns of sputter-deposited intermediate ZnO layers on the $(11\bar{2}0)$ sapphire substrate and the CVD films on them are shown in Fig.2.10. In Fig.2.10(a) and (c), the X-ray diffraction patterns of intermediate layers with 25 and 250 nm in thickness sputterd at a substrate temperature of 200°C respectively. The half value width of the ZnO sputtered layer with a 25nm thickness is narrower than that of 250nm. X-ray diffraction patterns of the CVD films grown on these intermediate layers are shown in Fig.2.10(b) and (d). It is found that the CVD ZnO films obtained on thin sputterd ZnO layer which had better crystallinity shows the better quality. In a word, the crystalline quality of films obtained by this CVD method depends on quality of intermediate sputterd layer.

Affinity of ZnO to the intermediate ZnO thin layer is much stronger than to the bare sapphire substrate. Furthermore, the ZnO particle deposited tightly by the sputtering method plays the role of dense nuclei in the succeeding CVD process. Therefore, depositing ZnO films as intermediate layers causes the surface binding energy to become very uniform over the entire surface area where the intermediate layer has been deposited. The inter-

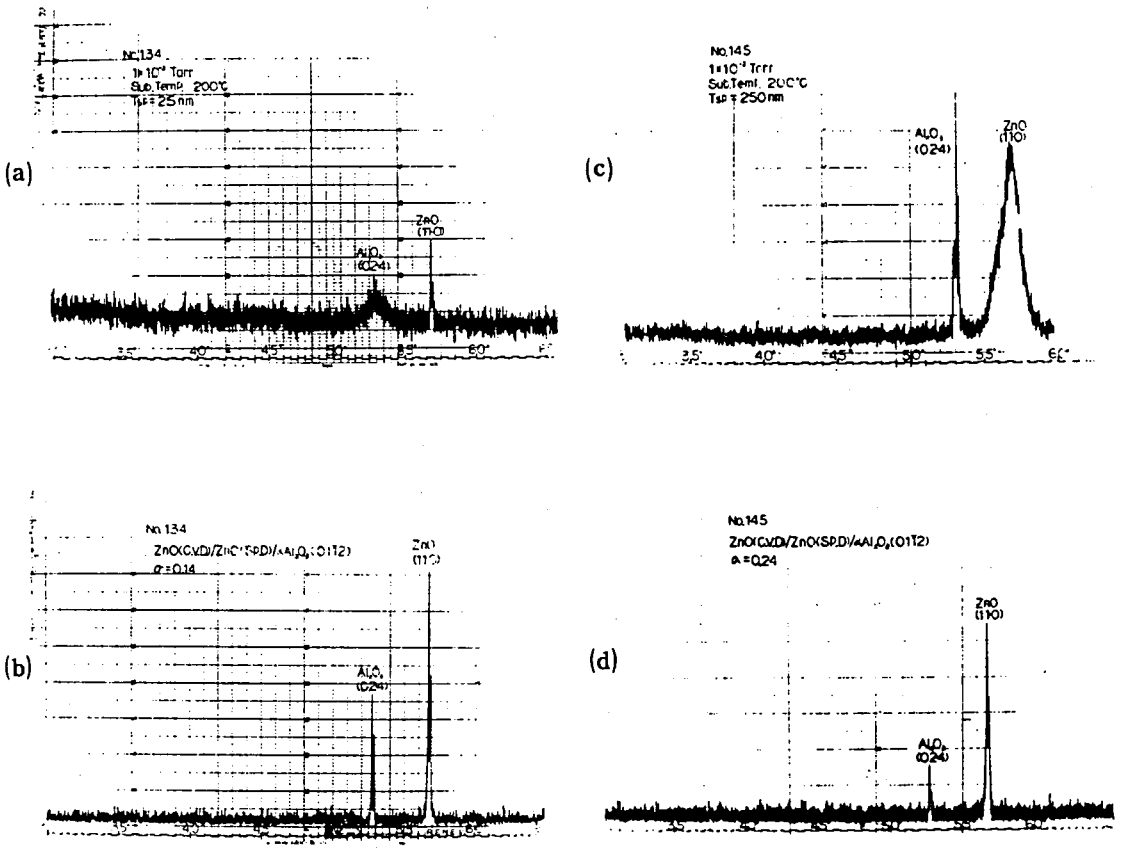

Fig.2.10. X-ray diffraction patterns and rocking curves of ZnO films on intermediate layers with different thickness.

mediate sputtered ZnO layer plays also a role as buffer layer which relaxes the difference of lattice constant and thermal expansion coefficient between ZnO and sapphire. For these reasons, a ZnO single crystal film can be grown only on an intermediate ZnO layered pattern when the growth condition for the CVD process are appropriate. Accordingly, successful selective crystal growth of the ZnO film is made by using this technique as shown in Fig.2.11.

2-4. Electrical Properties of Epitaxial Films

The electrical properties of bulk single crystals of ZnO have been studied by Heiland [11], Thomas [12], Hutson [13,14] and Kroger [15]. The studies on the electrical properties of single crystals ZnO doped with nickel and cobalt [16], and lithium and copper have been also carried out [17,18].

In contrast to the bulk ZnO crystals, there has been a few report about the electrical and optical properies of thin film ZnO because it has been difficult to obtain high quality ZnO films.

The electrical properties of the epitaxial ZnO $(11\bar{2}0)$ films on sapphire $(01\bar{1}2)$ have been examined. Measurements were carried out in the temperature range 77-400K by a van der Pauw method. Four point contacts of indium have been made as a ohmic contact. In order to investigate the dependence of electrical properties on film thickness, the film was reduced by lapping.

The as-grown films showed a n-type semiconductores with resistivity of 10^{-2}-10^{-1} Ωcm as shown in Fig.2.12. The film

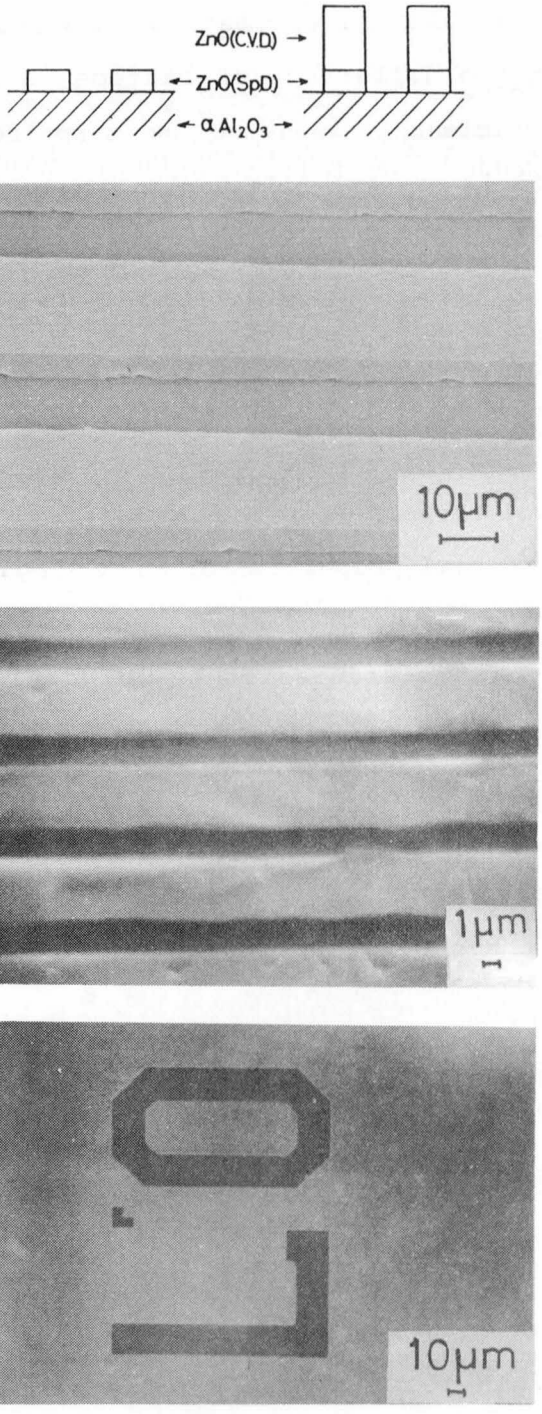

Fig.2.11. Process of the selective crystal growth and photograph of selectively grown ZnO.

resistivity does not show the temperature dependence in the measured temperature range. The carrier concentration in CVD films, which is shown in Fig.2.12., was about 10^{18} cm^{-3}, which is higher than in bulk sigle crystal by more than two order of magnitude [8,9]. The temperature dependence of carrier concentration also was weak. These experimental result suggested that the CVD film was degenerated typed.

Figure 2.12 and 2.13 show the dependence of resistivity, carrier concentration and Hall mobility on temperature. The specimens measured were prepared at 950°C. The electrical properties of as-grown samples show the weak temperature dependence. It ia also found that the thinner samples show the higher carrier concentration. These experiment facts suggest that ZnO films obtained are degenerated or have some shallow doners, and there exist highly conductive layer in the interface region.

In order to investigate to the distribution of electronic properties, measurements were carried out when sample's thickness was reduced to 143 μm and 17 μm by lapping from surface. The thickness dependence of resistivity, carrier concentration and Hall mobility are shown in Fig.2.14.. The resistivity and carrier concentration show the weak temperature dependence. The temperature dependence of Hall mobility also was weak when the film thickness were of 143 and 17 μm. The dependence of film thickness on electrical properties at 300K is also in Fig.2.15. Resistivity decreases as the film thickness decreases. This tendency means that the high conductive layers exist in the film-substrate interface region. The carrier concentration increases

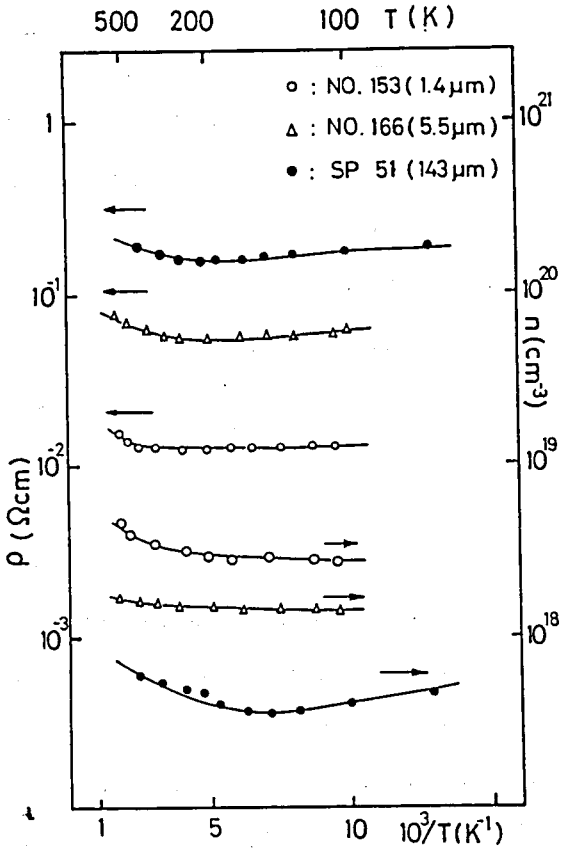

Fig.2.12. Temperature dependence of resistivity and carrier concentration in as-grown ZnO films.

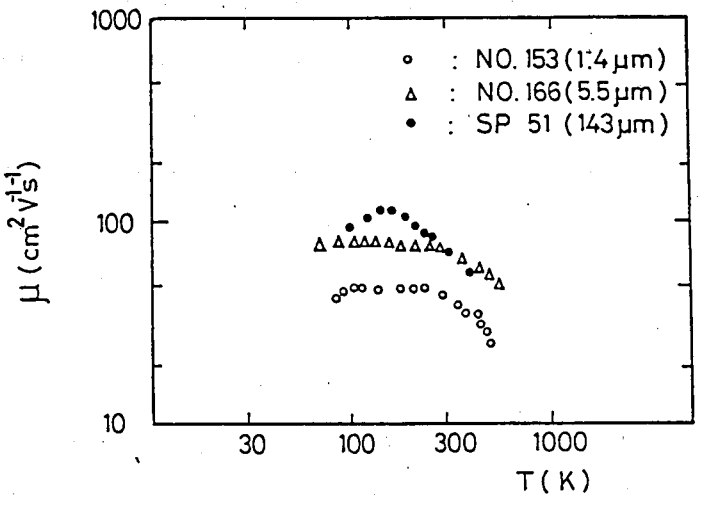

Fig.2.13. Temperature dependence of Hall mobility in as-grown ZnO films.

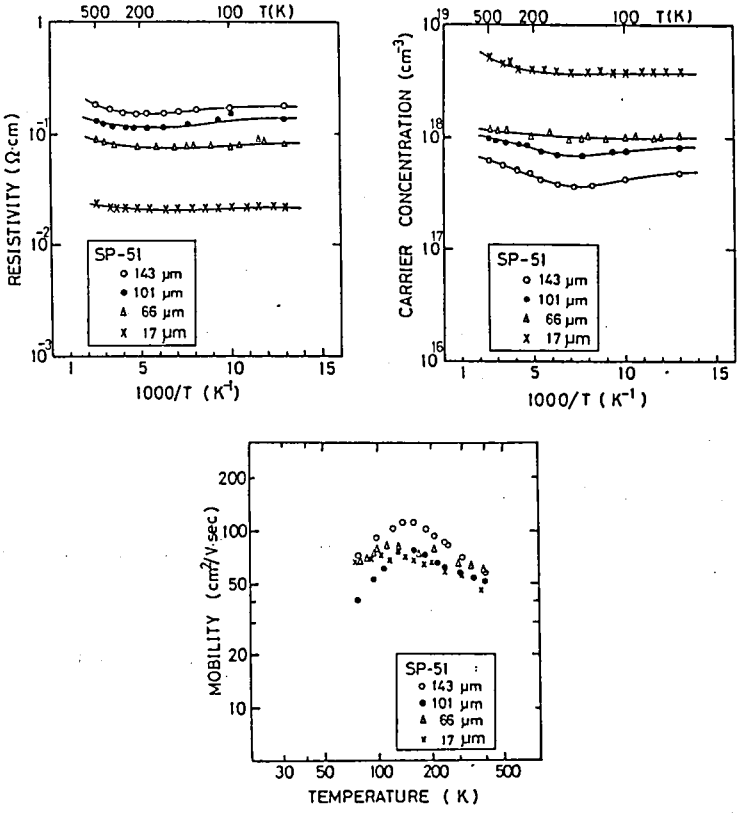

Fig.2.14. Temperature dependence of resistivity, carrier concentration and mobility for surface and rear lapped ZnO films.

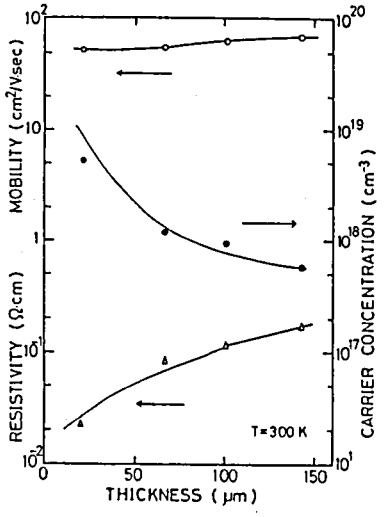

Fig.2.15. Electrical properties as a function of thickness.

with decreasing the film thickness and is very high in the interface region. This suggest that the carriers are localized and impurity conduction may occure in the interface region.

2-5. Optical Properties of Epitaxial Films

The optical transmission was measured for the CVD films which is shown in Fig.2.16. Transmission was measured by a double beam photospectroscopy(SHIMADZU:MPS-50L). The film showed a sharp absorption edge at about 380nm. The obtained films were coloreless and transparent. The average transmission of films of 2.4 μm thick (Sample No.10-18) and of 143 μm (Sample No.Sp-51) are about 80% and 76% in the visible region.

2-6. Dependence of Growth Conditions on Electrical and Optical Properties

The effect of the growth temperature on electrical and optical properties of ZnO films grown by CVD were mesured. The dependence of growth temperature on electrical prpoperties of films are shown in Fig.2.17. Electrical measurement was carried out by the van der Paw method. It was founded that resistivity and carrier concentration decrease with increaseing the substrate temperature. The increse of mobility with increasing substrate temperature was observed. This means that ZnO films grown at higher substrate temperatures have less native defects than when they grew at low substrate temperatures. Intensity of photolu-

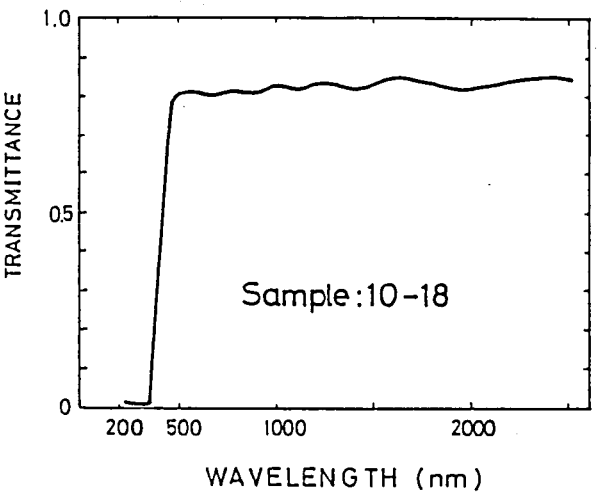

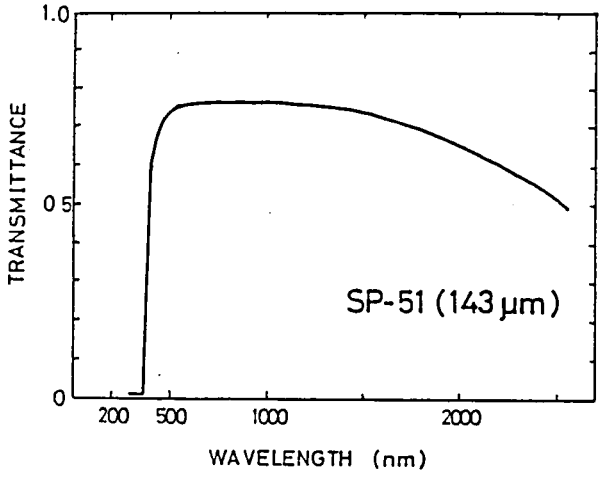

Fig.2.16. Optical transmission spectrum of ZnO films.

minescence spectrum also was measured, which is shown in Fig.2.17. The photoluminescence intensity increased as the substrate temperature increased. The strong intensity of photoluminescence also shows that the film contained less non radiative native defects which decresed mobility. This fact supported the change in mobility as shown in Fig. 2.17.

The dependence of growth rate on the electrical and optical properties of ZnO films were also measured, which is shown in Fig.2.18. The growth rate were controlled by changing the flow of water vapor. Electrical resistivity incresed and mobility decreased with increasing the growth rate. Photoluminescence intensity decreased. Thus, it was found that the number in non-radiative recombination center which decreased the mobility increased when films were grown at high growth rates. These results indicate that the electrical and optical properties can be controlled by changing the growth rate of film.

2-7. Conclusion

Single crystalline ZnO thin films were obtained by the chemical vapor deposition method using the $ZnO-H_2-H_2O-O_2$ system. The $(11\bar{2}0)$ and (0001) ZnO films were grown epitaxially on $(01\bar{1}2)$ and (0001) sapphire substrates, respectively. In this CVD method, an intermediate thin layer was first deposited on the sapphire substrate by sputtering and then the CVD growth was performed. The ZnO single crystal films were grown only on an intermediate ZnO layered pattern when the growth conditions for

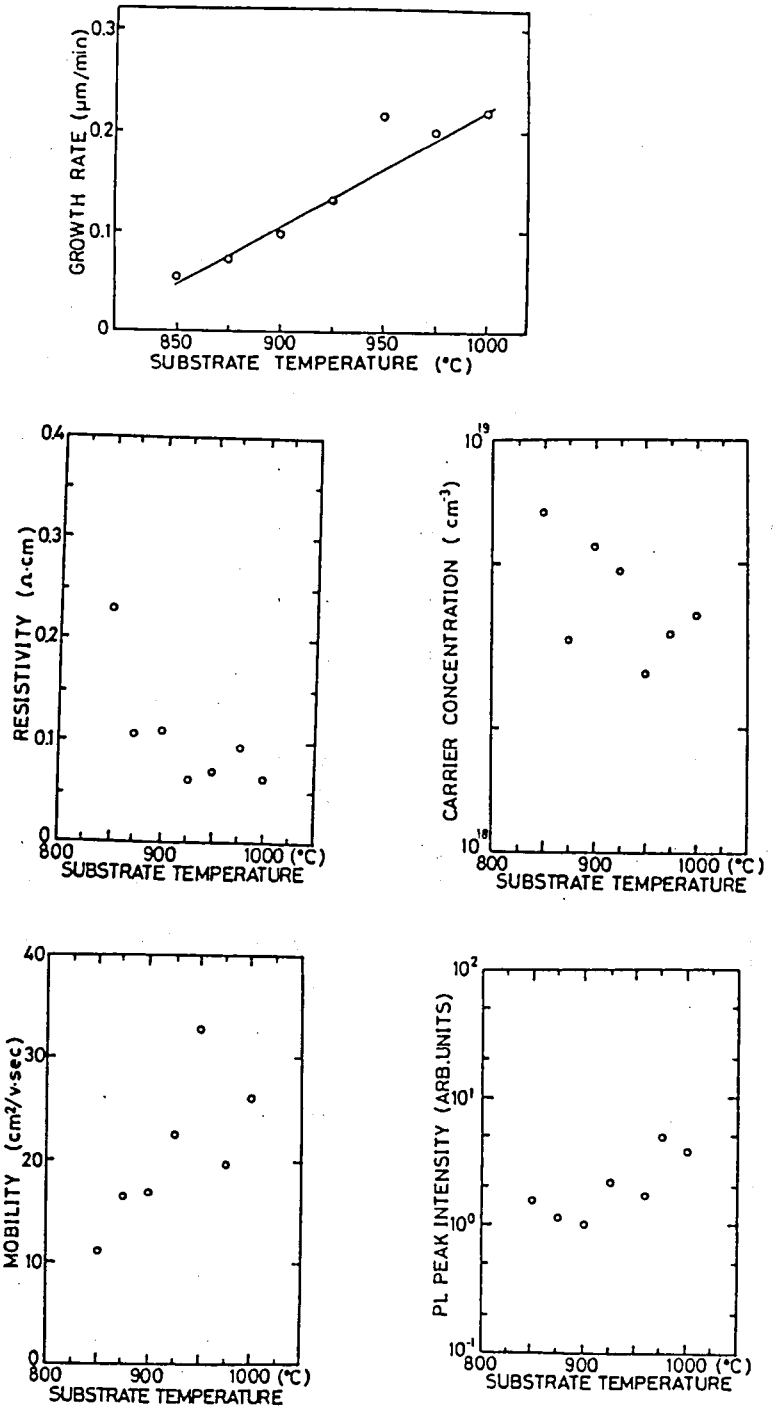

Fig.2.17. Effect of growth temperature on electrical and optical properties.

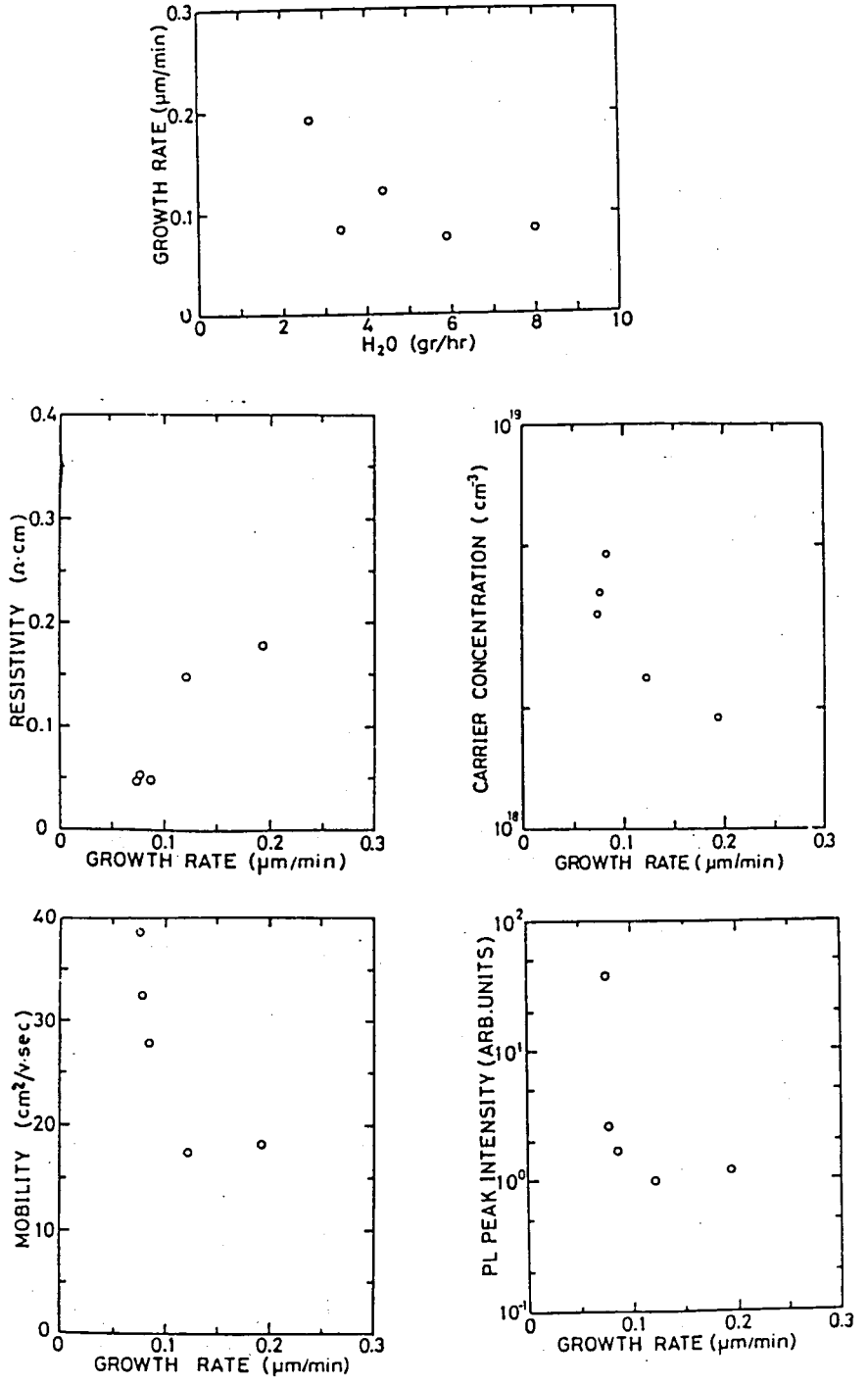

Fig.2.18. Effect of growth rate on electrical and optical properties.

the CVD process were appropriate. Accordingly, successful slective area growth of the ZnO films was made by using this technique.

The electrical properties of as grown samples were measured. The resistivity of films was 10^{-2}-10^{-1} Ωcm, Hall mobility of 40-120 $cm^2/V{\cdot}sec$ and carrier concentrations of 10^{18} cm^{-3}. The temperature dependence of them was weak and this result means that ZnO films obtained is degenerated or have some shallow doners. The dependence of film thickness on electrical properties showed carriers are localized and impurity conduction may occure in the interface between film and substrate. The optical transmission measure ments showed that the CVD films obtained had a sharp obsorption edge at 380nm and high transparency in visible region. The dependence of growth parameters (substrate temperature and growth rate) on electrical and optical propeerties also was investigated.

References

[1] I.Kubo, J.Phys.Soc.Jpn. 16(1961)2358.

[2] T.Takahashi, A.Ebina and A.Kamiyama, Jpn.J.Appl.Phys. 5(1966)560.

[3] Y.S.Park and D.C.Reynolds, J.Appl.Phys. 38(1967)756.

[4] H.Iwanaga and n.Shibata, Jpn.J.Appl.Phys. 11(1972)121.

[5] G.Galli and J.E.Coker, Appl.Phys.Letters 16(1970)439.

[6] R.A.Rabadanov, S.A.Semiletov and Z.A.Magomedov,

Sov.Phys.Solid State 12(1970)1124.

[7] F.Pizzarello, J.Appl.Phys. 43(1972)3627.

[8] J.M.Hammer, D.J.Channin, M.T.Duffy and J.P.Wittke, Appl.Phys.Letters 21(1972)358.

[9] M.Kasuga and S.Ishihara, Jpn.J.Appl.Phys. 15(1976)1835.

[10] M.Aoki, K.Tada and T.Murai and T.Inoue, Thin Solid Films 83(1981)283.

[11] G.Heiland, E.Mollow and Z.Stockman, Solid State Phys. 8(1959)191.

[12] D.G.Thomas, in: Semiconductors, Ed.N.B.Haannay (Reinhold, New York, 1959).

[13] A.R.Hutson, ibid.

[14] A.R.Hutson, Phys.Rev. 108(1957)222.

[15] F.A.Kroger, in: The Chemistry of Imperfect Crystals (North-Holland, Amsterdam, 1964)p.691.

[16] M.Sumita, Jpn.J.Appl.Phys. 6(1967)1469.

[17] E.D.Kolb and R.A.Laudise, J.Amer.Ceram.Soc. 49(1966)302.

[18] E.M.Dodson and J.A.Savage, J.Mater.Sci. 3(1968)19.

CHAPTERIII. FABRICATION OF OPTICAL WAVEGUIDES USING ZnO FILMS ON SAPPHIRE SUBSTRATES

3-1. Introduction

In the past twenty years, significant advances have been made in the field of integrated optics including optical waveguides. However the first study of an all dielectric guide was apparently that of D. Hondros et al. in 1910 [1]. They presented the first theoretical description of mode propagation along a dielectric rod. The subject then seems to have lain dormant until the development of high frequentcy sources. In the late 1930's and early 1940's, the dielectric rod came into consideration as an antenna which became a candidate for microwave antenna system. The early theory of dielectric aerials and its experimental verification was described by D.G. Kiely in 1953 [2].

In 1960's, the first dielectric waveguide to be studied at optical frequencies was the glass-coated, glass fiber developed originally for fibre optics imaging applications [3]. In 1971, the Corning Glass Works succeeded in fabricating single-mode glass fibers with loss rates of 20 dB/km. These guides are very promissing considerations for optical transmission lines in the communications system of the future.

On the other hand, the dielectric thin film waveguide at optical frequency is at least as old as the development of optical thin film technology. It was not until the rate 1960's, however, that thin film guides become candidates for potential communications applications. In 1969, the Bell Telephone Labo-

ratories published the theoretical and experimental studies in "integrated optics" [4]. This new concept promises to bring the techniques of electronic integrated circuit to optical waveguides, so that planer arrays of passive and active signal processing element can be fabricated. There does exist many literature on dielectric thin film, e.g. ZnS, ZnO, Si_3N_4, YIG, polymer glass, and charcogenide, optical waveguide.

In a ZnO thin film optical waveguide, the first theoretical and experimental studies were described by P.K.Tien et al. in 1969 [5]. In their work, thory and experiment of on modes of propagating light waves in sputter deposited ZnO films were described. In 1971, optical waveguide losses grater than 20 dB/cm were reported [6] and J.M.Hammer et al. reported the low losses (below 5 dB/cm) epitaxial ZnO optical waveguides in 1972 [7]. Since then, N.Chubachi et al. [8], E.L.Paradise et al. [9], and T.Shiosaki et al. [10] described the theoretical and experimental studies on ZnO thin film optical waveguide.

In this chapter, a simple theory of thin film waveguide and experimental studies are described.

3-2. Optical Waveguides (Planer Type) and their Properties

In this section, simple waveguide theory is described. If the media were perfect dielectrics, the Maxwell equation are

$$\nabla \times E = -\mu_o \partial H/\partial t \tag{3-1}$$

$$\nabla \times H = \varepsilon_o n^2 \partial E/\partial t \tag{3-2}$$

where, ε_o and μ_o are permitivity and permiability in free space, and n is refractive index, respectively.

We assume,

$$E=E(x,y)\exp j(\omega t-\beta z) \qquad (3\text{-}3)$$

$$H=H(x,y)\exp j(\omega t-\beta z) \qquad (3\text{-}4)$$

in where the direction of propergation is z, and the propagation constant is β , and $\omega=2\pi c/\lambda$. , as shown in Fig.3.1,

In step index waveguide, the electromagnetic component is not changed in the y direction. Therefore, $\partial/\partial t=j\omega$, $\partial/\partial z=-j\beta$, $\partial/\partial y=0$ are given, and from equation(3-1) and (3-2) the general wave equation are as follows,

$$\partial^2 E_y/\partial x^2 + (k_o^2 n^2-\beta^2)E_y =0 \qquad \text{TE mode} \quad (3\text{-}5)$$

$$\partial^2 H_y/\partial x^2 + (k_o^2 n^2-\beta^2)H_y =0 \qquad \text{TM mode} \quad (3\text{-}6)$$

where,

$$H_x=-\beta/\omega\mu_o E_y \quad H_z=-1/j\omega\mu_o \partial E_y/\partial x \quad \text{TE mode} \quad (3\text{-}7)$$

$$E_x=\beta/\omega\varepsilon_o n^2 H_y \quad E_z=1/j\omega\varepsilon_o n^2 \cdot \partial H_y/\partial x \quad \text{TM mode} \quad (3\text{-}8)$$

From the solution of the wave equations (3-5) and (3-6), and from the boundary conditions at x=0 and x= h, eigen value equation can be obtained, where h is film thickness.

As mentioned above, we considered the propergation of light in a waveguide as an electromagnetic field which mathematically represented a solution of Maxwell's wave equation, subject to certain boundary conditions at the interfaces between planes of different indices of refraction. Above mentiond description is generally called the physical-optic approach [11,12].

There is a another method which is the ray-optic approach [11]. In order to explain the waveguiding of light in a planer waveguide by the ray-optic method, only Snell's law of reflection which coupled with the phenomenon of total internal reflection.

Consider a ray of light propergating within a three-layer waveguide structure as shown in Fig.3.2.

From Snell's law,

$$\sin\phi_1 / \sin\phi_2 = n_2/n_1 \tag{3-9}$$

and

$$\sin\phi_2 / \sin\phi_3 = n_3/n_2 \tag{3-10}$$

where ϕ_3 is small, a ray of light passes freely through both interfaces, suffering only refraction, as shown in Fig.3.2(a). This case correspond to the radiation modes. As ϕ_3 is increased beyond the point at which ϕ_2 exceeds the critical angle for total internal reflection at the n_2-n_1 interface, the light wave passes as shown Fig.3.2(b). This case corresponds to a substrate radiation mode and the condition for total internal reflection at the n_2-n_1 inter face is given by

$$\phi_2 \geq \sin^{-1}(n_1/n_2) \tag{3.11}$$

and

$$\phi_3 \geq \sin^{-1}(n_1/n_3) \tag{3.12}$$

As ϕ_3 is further increased beyond the point at which ϕ_2 also exceeds the critical angle for total internal reflection at the n_2-n_3 interface, the light wave becomes confined as shown in Fig.3.2(c). This case correspondes to a guided mode and the critical angle by

$$\phi_2 \geq \sin^{-1}(n_3/n_2) \tag{3.13}$$

and

$$\phi_3 \geq \sin^{-1}(1)=90^{o} \tag{3.14}$$

Only when $\beta \geq kn_3$ can confined waveguide modes occur (because $\sin\phi_2=\beta/kn_2$).

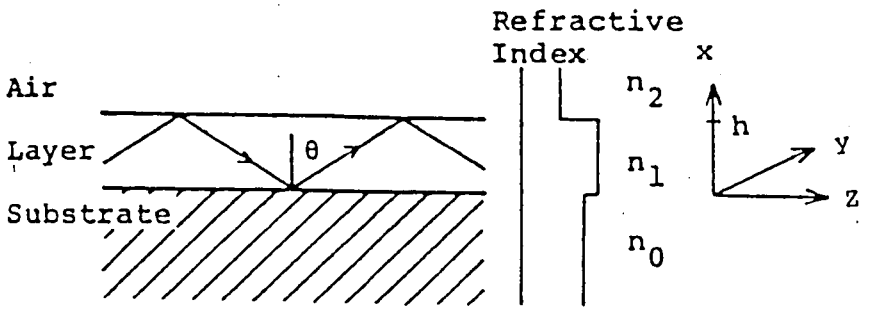

Fig.3.1. Schematic illustration of the basic three-layer planer waveguide structure.

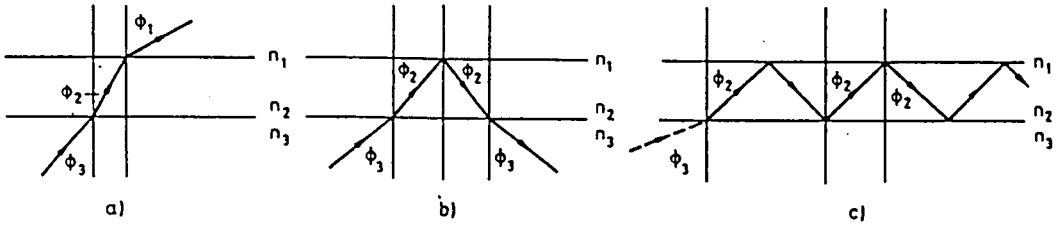

Fig.3.2. Optical ray patterns for (a) air radiation modes; (b) substrate radiation modes; (c) guided mode.

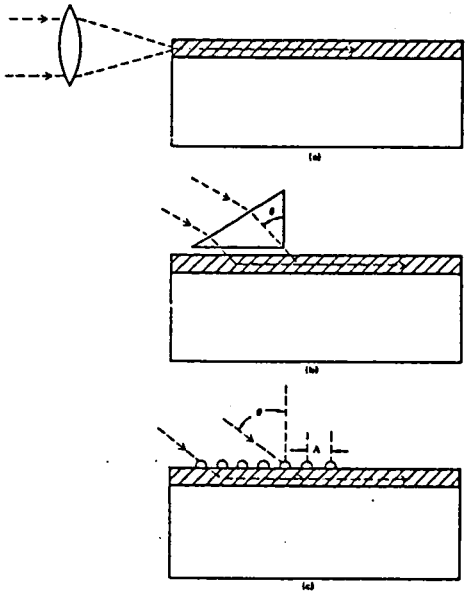

Fig.3.3. Techniques for coupling light into a thin-film waveguide; (a) Endfire, (b) Prism coupler, (c) Grating coupler.

In the waveguide modes, the total phase changes for a point on a wavefront that travels from the n_2-n_3 interface to the n_2-n_1 inter face and back again must be a multiple of 2π. Then the following condition given by

$$2kn_2t\sin\Theta_m-2\phi_{23}-2\phi_{21}=2m\pi \tag{3.15}$$

where t is the thickness of the waveguiding region, Θ_m is the angle of reflection with respect to the z direction, m is the mode number, and ϕ_{23} and ϕ_{21} are the phase changes sufferd upon total internal reflection at the interfaces. The values of ϕ_{23} and ϕ_{21} can be caluculated from

$$\tan\phi_{23}=(n^2{}_2\sin^2\phi_2-n^2{}_3)^{1/2}/(n_2\cos\phi_2) \tag{3.16}$$

$$\tan\phi_{21}=(n^2{}_2\sin^2\phi_2-n^2{}_1)^{1/2}/(n_2\cos\phi_2) \tag{3.17}$$

for TE wave, and

$$\tan\phi_{23}=n^2{}_2(n^2{}_2\sin^2\phi_2-n^2{}_3)^{1/2}/(n^2{}_3n_2\cos\phi_2) \tag{6.18}$$

$$\tan\phi_{21}=n^2{}_2(n^2{}_2\sin^2\phi_2-n^2{}_1)^{1/2}/(n^2{}_1n_2\cos\phi_2) \tag{6.19}$$

for TM waves. Where $\phi_m=\pi/2-\Theta_m$

For a given m, the parameters n_1, n_2, n_3 and t, ϕ_m (or Θ_m) can be caluculated. Thus a descrete set of reflection angle ϕ_m are obtained correspondending to the various mode. However, valid solutions do not exist for all waves m.

The excitation of guided wave is required in guided wave experiments. Efficient coupling of light into and out of thin film is an important consideration. Ttese coupling techniques have been commonly used as shown Fig.3.3. The end-fire coupling technique (Fig.3.3(a)) requres the good opticals surfaces at the edge of the film to avoid excessive scattering of the incident beam.

In the prism coupling method, light enters through the top surface of the film with the prism coupler. In order to excite all possible waveguide modes in the film, the refractive index of the prism should be larger than that of the film. An incoming laser power enters the film by tunneling through the gap which is air or other low refractive index materials and separates the prism from the film. For effective coupling, the spacing of the air gap is on the order of one-eighth to one-fourth of the vacuum optical wavelength. For most efficient power transfer, the phase velocity of the light wave in the prism must match that of a guided mode of the magnitude. In this case, the propagation constant of a particular mode in the film is

$$B=n_p k\sin\theta \quad k=2\pi/y \tag{3.20}$$

where n_p is the refractive index of the prism, θ is the angle between the incident beam in the prism and normal to the surface of the film, and y is the free-space wave length. The different modes of the film can be excited by varing θ.

The grating coupling method has been also used to provide efficient coupling (Fig.3.3(c)). In this case, the phase-match condition is

$$B=kn_1\sin\theta+2l\pi/\Lambda^2 \quad k=2\pi/y \tag{3.21}$$

where n_1 is the refractive index of the air or other medium in which the incident beam propergates, Λ^2 is the grating period, and l is the diffraction order of the grating.

In our experiment, the second coupling technique, prism coupling method, has been used because of high coupling efficiency, good selectivity of excited mode and good applicability.

Optical waveguided losses of ZnO films obtained have been measured by the scattering detection method [13]. In this method, if the scattered light intensity increases in proportion to the guided light intensity, the waveguided losses can be measured by measuring of the distribution of scattered light along the guided light. A fiber optic probe is then used to measure the intensity of the light scattered, as shown in Fig.3.4. The intensity of scattered light as measured by the optical fiber probe is plotted in Fig.3.5. This figure shows the average slope of TE_2 mode. Figure 3.6 shows an example of the relation between the optical loss and the effective refractive index of the mode. The loss measurement was carried out for TE modes propergating perpendicular to the c-axis of ZnO film. The loss value for the first mode is estimated as 0.87 dB/cm from the loss value and the standard deviation for higher modes. The refractive indecies, thickness and attenuation of the CVD films obtained are tabulated in Table 3-1. The values of the refractive indices are consistent with those of the ZnO bulk single crystal.

3-3. Fabrication of Ridge Optical Waveguides and their Properties

In the various optical waveguided devices with the function of optical modulation and switching, three dimensional waveguide is desirable to controll the waveguided light with good efficiencies. The three dimensional waveguide have been proposed, such as buried type, ridge type, loaded type and voltage-induced type. Various ways, such as thermal diffusion, ion exchange, ion injection and electron beam bombardment have been used to fabricate

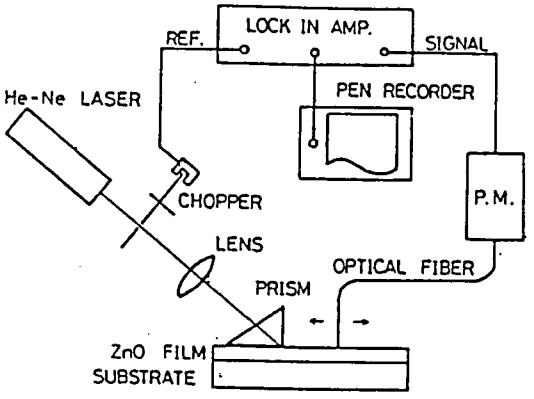

Fig.3.4. Schematic illustration of the scattering detection method.

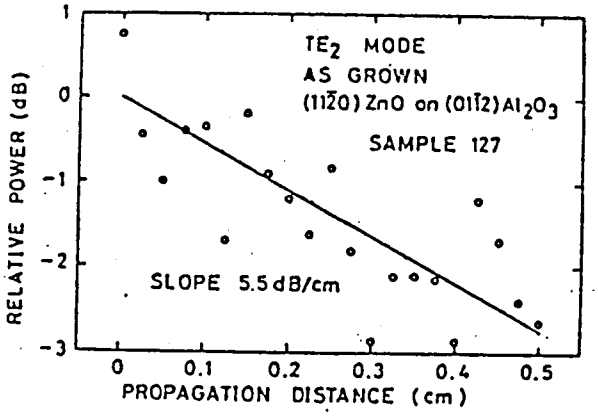

Fig.3.5. Scattering light intensity versus propagation distance.

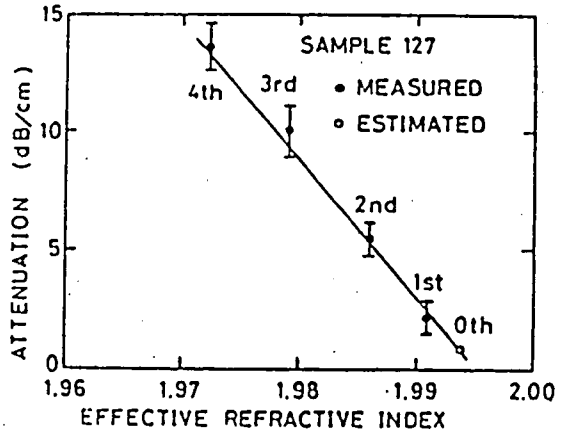

Fig.3.6. Loss attenuation versus effective refractive index.

Table 3-1. Results of light attenuation loss measurements.

SAMPLE	SUB. OR.	PROP. DIREC.	REFRACTIVE INDEX	THICKNESS (μm)	ATTENUATION 0th	1st	2nd	3rd	4th	5th	6th	7th
4-13-1	S-R	//	1.9877±0.0006	1.5401±0.0082	7.62	18.37	21.73	28.57	33.82			
4-16-1	S-R	//	1.9877±0.0005	1.3013±0.0067	11.04	17.54	23.91	25.65				
4-21-2	S-R	//	1.9842±0.0003	1.0318±0.0027	6.28	24.42	21.53					
4-21-2	S-R	⊥	1.9994±0.0001	1.0399±0.0006	7.68	19.68	18.19					
4-24-2	S-R	//	1.9913±0.0000	0.9508±0.0002	35.78	25.75	24.55					
4-24-2	S-R	⊥	1.9931±0.0002	0.9481±0.0013	7.84	19.62	23.12	17.70				
5-11-1	S-R	//	1.9893±0.0003	1.5140±0.0049	9.30	19.51	27.16	38.84				
5-15-1	S-R	//	1.9907±0.0000	1.4478±0.0003	7.64	13.49	25.83	30.36				
5-15-1	S-R	⊥	1.9995±0.0003	1.4522±0.0032	12.42	16.01	24.50	31.86				
5-31-2	S-R	//	1.9864±0.0002	0.8796±0.0009	11.82	34.00	34.19					
5-31-2	S-R	⊥	2.0016±0.0001	0.8942±0.0004	7.19	23.20	29.52					
6-1-1	S-R	//	1.9868±0.0007	1.0206±0.0059	10.73	29.24	48.14					
6-1-1	S-R	⊥	1.9994±0.0001	1.0013±0.0005	10.28	24.77	33.97					
CR45***	S-R	⊥	2.0061±0.0004	2.3611±0.0081	13.82	30.62	37.64	47.37	44.29			
CR67***	S-R	⊥	2.0081±0.0012	1.1869±0.0136	* 4.59	8.90	15.44					
CR97***	S-R	⊥	1.9992±0.0013	1.5621±0.0192	* 3.90	6.06	6.61	9.92				
CR117***	S-R	⊥	2.0033±0.0004	2.1563±0.0083	19.65	28.15	27.19	28.68	25.71	26.80	28.54	16.56
CR127	S-R	⊥	1.9939±0.0002	5.0216±0.0136	* 0.87	2.21	5.48	10.04	13.58	14.88	15.46	17.40

NOTE. SUB.OR. S-R $ZnO(11\bar{2}0)/Al_2O_3(01\bar{1}2)$

*** Polished Sample

** Nonmeasurable .

* Estimated from the attenuations of higher order modes

⊥ Perpendicular to the c-axis of ZnO

// Parallel to the c-axis

the buried type waveguides. This type waveguide has the good advantages of fabricating low loss optical waveguides, optical modulator and optical switching devices quite easily. Therefore, this buried type devices have been used mostly. In ridge type, the waveguides have been fabricated by removing thermal evaporated or sputtered layer using dry etchig or chemical etching technique. This type waveguide is multi mode waveguide and is suitable for the curved guide because of good confinement of the guided light. With the ridge type waveguide, for example, one of the most difficult problems lies in fabricating smooth side walls. The loaded type waveguide has two type waveguides, such as dielectric loading and metal loading type. This type waveguides have been not used widely, because the difference of refractive indices between waveguided region and clad region is too small, 10^{-3}. In electro-optic crystals, such as $LiNbO_3$ and $LiTaO_3$, voltage induced type waveguide have been proposed. The theory of dielectric three dimensional waveguide mode was presented by E.A.J.Marcatili [14].

In the following experiment, we propose the new technique to fabricate the ridge type optical waveguide using selective crystal growth technique in CVD and describe the scattering loss measurement.

In the first stage of fabrication process, an intermediate ZnO layer with 200Å thickness was sputtered on $(01\bar{1}2)$ sapphire substrate by an rf planer magnetron sputtering system. After that, the ridge was fabricated using photo lithographic technique as shown in Fig.3.7. AZ1350J was used as a photoresist and the

chemical etching was carried out using hydrogen chloride (HCl) for 5-8 sec. In succeeding process, the chemical vapor deposition was carried out and the ridge waveguide was fabricated as mentioned in Chapter 2. This wave guide has a 19.1 μm width and 1.05 μm thickness. Figure 3.8. shows a SEM photograph of the ridge waveguide fabricated.

A prism coupler at the top of the guide was used to inject the He-Ne laser light (6328 Å). Figure 3.9. shows a light propagating in a guide. From this figure it can be seen that a 6328A light beam for a distance longer than 1 cm. The optical propergation loss at E^{x}_{po} mode was measured by a scattering detection method, as mentioned in Sec.3-2. The ridge optical waveguide fabricated showed a propagation loss of 40.32 dB/cm, which is shown in Fig.3.10. It has been founded that the two dimensional thin film optical waveguides of ZnO on sapphire showed very low loss. Therefore, the high propergation loss of ridge waveguide obtained is attributed to the roughness of the side walls.

The selective area crystal growth technique was used for an application to three dimensional optical waveguide, as mentioned above, however an approach to smoothing side walls should be made. The appropriate choice of growth direction to the substrate and of growth conditions are applicable. These approach to reduceing scattering loss are now under investigation.

3-4. Conclusion

Optical propergation losses were measured in as-grown single crystalline ZnO films obtained on sapphire substrates by the

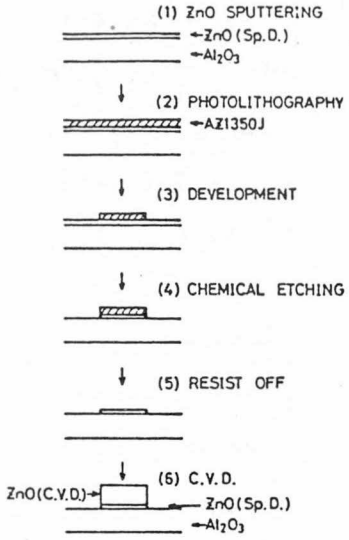

Fig.3.7. Fabrication process of ridge waveguide.

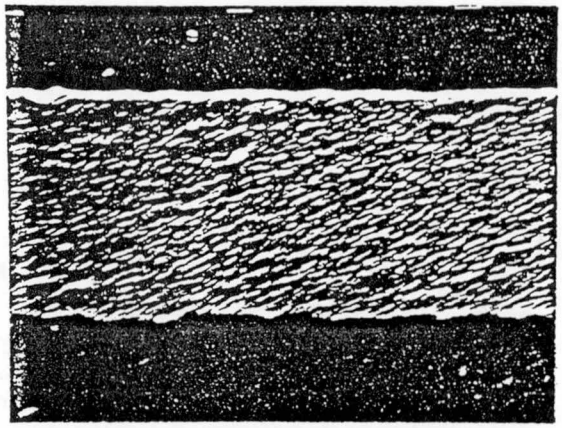

Fig.3.8. SEM photograph of ridge waveguide.

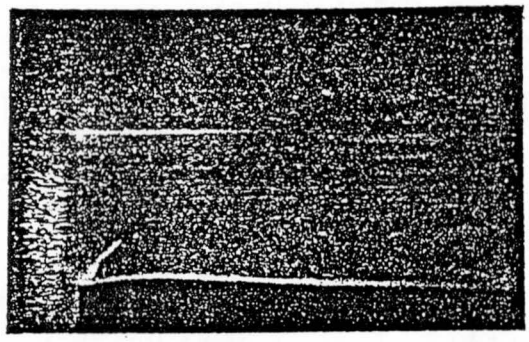

Fig.3.9. Light beam in ridge waveguide.

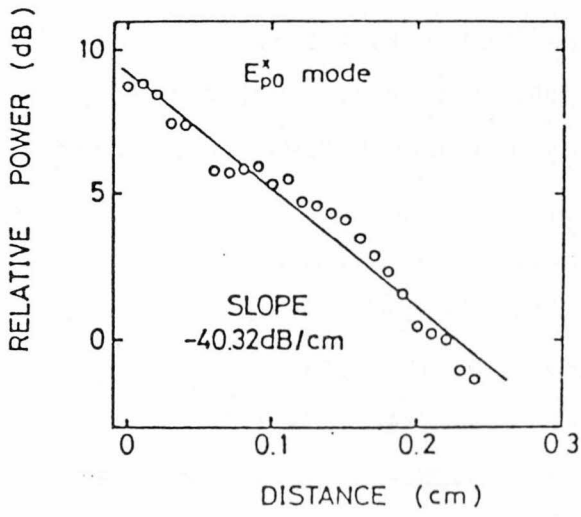

Fig.3.10. Scattering light intensity versus propagation distance.

chemical vapor deposition method. The loss measurement was carried out by the scattering detection method. The minimumm attenuation loss obtained are 0.87 dB/cm for TE_0 mode at 6328A. This attenuation loss is considerably small and the CVD method is proved to be a excellent technique to obtain the high quality ZnO films with low optical propagation losses.

The ridge type optical waveguide were also fabricated using the selective crystal growth technique in the CVD method. The ridge waveguide showed the attenuation loss of 40.3 dB/cm for TE^x_{po} mode at 6328Å. This high loss was attributed to the roughness of the side walls.

References

[1] D.Hondros and P.Debye, Ann.Phys. 32(1910)465.

[2] D.G.Kiely, in "Dielectric Aerials" (Mathuen, London, 1953).

[3] N.S.Kapany, in "Fiber Optics Principles and Applications" (Academic Press, New York, 1967).

[4] S.E.Miller, Bell Syst.Tech.J. 48(1969)2059.

[5] P.K.Tien, R.Ulrich and R.J.Martin, Appl. Phys.Letters 14(1969)291.

[6] P.K.Tien, Appl.Opt. 10(1971)2395.

[7] J.M.Hammer, D.J.Channin, M.T.Duffy and J.P.Wittke, Appl.Phys.Letters, 21(1972)358.

[8] N.Chubachi, Proc.IEEE. 64(1976)772.

[9] E.L.Paradise and A.J.Shuskus, Thin Solid Films, 38(1976)131.

[10] T.Shiosaki, S.Ohnishi and A.Kawabata, J.Appl.Phys. 50(1979)3113.

[11] R.G.Hunsperger, in "Integrated Optics"(Springer-Verlag, Berlin, 1984).

[12] N.S.Kapany and J.J.Burke, in "Optical Waveguides"(Academic Press, New York, 1972).

[13] J.E.Goell and R.D.Standley, Bell Syst.Tech.J. 48(1969)3445.

[14] E.A.J.Marcatili, Bell Syst.Tech.J. 48(1969)2071.

CHAPTER IV. GROWTH AND PROPERTIES OF ZnO FILMS ON SILICON SUBSTRATES BY CHEMICAL VAPOR DEPOSITION

4-1. Introduction

Several fabrication techniques of ZnO thin films, such as sputtering, ion-plating, ionized-cluster-beam deposition, spray pyrorysis and chemical vapor deposition, have been investigated for many purposes, as mentioned above. However it was very difficult to obtain high quality films with good c-axis orientation, good surface flatness, high transparency and high growth rate by these methods. And there has been no report about a crystal growth mechanism of ZnO films with good c-axis orientation by CVD on semiconductor substrates. In this chapter a CVD technique for obtaining a ZnO thin film with a good c-axis orientation at a high growth rate (3.6-90 μm/h) on a silicon substrate is reported.

Silicon is a suitable substrate for ZnO growth, because the thermal expansion coefficient of Si($3.57 \times 10^{-6}/^{\circ}C$) [1] is nearly equal to that of ZnO ($4.0 \times 10^{-6}/^{\circ}C$) [2]. The silicon is of course, a promising material of application to many kinds of electronic devices. This CVD method has a maximum growth rate of 90 μm/h which is higher than conventional methods, e.g. reactive magnetron sputtering with a deposition rate of 15 μm/h [3]. ZnO films obtained by this CVD method have a rather low resistivity (10^{-2}-10 Ω cm) and resistivity control by a diffusion process with lithium or other suitable acceptors is necessary to obtain a ZnO film with a high resistivity which is usually needed for applica-

tion to surface acoustic wave devices. However high conductive ZnO films obtained by this CVD method, which have also good transparency to most of the useful solar spectrum, can be used as a window layer of a solar cell. In this chapter we report the fabrication of ZnO films on Si by this CVD method and the characterization of these films by x-ray diffraction, reflection electron diffraction (RHEED), scanning electron microscopy (SEM), optical transmission measurement and photoluminescence measurement. Thin film solar cells of ZnO/Si were also fabricated and photovoltaic properties were studied.

4-2. Experimental Procedure

The grwoth apparatus similar to the one which is used in the previous work [4] is shown in Fig.4.1 , in which the reaction tubes have an internal diameter of 30 and 84 mm respectively. The small and large tubes are 100 and 145 cm long respectively. The purified ZnO powder (99.99%) and Si substrates are placed in the inner tube. A temperature profile of the furnace with the growing region temperature of 950°C is shown in Fig.4.1. A mixture of H_2, H_2O and N_2 gases is introduced into the inner tube. The deoxidation reactions take place at the source, according to the next equation:

$$ZnO + H_2 \rightleftarrows Zn + H_2O \quad \text{with} \quad P_{Zn} = K \cdot P_{H_2}/P_{H_2O} \tag{4-1}$$

On the other hand, a mixture gas of O_2 and N_2 is introduced into the outer tube and the oxidation reactions may take place at the

substrates, following the equations:

$$2Zn + O_2 \rightleftarrows 2ZnO \quad (4\text{-}2)$$

$$Zn + H_2O \rightleftarrows ZnO + H_2 \quad (4\text{-}3)$$

$$2H_2 + O_2 \rightleftarrows 2H_2O \quad (4\text{-}4)$$

$$Si + O_2 \rightarrow SiO_2 \quad (4\text{-}5)$$

$$2Si + O_2 \rightleftarrows 2SiO(g) \quad (4\text{-}6)$$

$$Si + H_2O \rightleftarrows SiO + H_2 \quad (4\text{-}7)$$

ZnO is formed on the substrate by the chemical reactions according to the above equations. The substrare was (111) oriented silicon on which a 300-2500Å thick ZnO layer was sputter-deposited followign the process shown in ref.[5]. In order to investigate the effect of the sputtered thin ZnO layer on the crystallinity of the CVD ZnO film, chemical vapor deposition of a ZnO film was also tried directly on a silicon substrate without a sputtered ZnO layer. The thin intermediate ZnO film on the substrate was deposited by a planer magnetron rf sputtering system at a substrate temperature of 300-350°C. A (111) Si single crystal wafer was used as a substrate because its three-fold symmetry may give rise to the growth of a more highly c-axis oriented ZnO film due to the similarity of the six-fold symmetry of ZnO to the three-fold symmetry of silicon.

4-3. Film Growth

Attempts to grow ZnO films directly on bare silicon substrates have been unsuccessful. Even if a film was deposited,

it had a very rough surface and the affinity of ZnO to the silicon substrate was very weak and the ZnO layer was easily pealed off. On the otehr hand, ZnO thin films were reproducibly obtained on a silicon substrate with the intermediately-sputtered ZnO thin layer. By using this method ZnO films could be obtained all over the substrate surface uniformly and the affinity of the ZnO film to substrate was strong. The appropriate flow rates of N_2, H_2O and H_2 from the source side were 150cc/min, 5.5gr/h and 55cc/min, and those of N_2 and O_2 from the substrate side were 200cc/min and 50cc/min respectively. The appropriate thickness of the intermediately-sputtered layer was 1500 to 2500Å. In this CVD system, highly oriented films were obtained at a substrate temperature of 850 to 1000°C.

The typical x-ray diffraction pattern of a ZnO film deposited on a (111) Si substrate is shown in Fig.4.2. Fig.4.2(a) shows the patten of an intermediately-sputtered ZnO layer prior to CVD growth and Fig.4.2(b) shows that of a CVD ZnO film. From Fig.4.2(b) it is seen that only the (002) peak of ZnO is present and the separation of the Cu-$K_{\alpha 1}$ and $K_{\alpha 2}$ lines of the (002) peak is clearly shown. This indicates that a highly c-axis oriented ZnO film was deposited on the (111) silicon substrate. The c-axis of the ZnO film was perpendicular to the silicon surface. An x-ray rocking curve of this CVD film was measured to estimate the distribution of the c-axis orientation. The value of standard deviation angle of the c-axis orientation distribution was 0.47°, taking the distribution as Gaussian to a good approximation. It is shown in Fig.4.2(a) that an itnermediately-sputtered

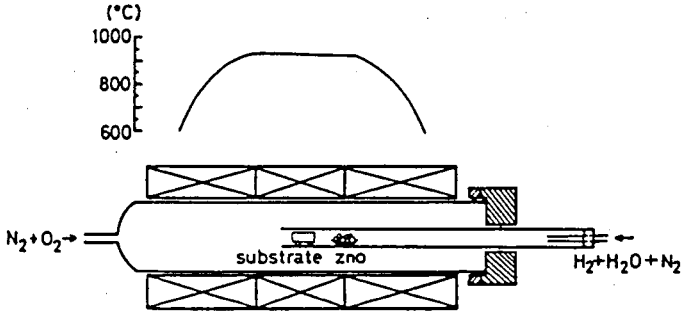

Fig.4.1. Schematic diagram of the growth furnace and a temperature profile.

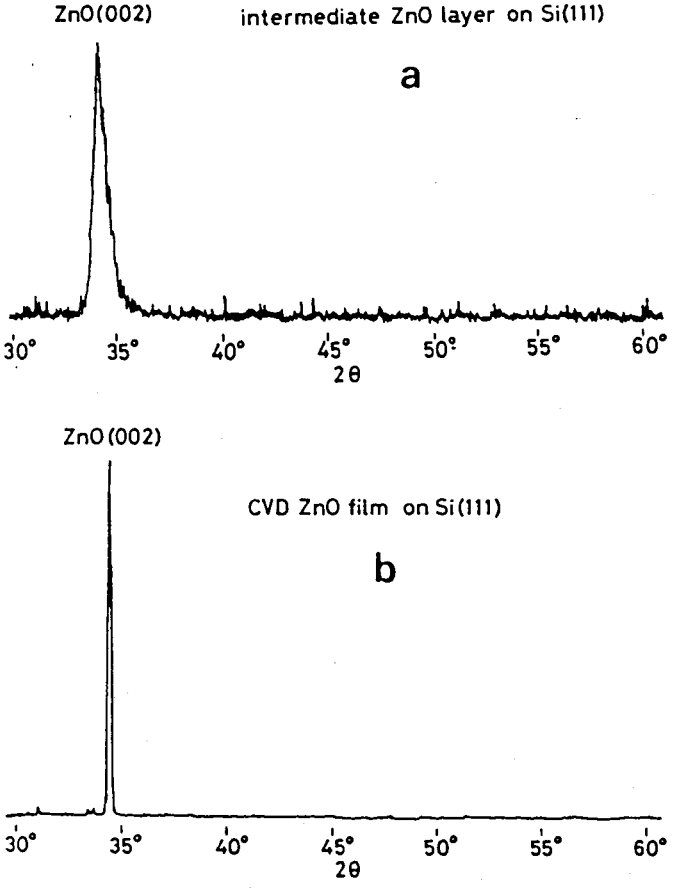

Fig.4.2. X-ray diffraction pattern of a ZnO film on (111) Si: (a) the pattern of an intermediately sputtered ZnO layer prior to CVD growth, (b) that of a CVD ZnO film.

ZnO layer on a (111) silicon substrate also had a c-axis orientation. It has been reported by M.S. Raven et al. that sputter-deposited ZnO films on SiO_2/(111)Si had only (002) reflections [6]. In our case the (111) silicon substrates had been chemically cleaned but had not been sputter cleaned just prior to growth. And also sputtering deposition was performed in oxygen and argon (1:1). For these reasons the silicon surface might have a very thin SiO_2 layer prior to sputtering deposition, if thus could be possible that the ZnO particles have been deposited on the SiO_2 layer giving the sputtered ZnO layer a c-axis orientation.

Figure 4.3(a) is a RHEED pattern of an intermediately sputtered ZnO layer sputter-deposited prior to the CVD growth and Fig.4.3(b) is that of a CVD ZnO film. Figure 4.3(c) is the theoretical pattern in which an electron beam is incident in the $[11\bar{2}0]$ and $[10\bar{1}0]$ directions of ZnO. The pattern of an intermediately sputtered ZnO layer had spots and rings. This shows the sputter deposited ZnO layer to have a poor c-axis orientation. However the CVD ZnO film on the sputtered ZnO layer had a good c-axis orientation so that the RHEED pattern had well-defined spots and had no rings. By comparing this RHEED pattern (Fig.4-3(b)) with that of the theoretical pattern (Fig.4.3(c)), it was found that these patterns were coincident. This shows that CVD ZnO films on (111) silicon had c-axis orientation perpendicular to the substrate surface while the a-axis of those films was in random orientation parallel to the substrate surface.

Figure 4.4 shows an SEM photograph of a ZnO film on (111) silicon. This photograph shows a columnar structure of the layer,

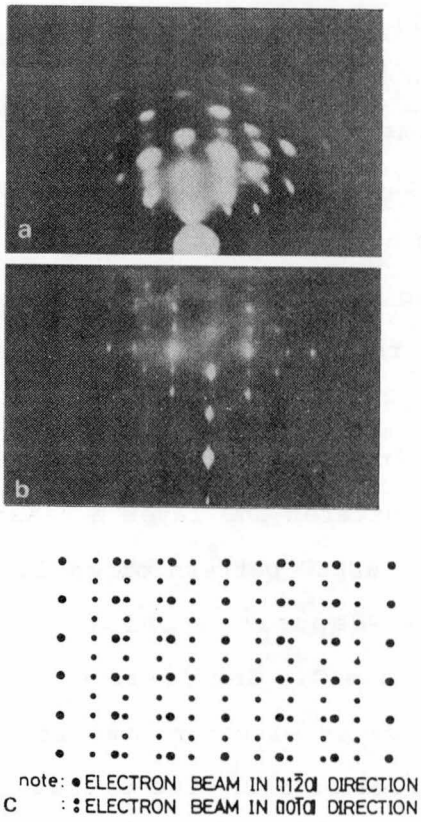

Fig.4.3. RHEED pattern of a ZnO film on (111) Si: (a) the pattern of an intermediately sputtered ZnO layer prior to CVD growth, (b) that of a CVD ZnO film.

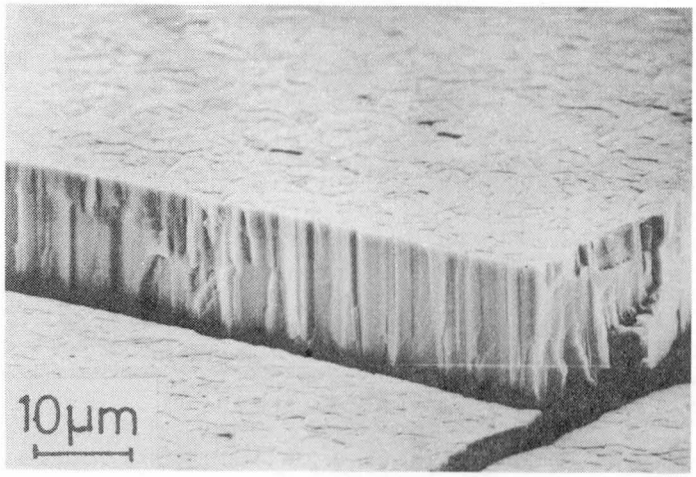

Fig.4.4. SEM photograph of a ZnO film on (111) Si.

where the c-axis of ZnO is perpendicular to the substrate. The crystallite diameter was about 1 μm.

The thickness of the ZnO film increases linearly with the growth time as shown in Fig.4.5. This growth rate was obtained at a substrate temperature of 950°C, gas flow rates of 55cc/min for H_2, 5.5gr/h for H_2O and 150cc/min for N_2 at the source side, and of 50cc/min for O_2 and 200cc/min for N_2 at the substrate side.

The growth rate of the ZnO film was dependent on the flow rate of H_2O. The H_2O gas flow rate was controlled by changing the temperature of the water source in the bubbler and the flow rates of N_2 and H_2 gases which were introduced to the reaction tube through H_2O in the bubbler. Fig. 4.6 shows the relationship between the H_2O gas flow rate and the growth rate. In this case the flow rates of N_2 and H_2 gases were constant and the H_2O gas flow rate was controlled by changing temperature of H_2O. The growth rate was increased from 0.06 μm/min to 1.5μm/min when decreasing the H_2O gas flow rate.

As previously mentioned, the intermediately sputter-deposited ZnO layer played an important role in this CVD method. A ZnO film was not deposited on a silicon substrate without sputtered layer. The well adhering ZnO thin layer deposited by sputtering plays a role of providing a high density of nuclei in the succeeding CVD process. Depositing ZnO as an intermediate layer at low temperatures causes the surface binding energy to become very uniform over the entire surface area. For these reasons, a ZnO film can be grown only on an intermediate ZnO

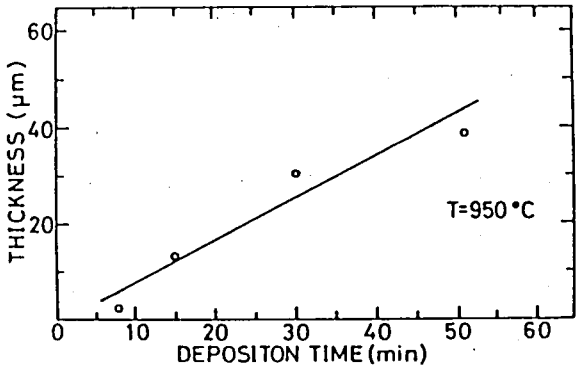

Fig.4.5. Relation between deposition time and thickness of ZnO film.

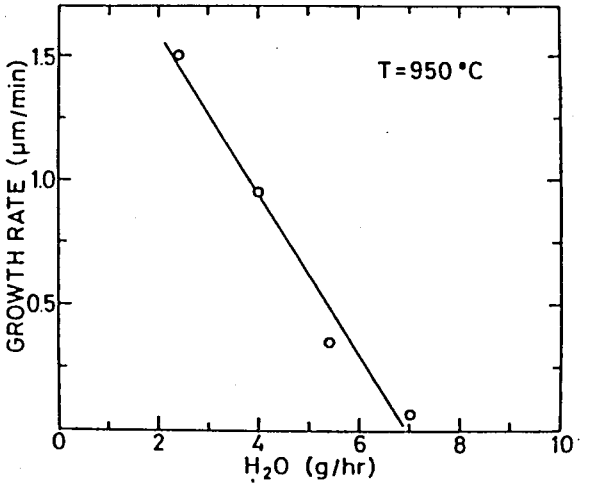

Fig.4.6. Relation between H_2O gas flow rate and film growth rate at a substrate temperature of 950°C, gas flow rate of 55cm^3/min for H_2, 150cm^3/min for N_2 at source side and of 50cm^3/min for O_2 and 200cm^3/min for N_2 at substrate side.

layer. The sputtered thin ZnO layer also acted as a buffer layer which reduced the difference of thermal expansion coefficient and lattice constant between ZnO and silicon. A CVD ZnO film is tightly deposited on a Si substrate because the intermediate layer is deposited tightly on the substrate by sputtering and the affinity of the CVD-deposited ZnO to the intermediate ZnO layer is strong because of the homo-epitaxy.

Utilizing these techniques a ZnO film can be selectively grown only on the pattern written by an intermediate ZnO layer when the growth conditions for the CVD process are appropriate. Figs. 4.7 shows a successful selective growth of a ZnO film on (111) Si made by using this technique. Here the intermediate ZnO layer pattern was sputter-deposited on the Si substrate using a metal mask and then CVD growth was performed on the Si substratre with the pattern. The edge of the ZnO strips is not flat and has irregular planes. This is because the c-axes of the polycrystallites are normal to the substrate but the a-axes are in random orientations. When the a-axis had a good orientation as in an epitaxial growth of a ZnO film on (0001) sapphire, the edge of strips had a more regular plane.

4-4. Optical Properties

Optical transmission measurements in the 3500 to 7400Å region were made on a ZnO thin film about 15 μm thick using a double beam spectrophotometer (SHIMADZU MPS-50L). This thin film sample was obtained when a sample of ZnO on silicon was quenched from 950°C to room temperature and pealed off from the substrate

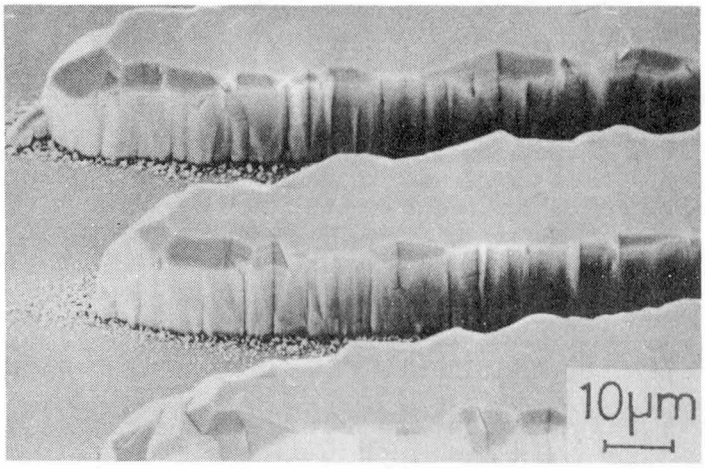

Fig.4.7. Photograph of selectively grown ZnO strips of 35μm width obtained by selective crystal growth technique.

silicon due to the difference of the thermal expansion coefficients between ZnO and Si. The optical transmission as a function of wavelength is shown in Fig.4.8. It is found that the absorption edge of the ZnO film obtained by this CVD is about 3900Å and the film has a good transparency although the film is as thick as 15 μm thick.

Photoluminescence measurements in a ZnO film on a Si substrate were made. For the measurements of photoluminescence spectra the sample was excited by 3650Å radiation from a 250W high-pressure mercury lamp. The emission peak was located at about 5200Å at room temperature as shown in Fig.4.9. This green luminescence band is usually observed in a single crystalline ZnO and attributed by many authors to interstitial zinc or an oxygen vacancy. The result that no other luminescence peak was observed shows that the ZnO film obtained did not contain prominent impurities.

4-5. Application

Thin film solar cells of n-ZnO/p-Si were fabricated. The substrates were 250 μm thick B-doped p-type Si single crystal wafers which had a resistivity of 0.005-0.015 Ωcm; the n-type ZnO layers had a thickness of about 0.9 μm. The samples were cut into about 6 x 7mm^2 squares. The dark I-V characteristics of the cells were poor, but a treatment of the cells in hydrogen improved the I-V characteristics as well as the photoelectric conversion efficiency. The typical current-voltage characteristics of the cells are shown in Fig.4.10. The best cell showed a

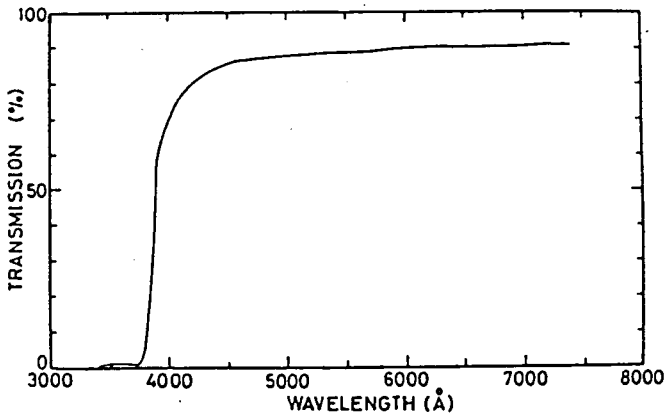

Fig.4.8. Optical transmittance spectrum of a ZnO thin film of about 15 μm thick.

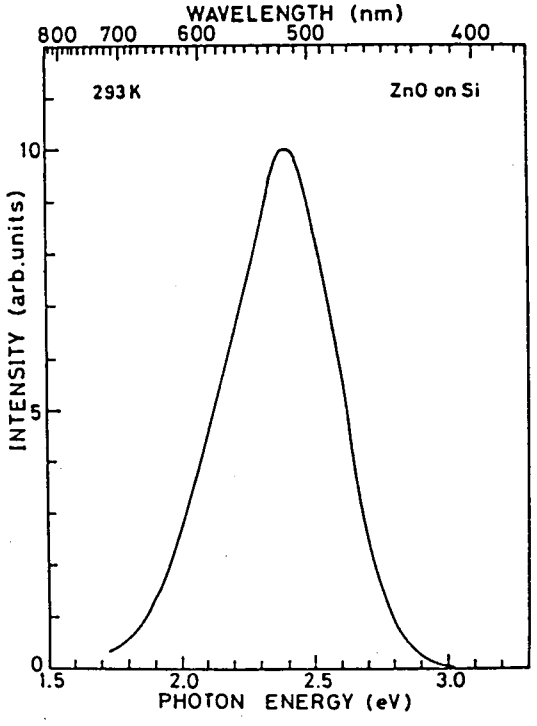

Fig.4.9. Photoluminescence spectrum of a ZnO film on Si.

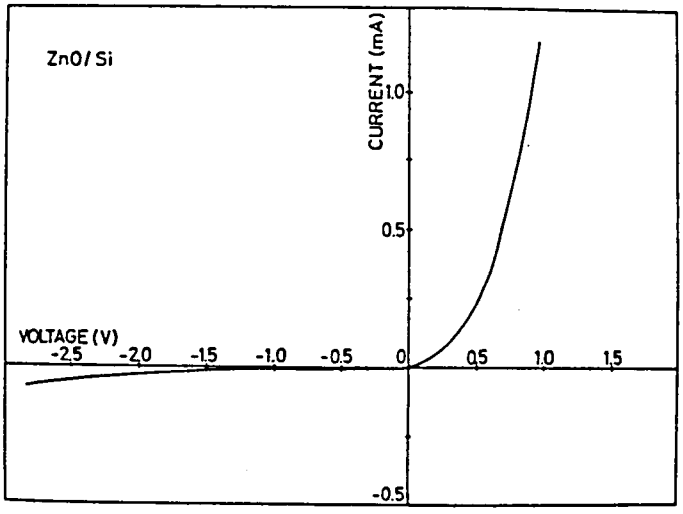

Fig.4.10. Dark current-voltage characteristics of ZnO/Si cell.

photovoltaic effect with open-circuit photovoltage of 115mV and short-circuit photocurrent of about 32μA/cm^2 under an irradiation of 100mW/cm^2. This cell showed a conversion efficiency of 0.92%. The current-voltage characteristics and photovoltaic effect of the cells may be effected mainly by the interfacial layer, caused by interfacial defects at the junction and series resistance effects. Therefore, the improvement of conversion efficiency of our solar cells may be expected by decreasing series resistitivy and controlling interfacial states.

4-6. Conclusion

A highly oriented ZnO single crystal thin film with high deposition rate was obtained by the ZnO-H_2-H_2O-O_2 CVD system on the (111) silicon substrate with a very thin ZnO sputtered layer (1500-2500Å) on it. The growth rate was increased from 3.6 μm/h

to 90μm/h and can be controlled by changing the H_2O gas flow rate. The ZnO sputtered layer gives a high density of nuclei and a buffer layer for the succeeding CVD process. When a thin ZnO layer was not sputter-deposited on the silicon substrate, a CVD ZnO film was not deposited. By using this technique, in which both sputtering at the first step and CVD at the second step were used for the film growth, a selective crystal growth of the ZnO film was successfully made.

n-ZnO/p-Si solar cells have been prepared and the best cell showed a conversion efficiency of 0.92%.

References

[1] W.M.Yim and R.J.Paff, J.Appl.Phys. 45(1974)1456.

[2] S.Ono, K.Wasa and S.Hayakawa, Wave Electron. 3(1977)35.

[3] T.Hata, E.Noda, O.Morimoto and T.Hada, Appl.Phys.Letters 37(1980)633.

[4] T.Shiosaki, S.Ohonishi, Y.Hirokawa and A.Kawabata, Appl.Phys.Letters 33(1987)406.

[5] T.Yamamoto, T.Shiosaki and A.Kawabata, J.Appl.Phys. 51(1980)3113.

[6] M.S.Raven, M.H.T.Al-Sinaid, S.J.T.Owen and T.L.Tanslay, Thin Solid Films 71(1980)23.

CHAPTER V. GROWTH AND PROPERTIES OF ZnO FILMS ON DIFFERENT SUBSTRATES BY PLASMA-ENHANCED METALORGANIC CHEMICAL VAPOR DEPOSITION

5-1. Introduction

In 1968 Manasevit first reported the successful use of Metalorganic Chemical Vapor Deposition (MO-CVD), also named Metalorganic Vapor Phase Epitaxy (MO-VPE) or Organometallic Vapor Phase Epitaxy (OM-VPE), in a open system for the epitaxial growth of compound semiconductors [1]. In his work, single crystal GaAs films was grown on a number of single crystal insulating oxide substrates by the decomposition of alkyl-gallium which was first applied as a source of Ga. Since his pioneering study, his group have reported actively the growth of epitaxial compound semiconductor films and alloys, GaAs, GaP, InP, GaN, AlN, $Ga_{1-x}Al_xAs$, $Ga_{1-x}In_xAs$ and $GaAs_{1-x}P_x$, on insulataing substrates and semiconductors i.e. α-Al_2O_3, $MgAl_2O_4$, BeO, ThO_2, Ge, GaAs, Si and α-SiC [2-6].

In their process semiconductor films of III-V compounds and alloys are produced by decomposing appropriate Group III metalorganic compounds, such as triethylgallium (TEG), trimethylgallium (TMG) and trimethylalumium (TMA), in the presence of the appropriate Group V hydrides. At the first stage of the work of MO-CVD, the fundamental basic problem to be solved was that due to poor purity of the source used, metalorganaic compounds, crystalline quality of semiconductor films obtained by MO-CVD was inferior to that obtained by the other epitaxial growth method. For

this reason various devices fabricated by the MO-CVD technique were not resulted in practical use in the 1970s. However, in 1977 R.D. Dupuis and co-workers succeeded in achieving the room-temperature pulsed laser operation of $Ga_{(1-x)}As_xAs$-GaAs double-heterostructure lasers [7]. Within only few years following this work, their group reported successful continuous room-temperature operation of $Ga_{(1-x)}Al_xAs$-GaAs double-heterostructure lasers [8], distributed-Bragg-confirement $Ga_{(1-x)}Al_xAs$-GaAs lasers [9], quantum well $Ga_{(1-x)}Al_xAs$-GaAs and $Al_xGa_{(1-x)}As$-GaAs-$Al_xGa_{(1-x)}As$ lasers [10,11], high efficiency GaAlAs/GaAs heterostructive solar cells [12] and $Al_{0.5}Ga_{0.5}As$-GaAs heterojunction phototransistors [13]. Since their work allowing realization of favorable practical devices, many studies have been published by other workers, on various kind of heterostructure lasers [14-21], heterostructure solar cells [22-25], and photocathods [26,27] etc.. On these studies stimulating the development of the device technology utilizing single crystal film growth technique, the First International Conference on Metalorganic Vapor Phase Epitaxy was held at Ajaccio, France in May 1981.

In the growth of II-VI compounds, the successful use of the metalorganic technique for the preparation of selenides, sulfides and telluride of zinc and cadmium was first reported by H.M. Manasevit in 1971 [28]. His group reacted $(C_2H_5)_2Zn$ and also $(CH_3)Cd$ with H_2S, H_2Se or $(CH_3)_2Te$ to obtain ZnSe, ZnS, SnTe, CdSe, CdS and CdTe on insulating substrates. After their works, many studies of epitaxial growth of ZnO for surface acoustic wave devices [29-36], of ZnS and ZnSe for electroluminescent and high emitting

devices [37-42], of CdS and CdTe for solar cells [43-45], and of HgTe and $Cd_xHg_{1-x}Te$ for infrared detectors [46-51] have been reported. However, in comparing with the study of III-V compound semiconductor by MO-CVD that of II-VI's have delayed and there have been proposed many problems for obtaining practical devices. Recently studies in this field have grown very actively. In order to discuss the problem to be overcome, International Conference on II-VI compounds was held at Durham, UK, in April 1982.

From many studies mentioned above, the MO-CVD technique proved to be very promising technique with good features as follows: 1) The composition, carrier concentration, conduction type, film thickness and growth rate of the films etc. can be easily controlled, since all of the constituent elements and dopants can be introduced into the reaction chamber in the vapor phase. Therefore, even mixed crystals and multi-layered structures can be easily obtained. 2) The gas introduced into the reaction chamber can be exchanged easily, because of a high gas flow rate comparing with that of ordinary CVD, and for this reason favorable abrupt change of component and impurity distribution can be achieved. 3) The growth apparatus is equipped with a heating system which produces only a single hot region for deposition. 4) The MO-CVD system is superior in productivity comparing with a conventional LPE system. 5) The reaction of crystal growth is caused by thermal decomposition and the epitaxial film growth on insulating oxide substrates is possible. 6) The component materials of this growth system, such as metal, quartz and graphite, are not affected by the raw material gases.

7) The crystals with discrepancy of stoichiometry can be obtained by changing the ratio of compositions introduced as soruce materials, e.g., III/V and II/VI.

On the other hand in addition to the recent increasing interest in the MO-CVD technique, the plasma-enhanced CVD (PE-CVD) technique has been developed actively in recent years. In PE-CVD, numerous films of interest in semiconducstor processing and devices are deposited by utilizing decomposition of source materials by the action of the glow discharge at low temperatures.

This plasma-enhancement technique employs a glow discharge to generate active species such as ions, atoms, molecules or free radicals. The nonequilibrium steady-state condition produced by a glow discharge transforms inert molecules into reactive species which can be produced generally only at high temperatures. By the use of this action of the glow discharge reaction, usually required high temperatures of substrates can be reduced considerably to lower-temperature region. The early works in this field were reviewed by Kirk [52].

A system equipped with a large reactor for commercial use was first presented by Reinberg in 1974 [54]. His system is a capacitively coupled circular parallel plate system with a top electrode and a heated lower grounded wafer plate. After his work, in early 1976 Rosler et al. first proposed a commercially available production system to obtain the silicon nitride film as the passivation coating for silicon device [55]. The deposition rate, refractive index and etch rate were studied by them. They

indicated that the plasma silicon nitride films practically without pinholes are scratch resistant and good step coverage, and are an effective barrier to alkali ions. Since their work allows realization of practical use, many studies on applications have been published, such as device passivation overcoat, diffusion masks for LED, an antireflection coating over LED, a coating over photolithographic masks, a backseal film which minimizes epitaxial film autodoping on highly doped substrates and a matrix for dopant in solid-to-solid diffusion. The successful application of silicon nitride films obtained by PE-CVD has promoted its application to other plasma-promoted reactions. The plasma-enhanced deposition of films such as SiO_2, Al_2O_3, TiC, SiC, and amorphous Si has been also reported and is now being studied by many workers.

In this chapter we propose a new method for obtaining ZnO films at low substrate temperatures by plasma-enhanced metalorganic chemical vapor deposition (PE-MO-CVD). This PE-MO-CVD method has the advantageous features of both MO-CVD and PE-CVD methods as mentioned above. In the following, film growth, electrical and optical properties of films and their applications are described.

5-2. Experimental Procedure

In PE-MO-CVD, the suitable metalorganic compound used as the Zn source reacts with oxidizing gas, such as O_2, CO_2 and N_2O, in the plasma discharge, resulting to ZnO films. For MO-CVD, in general, semiconductor films of II-VI and III-V compounds are

produced by decomposing appropriate Group II and Group III metal-organic compounds as shown in Table 5-1. In our study, diethlzinc (DEZ, $(C_2H_5)_2Zn$) is used as the Zn source. Diethlzinc is one of stable metalorganic compounds in N_2 and Ar atmosphere at room temperature, but reacts with air and water rapidly, and ignites by itself. The saturated vapor pressure curve and other properties are shown in Fig.5.1. At the first state of our work oxygen was used as an oxidizing gas. However, when it was used, the reaction with DEZ was too rapid and the nozzles for introducing gas to reaction chamber were soon choked with deposited ZnO. Moreover, the reaction of O_2 with DEZ took place whether the electric power for plasma generation was applied or not. After recognizing these results, CO_2, or N_2O gas reacted with DEZ to produce ZnO. CO_2 or N_2O was chosen as an oxidizing gas based on the following consideration. First, CO_2 and N_2O do not react with DEZ rapidly and the reaction between DEZ and CO_2 or N_2O does not take place below 400^{o}C without applying the electric power for plasma generation. For this reason, the effect of glow discharge plasma on the chemical reactions is investigated definitely. Second, CO_2 and N_2O are fairly safe gas.

The external aspect of the PE-MO-CVD system used in this study is shown in Fig.5.2. Figure 5.3 shows the schematic diagram of the apparatus. This system consists principally of a gas supplying system and a plasma CVD system (ANELVA PED-301). The gas system has flow meters, valves, and a stainless steel bubbler containing a liquid metalorganic compound (DEZ) (Sumitomo Chemical Co., Ltd.). These parts are connected with each other

Table 5-1. Metalorganic compounds.

	IIb	IIIb	IVb	Vb	VIb
2		$(CH_3)_3B$			
3		$(CH_3)_3Al$ $(C_2H_5)_3Al$		$(C_2H_5)_3P$	
4	$(CH_3)_2Zn$ $(C_2H_5)_2Zn$	$(CH_3)_3Ga$ $(C_2H_5)_3Ga$ $(C_2H_5)_2GaCl$*		$(CH_3)_3As$	$(CH_3)_2Se$ $(C_2H_5)_2Se$*
5	$(C_2H_5)_2Cd$	$(CH_3)_3In$* $(C_2H_5)_3In$		$(CH_3)_3Sb$	$(CH_3)_2Te$
6	$(CH_3)_2Hg$ $(C_2H_5)_2Hg$		$(CH_3)_4Pb$ $(C_2H_5)_4Pb$		

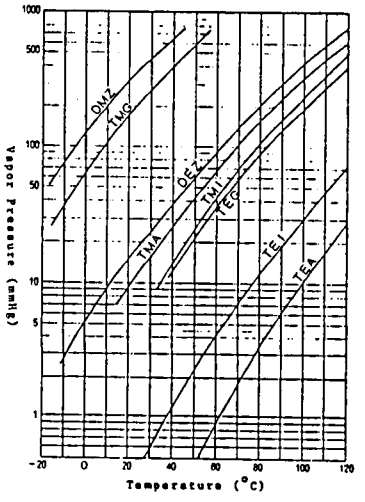

Diethyl Zinc Properties

$(C_2H_5)_2Zn$

Molecular Weight	123.5
Boiling Point	118°C
Melting Point	-28°C
Specific Gravity	1.2065
Refractive Index	1.4936
Expansion Coefficient	0.0019

Fig.5.1. Vapor pressure versus temperature for metalorganic compounds and properties of diethylzinc.

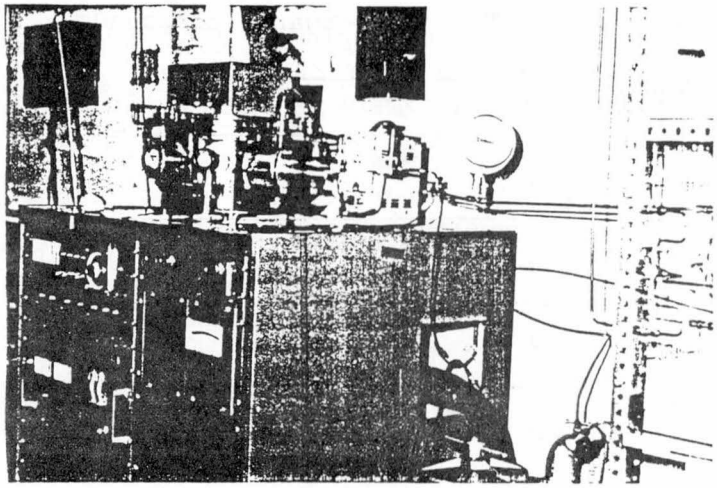

Fig.5.2. External aspect of the PE-MO-CVD system.

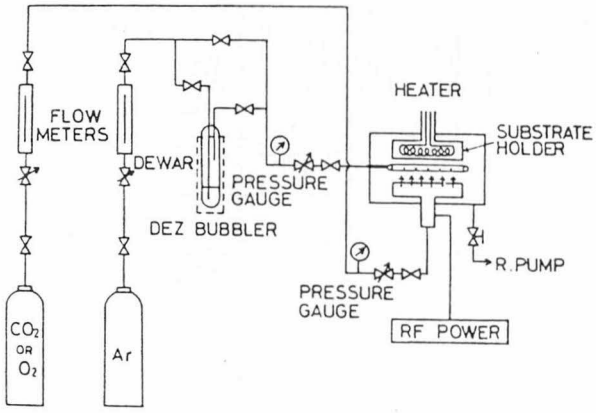

Fig.5.3. Schematic diagram of the PE-MO-CVD system.

by 1/4 inch stainless-steel tubes. Ar gas is used as a carrier gas. A bubbler containing DEZ is set in a thermostatic controled bath and the vapor pressure of DEZ is controlled by changing temperature of bubbler. The plasma CVD system is a capacitively coupled circular parallel electrode system. Plasma is generated by applying RF power of 20-300W at 13.56MHz. The chamber size is 30cm in diameter and 18cm in height. The electrodes are 21cm in diameter. Substrates materials such as glass, silicon, ceramic, sapphire and polyimide are set on upper electrode with heating system, as shown in Fig.5.3.

An oxidizing gas such as O_2, CO_2 and N_2O is introduced into the reaction chamber through many small holes bored in the lower electrode. DEZ is also introduced through an inlet nozzle with many holes. The temperature of the substrate is measured with the thermocouple. The reactor is evacuated by a rotary pump (500 l/min), and reactor pressure, which is measured by MKS BARATRON pressure transducer, about 1.5 Torr during the growth run.

5-3. Crystal Growth Using the Reaction between Diethylzinc and CO_2

In this section, c-axis oriented and epitaxial ZnO film growth by using the reaction of DEZ with CO_2 is described. Crystalographic properties of ZnO films dependent on the materials of substrate.

5-3-1. Films Grown on Glass

A Corning 7059 glass was used as substrate because of

its low price and its potential for the substrate of surface acoustic devices. The growth condition employed in the present work was that the flow rate of Ar was 200 sccm and of CO_2 was 300 sccm. The DEZ saturated gas pressure was 10mmHg. The gas pressure of reactor was kept at 1.2mmHg during plasma discharge.

In the PE-CVD system, the growth rate and the properties of the grown films seem to be greatly affected by the gas flow rate, the DEZ saturated gas pressure, the rf input power and the substrate temperature. Film thickness was measured by a profilometer (Rank Taylor Hobson Co. Ltd., Talysurf 4). Figure 5.4 shows the deposition rate as a function of these parameters. The growth conditions in changing the parameters are shown in Table 5-2. From Fig.5.4(a) and (b), we can see that the deposition rate increases rapidly as the gas flow rate is increased, however, that increases gradually as the substrate temperature and rf input power are increased. Both O_2 and CO_2 gas atmospheres are used. The growth rate by reacting DEZ with O_2 is higher than that obtained by DEZ with CO_2. As is well known, DEZ burns very violently in oxygen atmosphere. This too-rapid reaction harms the uniform mixing of the DEZ and the O_2 gas in the whole chamber and thus the uniformity of the film thickness, though DEZ is diluted in the carrier Ar gas by bubbling. On the other hand, the CO_2 gas is a fire extinguishing agent for fire accidents in using DEZ, and no reaction takes place without plasma discharge. The CO_2 gas mixes more uniformly with DEZ and gives more uniform film thickness. The reproducibility of the films is also lower when the O_2 gas is used as the oxidizing agent, because this

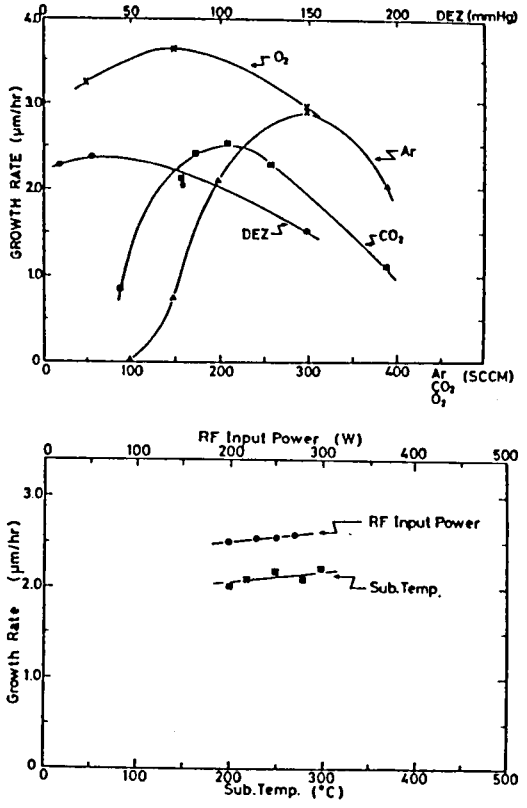

Fig.5.4. Deposition rate of ZnO films as a function of (a): Ar gas flow rate, CO_2 gas flow rate and DEZ standard gas pressure, and (b): substrate temperature and rf input power. Refer to Table 5-2.

Table 5-2. The film growth parameters supplement to Fig.5.4.

Ar flow rate (sccm)	CO_2 flow rate ($^{\circ}O_2$ flow rate) (sccm)	DEZ saturated gas pressure (mm Hg)	Substrate Temperature ($^{\circ}$C)	rf input power (W)
100-400	300	10	230	230
200	80-390	10	230	230
200	($^{\circ}$50-300)	10	230	230
200	300	10-150	230	230
200	300	10	200-300	230
200	300	10	230	200-270

rapid reaction takes place and deposits ZnO powders at the nozzle tip of the DEZ inlet and disturbs a smooth flow of DEZ.

Figure 5.5 shows the x-ray diffraction pattern of a ZnO film grown on a Corning 7059 glass substrate at a substrate temperature of 200°C and an rf input power of 220W. It is shown that only the (0001) face of ZnO is grown parallel to the substrate surface.

The effects of substrate temperature on film properties were investigated. Figure 5.6 shows the relation between the x-ray peak intensity and the substrate temperature keeping the rf input at 230W. The value of standard deviation of the x-ray rocking curve for the (002) peak, which represents the distribution of the c-axis of polycrystallites around the substrate normal, is also shown in Fig.5.6. The x-ray peak intensity increases as the substrate temperature increases. It increases rapidly at a substrate temperature of 200°C. The value of standard deviation decreases from 5° to 3° as the substrate temperature increases. This shows that the films grown at higher substrate temperatures have better c-axis orientations. When the rf input power is not applied, no x-ray peak is observed even if the substrate temperature is increased from 200 to 350°C. This suggests that the reaction of DEZ and CO_2 gas is caused by the energy of the plasma discharge and not by the thermal energy of the substrate alone.

The typical x-ray diffraction patterns of films prepared at different substrate temperatures are shown in Fig.5.7. The ZnO films grown at a substrate temperature of 150°C have a mixed orientation, however those grown above 200°C have only c-axis

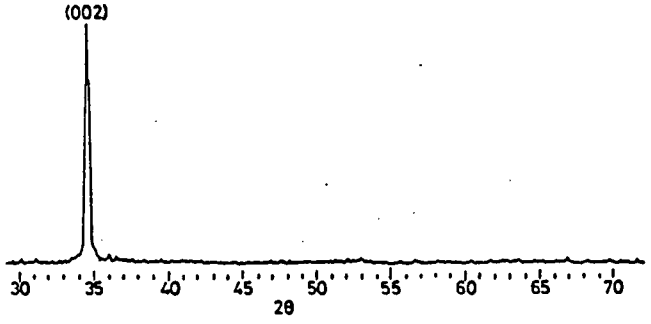

Fig.5.5. X-ray diffraction pattern of a ZnO film grown on a Corning 7059 glass substrate.

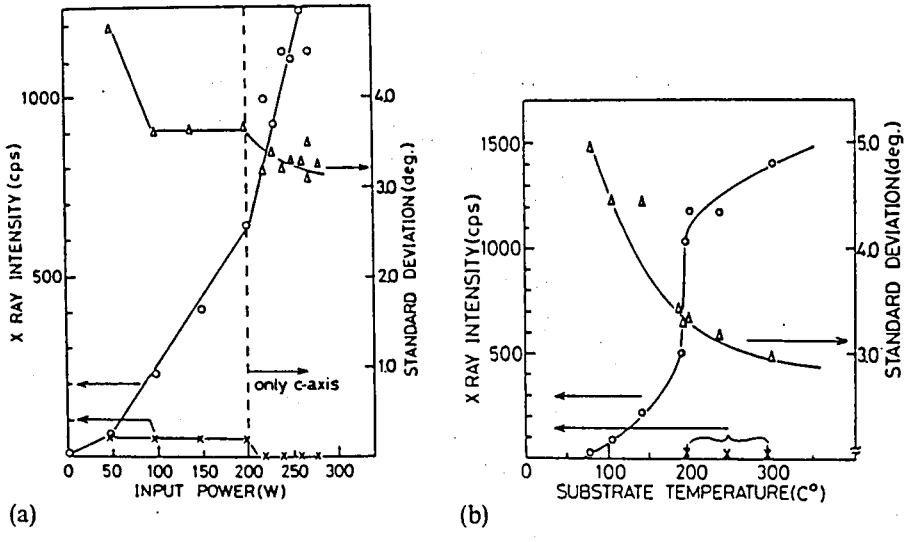

Fig.5.6. The relation between x-ray intensity, standard deviation angle and (a) rf input power (O, (00·2); x, (10·1)) and (b) substrate temperature (O, △, 230W; x, 0W).

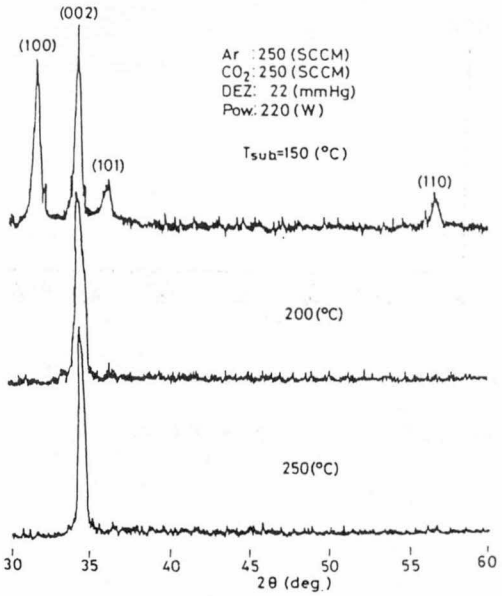

Fig.5.7. X-ray diffraction patterns of films prepared at different substrate temperatures.

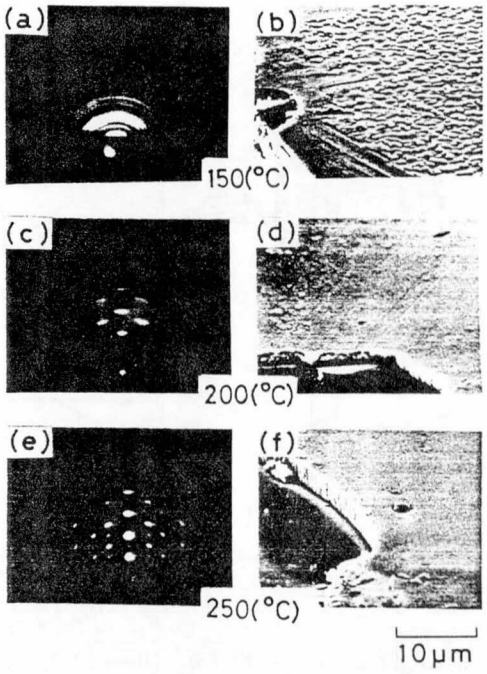

Fig.5.8. RHEED patterns and SEM micrographs of films prepared at different substrate temperatures: (a) and (b) 150°C, (c) and (d) 200°C, and (e) and (f) 250°C.

orientation. The substrate temperature higher than 200°C is also essential for the good c-axis normal orientation of the ZnO film. The structural nature of the deposited films was also examined by reflection high energy electron diffraction (RHEED) and scanning electron microscopy (SEM).

The RHEED patterns and SEM micrographs of ZnO films grown at 150°C, 200°C and 250°C at an rf input power of 230W are shown in Fig.5.8. The film grown at 150°C has ring patterns, indicating that it has a mixed orientation and is a polycrystal. The patterns of the films grown at 200°C and 250°C have spread spots; films grown at these temperatures also have better surface flatness than that grown at 150°C. From the RHEED and SEM we can see that the films obtained at a substrate temperature higher than 200°C have good crystalline quality and smooth surface.

The effects of rf input power levels on film properties were also investigated. Figure 5.9 shows the typical x-ray diffraction patterns of films prepared at different rf input powers. The ZnO films grown on a Corning 7059 glass substrate, keeping the substrate temperature at 200°C at an rf input power of 150W, have mixed orientation as shown in Fig.5.9. However, in the films obtained at rf input power above 220W the (00·2) peak becomes dominant, which shows that the c-axis is oriented perpendicularly to the substrate. As rf input power decreases below 220W, x-ray intensity of the (00·2) peak decreases. On the other hand, x-ray intensity of the (00·2) peak increases at rf input power above 220W. The value of standard deviation of the x-ray rocking curve for the (00·2) peak, varies from 4.8 to 3.0° as the

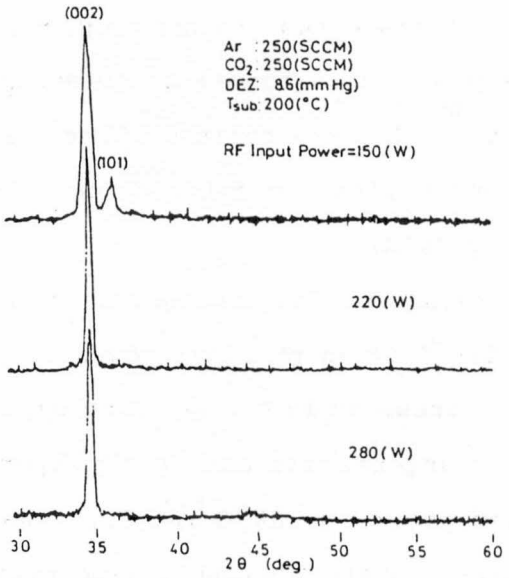

Fig.5.9. X-ray diffraction patterns of films prepared at different rf input powers.

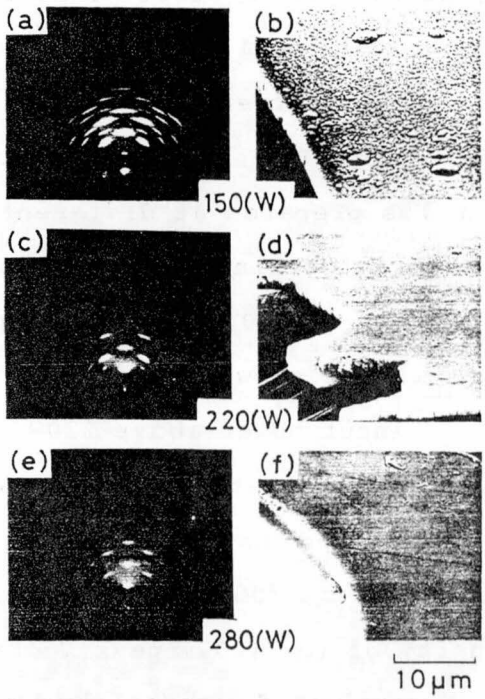

Fig.5.10. RHEED patterns and SEM micrographs of films prepared at different rf input powers: (a) and (b) 150W, (c) and (d) 220W, and (e) and (f) 280W.

rf input power increases from 50 to 280W, as shown in Fig.5.9. From these facts it is found that the films obtained at higher rf input power have better c-axis orientation than those obtained at lower rf input power. The RHEED patterns and SEM micrographs of ZnO films obtained at an rf input power of 150W, 220W and 280W at a substrate temperature of 200°C are shown in Fig.5.10. The RHEED pattern of ZnO films grown at an rf input power of 150W have a scattered ring pattern accompanied by widely spread spots. The RHEED patterns of the films grown at 220W and 280W have only spread spots, which indicate that the films have better crystalline quality than those obtained at 150W. The ZnO films obtained at 220W and 280W have a smoother surface than those obtained at 150W as shown in Fig.5.10. The effects of rf input power levels on film properties are presumably caused by the change in condition of plasma discharge and by the change in generation rate of active species with the change of rf input power levels.

In the PE-MO-CVD system the growth rate of ZnO films can be controlled by changing the gas flow rate, saturated gas pressure of DEZ, rf input power and substrate temperature as shown in Fig. 5.4. The RHEED patterns and SEM micrographs of film obtained at different growth rates are shown in Fig.5.11. The growth rate of the samples shown in this figure was controlled from 0.7μm/hr to 6 μm/hr by changing the Ar gas flow rate. The RHEED patterns of the films grown at growth rates of 0.7μm/hr and 6μm/hr indicate that the films have poor quality. However, the RHEED pattern of the film grown at a growth rate of 1.8 μm/hr shows good crystalline quality. From the SEM we can see that the film grown at a

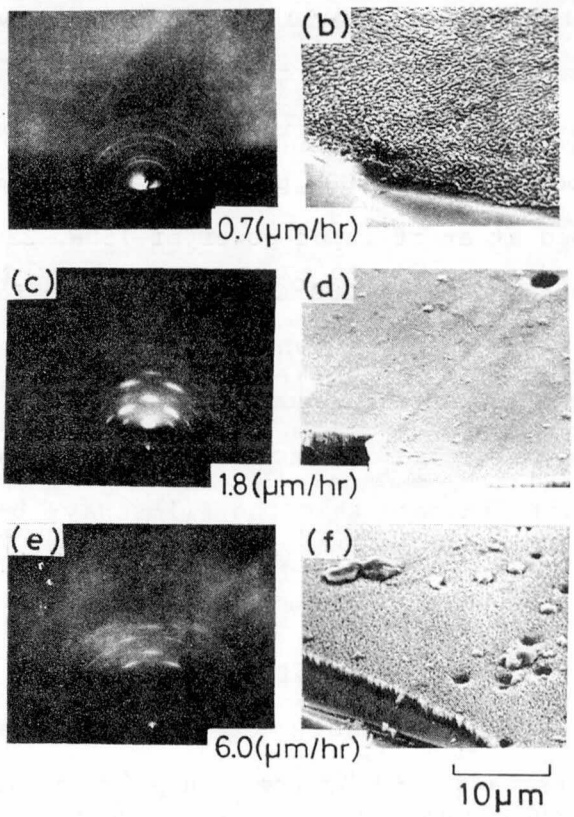

Fig.5.11. RHEED patterns and SEM micrographs of films prepared at different growth rates: (a) and (b) 0.7μm/hr, (c) and (d) 1.8μm/hr, and (e) and (f) 6.0μm/hr.

growth rate of 1.8 μm/hr has a smooth surface, while those grown at a rate of 0.7 μm/hr and 6 μm/hr have rough surfaces. These facts shows that films grown at an appropriate growth rate have good crystalline quality and a smooth surface.

5-3-2. Films Grown on Si

Silicon was used as a substrate, because of its potential for many applications such as optical waveguides, surface acoustic wave devices and heterojunction devices. The film properties were also affected by the substrate temperature, rf input power level and gas flow rate.

The growth condition employed in the present work was that 400sccm of Ar flow through the DEZ bubbler and 200sccm of CO_2 flow directly into the reaction chamber. A stainless steel bubbler containing DEZ was maintained at 20°C. (The partial pressure of DEZ was 15 Torr). The ratio of $[CO_2]/[DEZ]$ was equal to about 10.

The c-axis oriented ZnO films were obtained on (111) Si at a substrate temperature of 350°C. A typical x-ray diffraction pattern, RHEED pattern and surface morphology of ZnO on (111) Si grown at 350°C are shown in Fig.5.12. The films grown on Si show only a diffraction peak from the (002) plane. The RHEED patterns exhibit spread spots. These x-ray and RHEED observations indicate that the films have high c-axis orientation normal to the substrate. From the surface morphology and cleaved cross section of SEM photographs, we can see that the film surface morphology is something like that of films grown on the glass

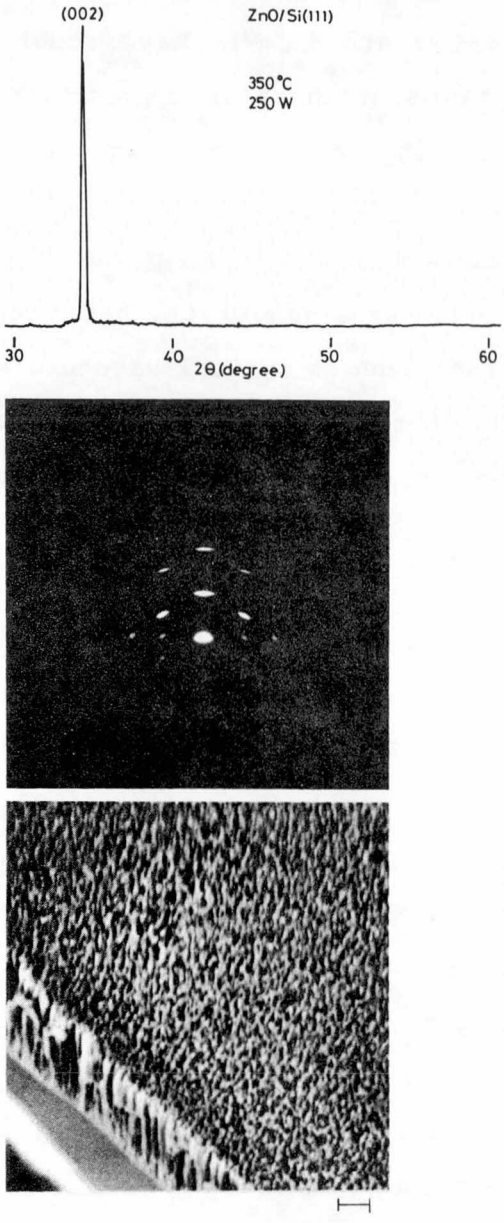

Fig.5.12. A typical x-ray diffraction pattern, RHEED pattern and SEM photograph of a ZnO film on (111) Si. Marker represents 1 μm.

substrate, previously mentioned in section 5-3-1, and c-axis is aligned perpendicular to the substrate surface. It is noted that non-c-axis oriented films had rough surfaces.

The c-axis orientation of the films was also affected by the substrate temperature and rf input power. Figure 5.13 shows the dependence of the c-axis orientation on substrate temperature and rf input power, evaluated by the standard deviation angle. In film growth on Si, higher c-axis oriented films were grown as the substrate temperature and the rf input power increased. Generally, crystalline films prepared by the other methods tend to have good quality when they are grown at higher substrate temperatures. ZnO films obtaiend on Si by PE-MO-CVD showed the similar tendency. The dependence of the c-axis orientation on rf input power level suggests that the quantitative change of the active species with increasing rf input power influences the film quality. The degradation of standard deviation at high rf input power levels is probably caused by the damage of films being due to plasma discharge.

5-3-3. Films Grown on SiO_2/Si

The preparation of ZnO thin films on SiO_2/(100)Si is described in this section. Thermally grown SiO_2 layer on (100)Si used was 1.3 μm thick. The c-axis oriented ZnO films were grown at substrate temperatures higher than 300°C and rf input power levels of more than 200W. A typical x-ray diffraction pattern, RHEED pattern and SEM photograph of film grown at 300°C are shown in Fig.5.14. An x-ray diffraction pattern shows only the sharp

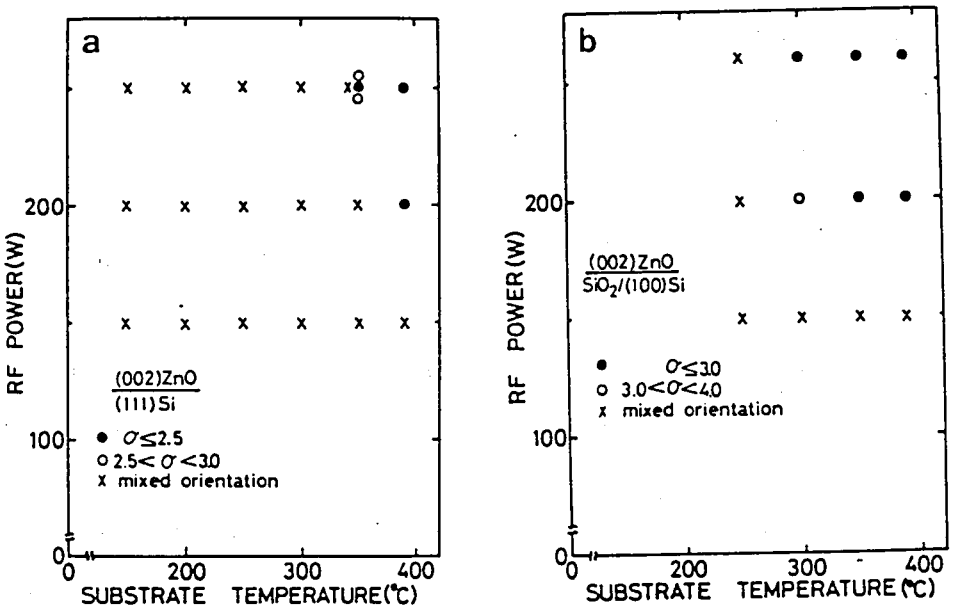

Fig.5.13. Film quality of ZnO film on (a) (111) Si, (b) on SiO_2/(100)Si.

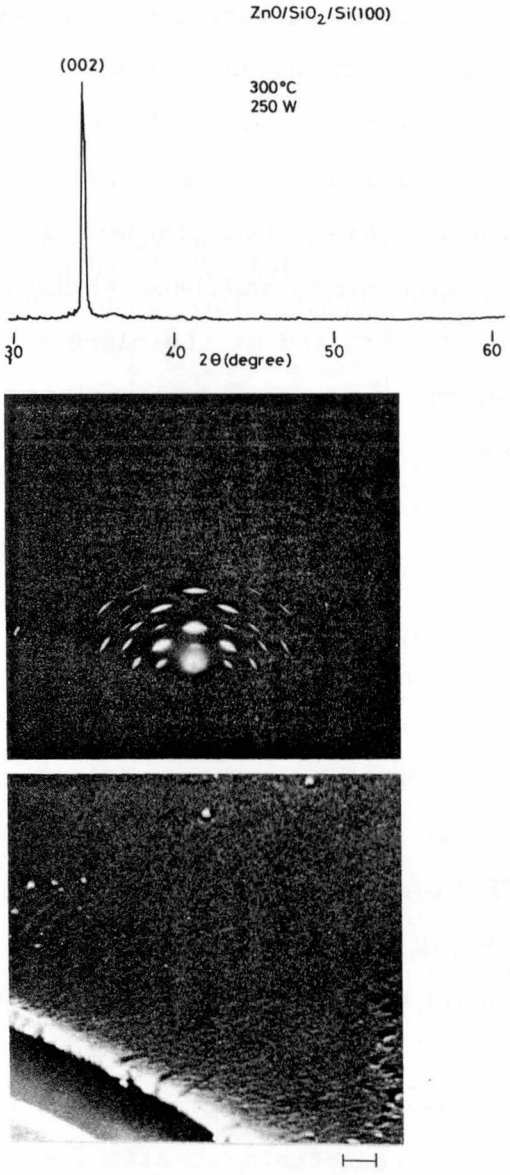

Fig.5.14. A typical x-ray diffraction pattern and SEM photograph of a ZnO film on SiO_2/(100)Si. Marker represents 1μm.

ZnO (002) peak. The RHEED pattern shows no Debye rings but well-defined spread spots which indicate that the film had a so-called fibre structure. The dependence of the c-axis orientation on substrate temperataure and of rf input power was also studied, as shown in Fig.5.13(b). From this standard deviation measurements of the x-ray rocking curve and from RHEED measurements it is found that the films obtained at the higher substrate temperature and at the higher rf input power had the better c-axis orientation. This tendency shows same one of films grown on other substrates.

5-3-4. Films Grown on Ceramics

It has recently been reported that a translucent Al_2O_3 ceramic is one of very promising substrates for the surface acoustic wave devices and can be used as an inexpensive and versatile substitute for the sapphire substrate [56]. The ceramic (Sumimoto Chemical Co., Ltd.) used as a substrate in the present work was 600 μm in thickness and its surface roughness was 500-1000Å. The growth rate was investigated as a function of substrate temperature. As shown in Fig.5.15 , the growth rate is decreased with increasing substrate temperature. The ZnO films grown on this ceramic substrate at different temperatures showed c-axis orientation below the temperature of 350°C, and (002) and (101) planes were observed at 400°C, as shown in Fig.5.16. The minimum standard deviation was 3° at a substrate temperature of 200°C and increased as the temperature increased. Figure 5.17 shows the dependence of the c-axis orientation (σ) on substrate

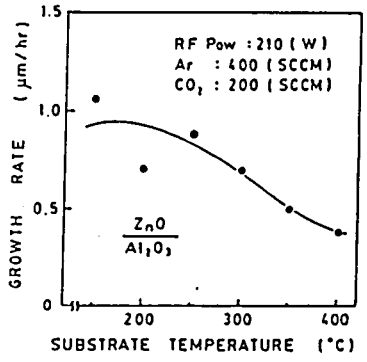

Fig.5.15. Relation between growth rate and substrate temperature.

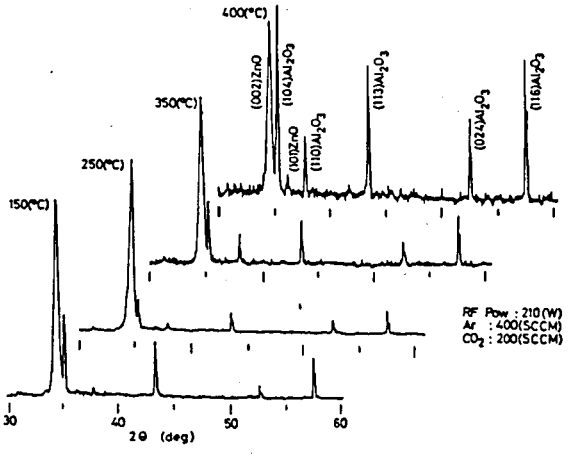

Fig.5.16. X-ray diffraction patterns of ZnO films grown on ceramic substrates at substrate temperatures of 150-400°C.

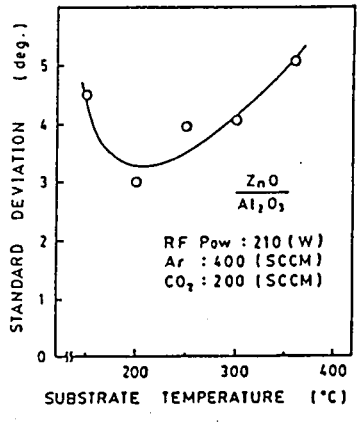

Fig.5.17. Standard deviation angle versus substrate temperature for ZnO films on ceramic substrates.

temperature.

RHEED and SEM photographs of ZnO films grown between 150-400°C are shown in Fig.5.18 and 5.19. The films grown under optimum condition (at a substrate temperature of 200°C) shows well-defined spread spots of RHEED pattern and good surface flatness.

In the growth of materials with hexagonal structure (wurtzite type), e.g. ZnO, AlN and BeO, their c-axes tend to be oriented perpendicular to the substrate surfaces. At substrate temperatures below 350°C the crystal growth mechanism is strongly affected by this tendency as mentioned above and the ZnO film had a c-axis orientation. However, at substrate temperatures above 350°C, overcoming the preferential c-axis orientation ZnO grew optionally on the substrate surface which was formed by many fine aluminum oxide crystals with different oriented planes. In this case different peaks form (00·2) and (10·1) planes of ZnO were observed, as can be seen in Fig.5.16.

5-3-5. Films Grown on Polymide

In the PE-MO-CVD method non-heatproof substrates can be used, because the lower growth temperatures are applicable in this method. Utilizing this advantage polyimide film can be used as a substrate material. Recently polyimides films have been adopted as flexible substrates for electronic circuits and solar cells. The polyimide film (Ube Industries Ltd.) used in the present work was 100 μm in thickness. The decomposition temperature of polyimide used is 478°C in air and 510°C in N_2 atmos-

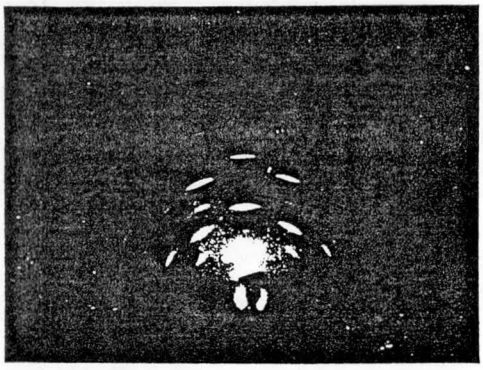

150 ℃

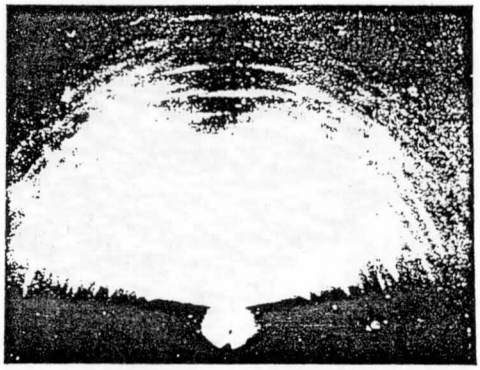

200 ℃

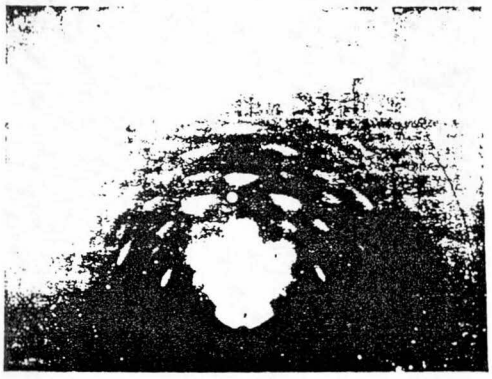

250 ℃

300 ℃

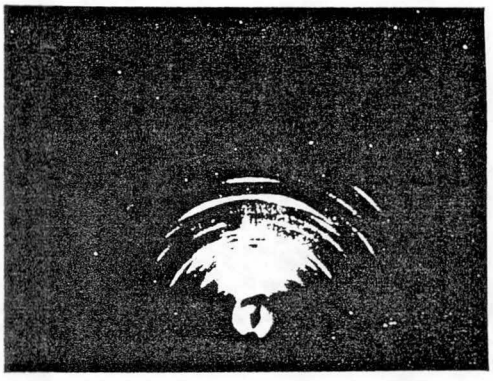

350 ℃

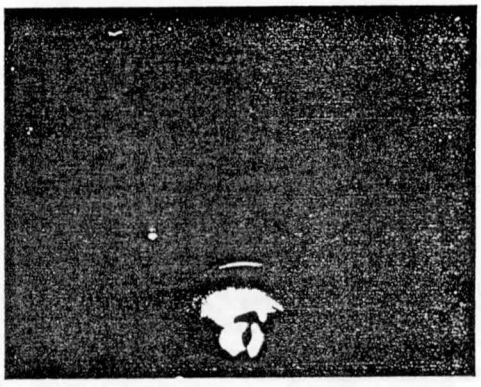

400 ℃

Fig.5.18. RHEED patterns of ZnO films on ceramic substrates.

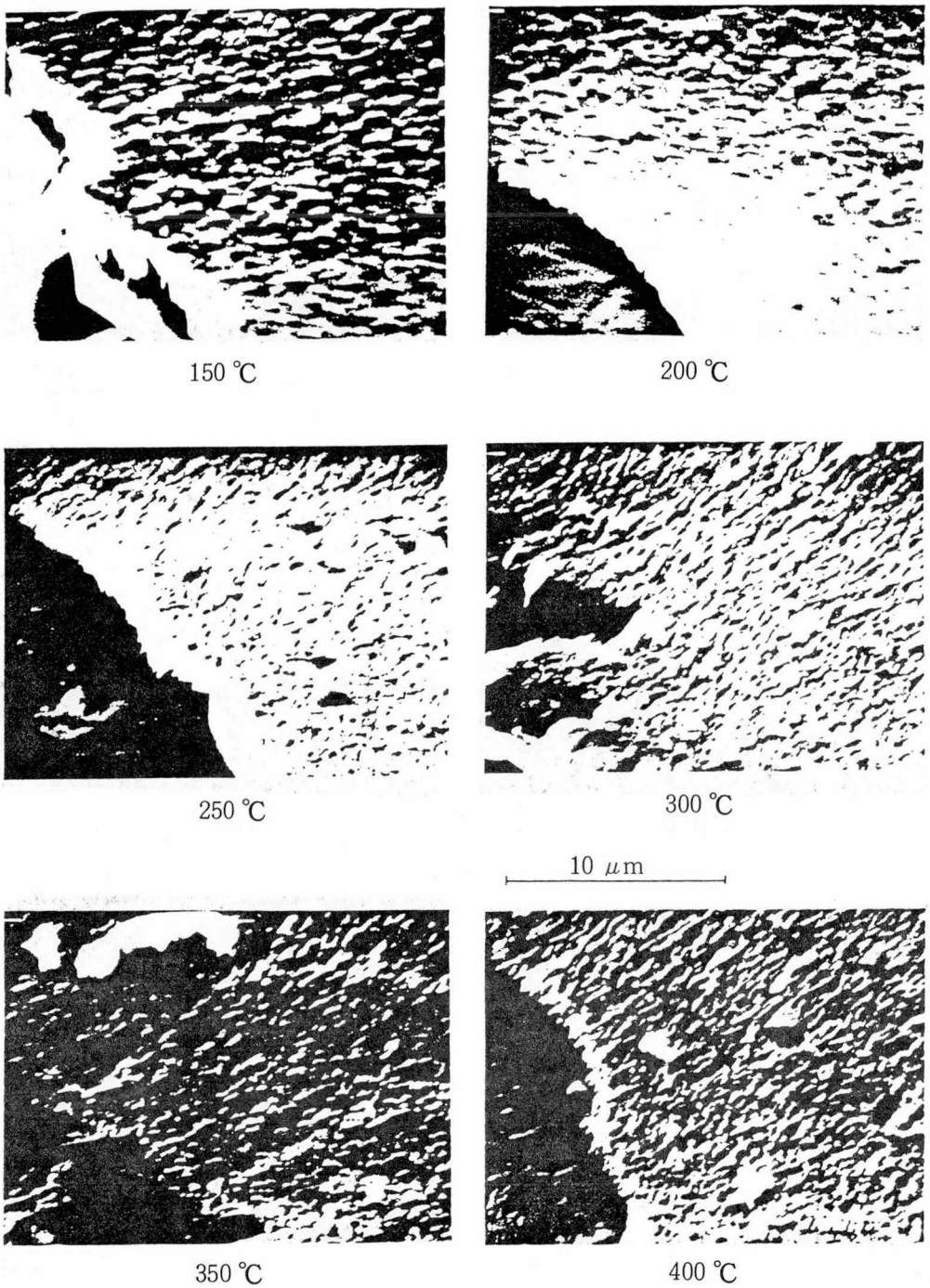

Fig.5.19. SEM photographs of ZnO film on ceramic substrates.

phere, and its resistivity is 10^{16}-10^{17} Ωcm.

Highly c-axis oriented ZnO films were prepared at the substrate temperatures above 350°C, as shown in Fig.5.20. The surface morphology of the film resembled that prepared on other substrates. The dependence of c-axis orientation on the substrate temperatue and rf input power is shown in Fig.5.20 exhibiting the same tendency as that of films grown on other substrates. The c-axis orientation of the film becomes higher with increases of both substrate temperature and rf input power.

It is noted here that films of about 1 μm thickness did not peel from polyimide substrates, and adhesion to this flexible substrate was relatively strong, as will be mentioned in Appendix.

5-3-6. Epitaxial Films

It has been also found that the epitaxial growth of $(11\bar{2}0)$ ZnO films on $(01\bar{1}2)$ sapphire substrates and of (0001) ZnO films on (0001) sapphire substrates is also achieved at low substrate temperatures. The growth condition employed in the present work was that the flow rate of Ar was 500sccm and of CO_2 was 300sccm. The vapor pressure of DEZ was kept 15Torr during the growth runs.

The $(11\bar{2}0)$ ZnO films were grown on $(01\bar{1}2)$ sapphire substrates at a substrate temperature of 200°C as shown in Fig. 5.21. ZnO films grown at a substrate temperature lower than 200°C and/or at lower rf input power show the (0002), $(10\bar{1}1)$ and $(11\bar{2}0)$ peaks as illustrated in Fig.5.21 , indicating that these films were not grown epitaxially. Figure 5.22 shows RHEED pat-

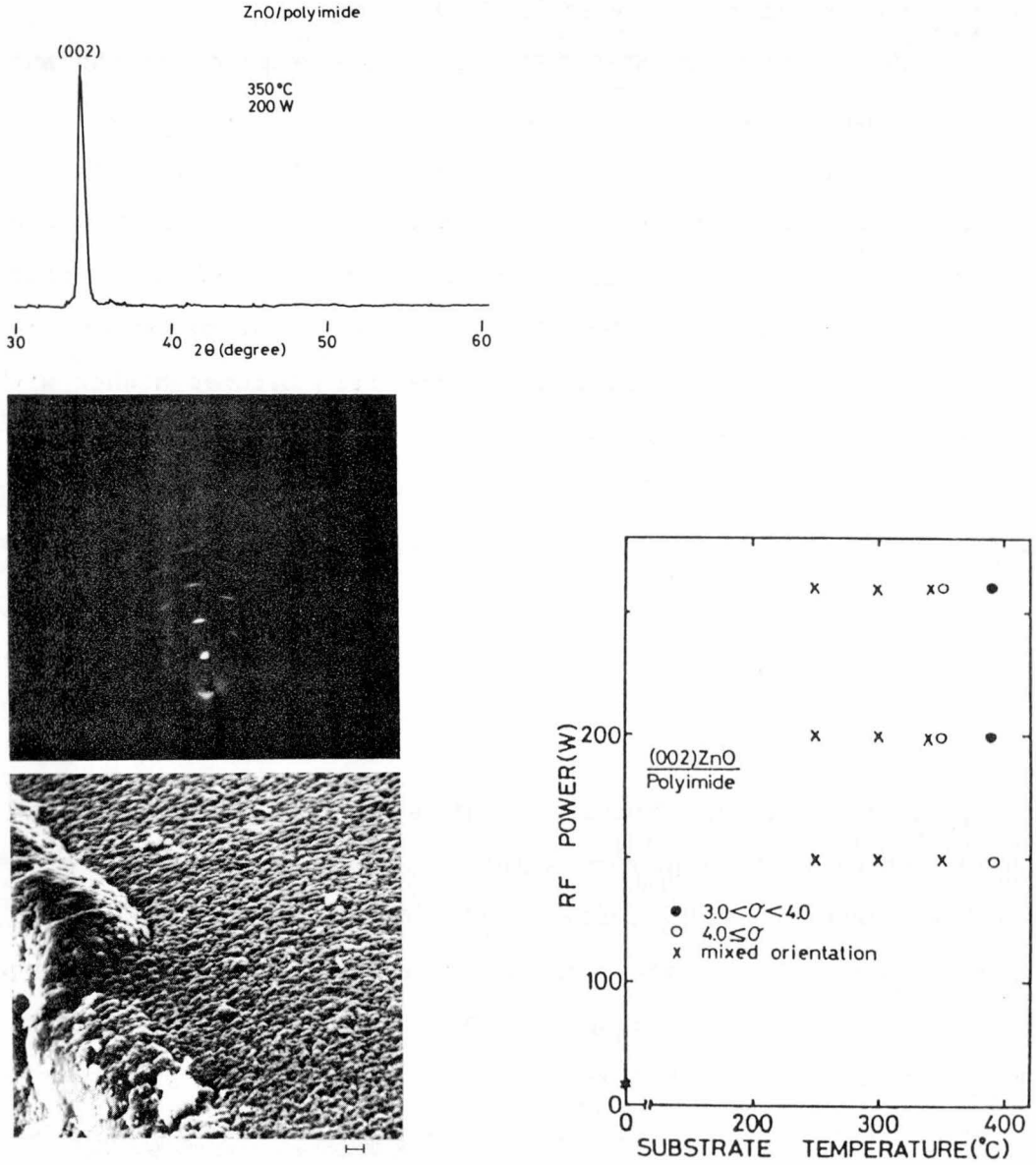

Fig.5.20. A typical x-ray diffraction pattern, RHEED pattern and SEM photograph of a ZnO film on polyimide. Marker represents 1 μm.

Film quality chart of ZnO film on polyimide.

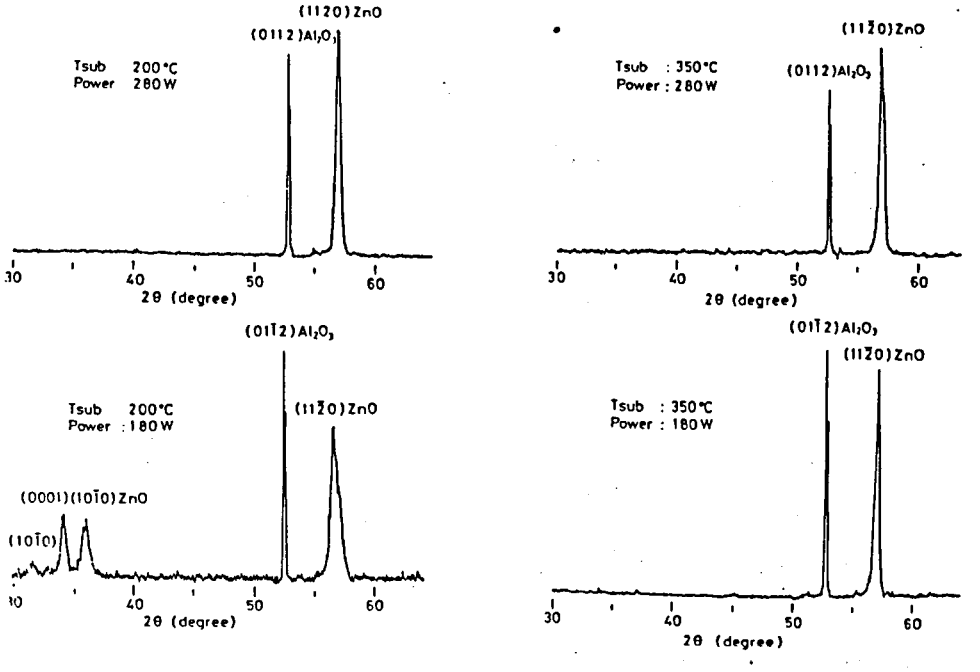

Fig.5.21. X-ray diffraction patterns of ZnO thin films on (01$\bar{1}$2) sapphire substrates.

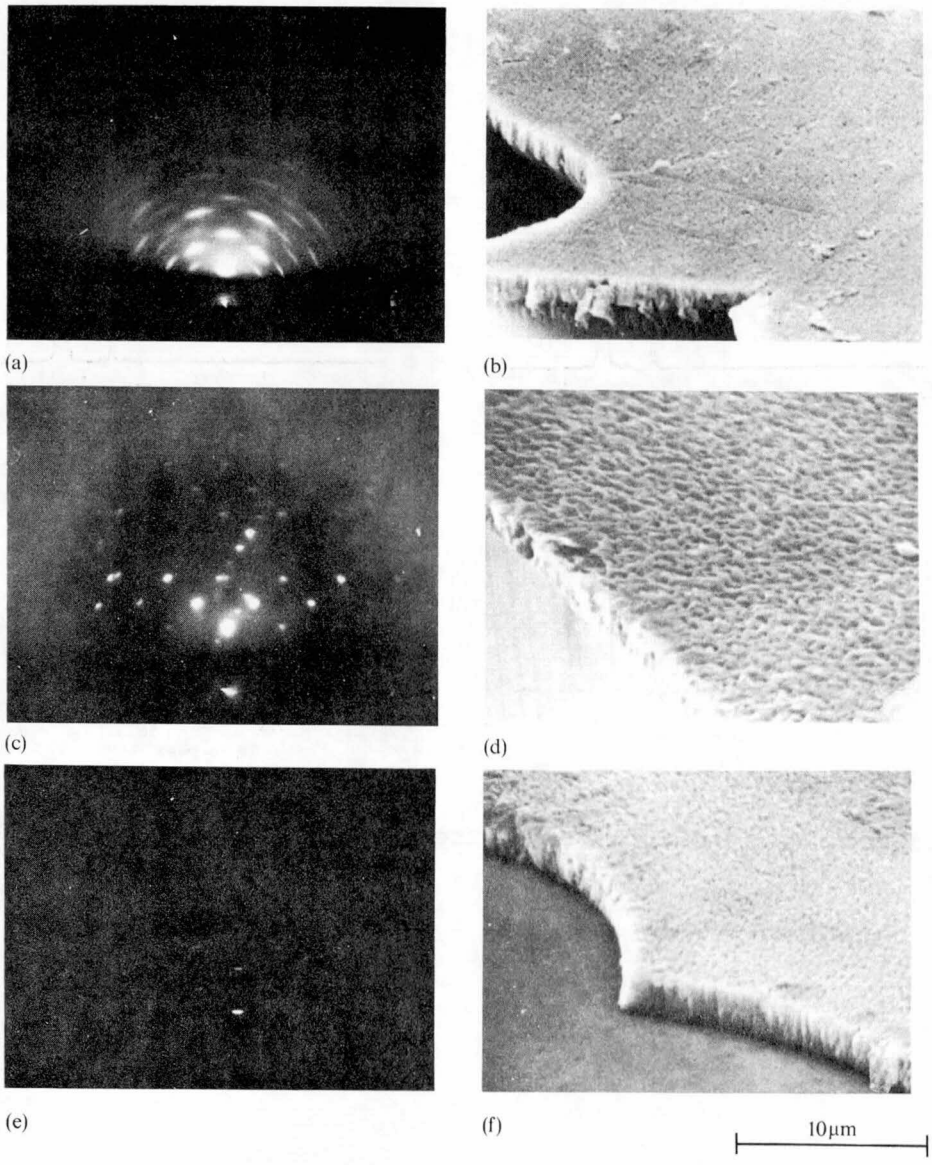

Fig.5.22. RHEED and SEM photographs for ZnO films: (a), (b) prepared on glass at 200°C and 220W; (c), (d) prepared on sapphire $(01\bar{1}2)$ at 200°C and 280W; (e), (f) prepared on sapphire (0001) at 150°C and 280W.

terns and SEM photographs for ZnO films grown at different substrate temperatures and at same rf input power. Film quality is also affected by rf input power as shown in Fig.5.21. From these figures we can see that films grown under optimum conditions have better crystalline properties and smooth surfaces. The RHEED pattern of films grown under optimum conditions consists of well-defined spots; when the direction of the incident electron beam was changed, two kinds of RHEED pattern appeared alternately and periodically, indicating that the grown films were almost single crystals. Film properties were evaluated by standard deviation measurements and a film quality chart of $(11\bar{2}0)$ZnO film on $(01\bar{1}2)$ sapphire substrate is illustrated in Fig.5.23. These x-ray rocking curve measurements and RHEED measurements shows that the films obtained at the higher substrate temperature and at the higher rf input power had the better quality. However, when the films were grown at too high rf input power, the degradation of the standard deviation angle of films was observed as shown in Fig.5.24 , illustrating the dependence of standard deviation on the substrate temperature (Fig.5.24(a)) and on the rf input power (Fig.5.24(b)). The degradation of the standard deviation with increasing rf input power is probably caused by the damage of films being to plasma discharge. The improvement of the standard deviation with increasing rf input power below a certain power level is presumably caused by the change in the generation rate of active species. The effects of substrate temeprature on the film properties are caused by adsorption, evaporation and surface migration of atoms

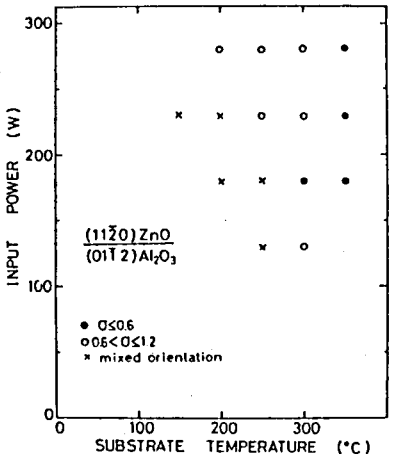

Fig.5.23. Film quality chart of ZnO films on (01$\bar{1}$2) sapphire substrate.

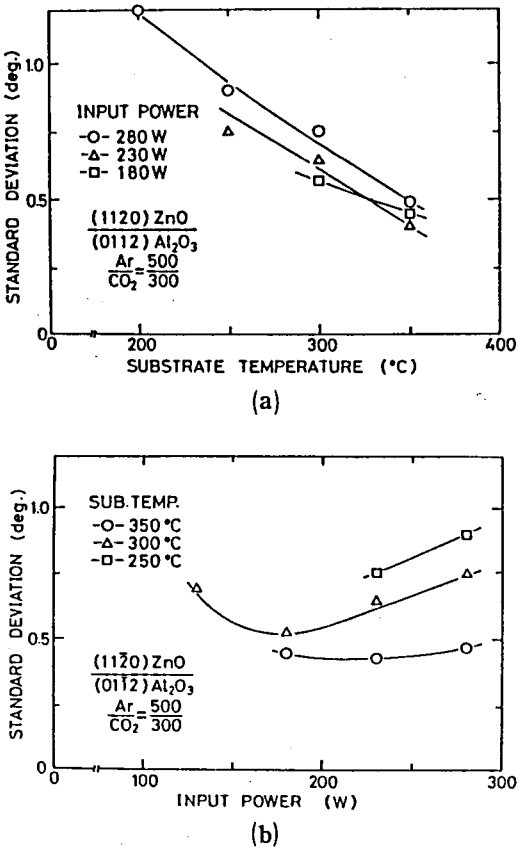

Fig.5.24. The dependence of standard deviation on (a) substrate temperature, (b) rf input power.

etc..

The (0001)ZnO films were grown on (0001) sapphire substrates at substrate temperatures higher than 150°C. The typical x-ray diffraction pattern, RHEED pattern and SEM photograph are shown in Fig. 5.22 and 5.25. The RHEED patterns of films grown at different substsrate temperatures and rf input powers show slightly spread and arced spots, which indicates that the films was not completely single crystal. X-ray rocking curve measurements shows in Fig. 5.26 and 5.27. The tendency of the dependence of standard deviation on the substrate temperatue, as shown in Fig.5.27(a), is different from one of the case of (11 $\bar{2}$0) ZnO films. The degree of standard deviation does not change at substrate temperature higher than 200°C. This difference of tendency is presumably caused by the difference of adsorption coefficient and surface migration energy. From Fig.5.27(b) we can see the degradation of standard deviation with increasing rf input power. However, standard deviation of films grown at 350°C does not increase. In these films, the effect of film properties on substrate temperature probably overcomes the effect on rf imput power.

5-4. Influence of Growth Conditions on Electrical Properties

Preparation of ZnO films on different substrate is described in previous section. In this section the relations between electrical properties and growth conditions are described. The electrical properties of films grown on Corning 7059 glass substrate by PE-MO-CVD were measured at room temperature by a van

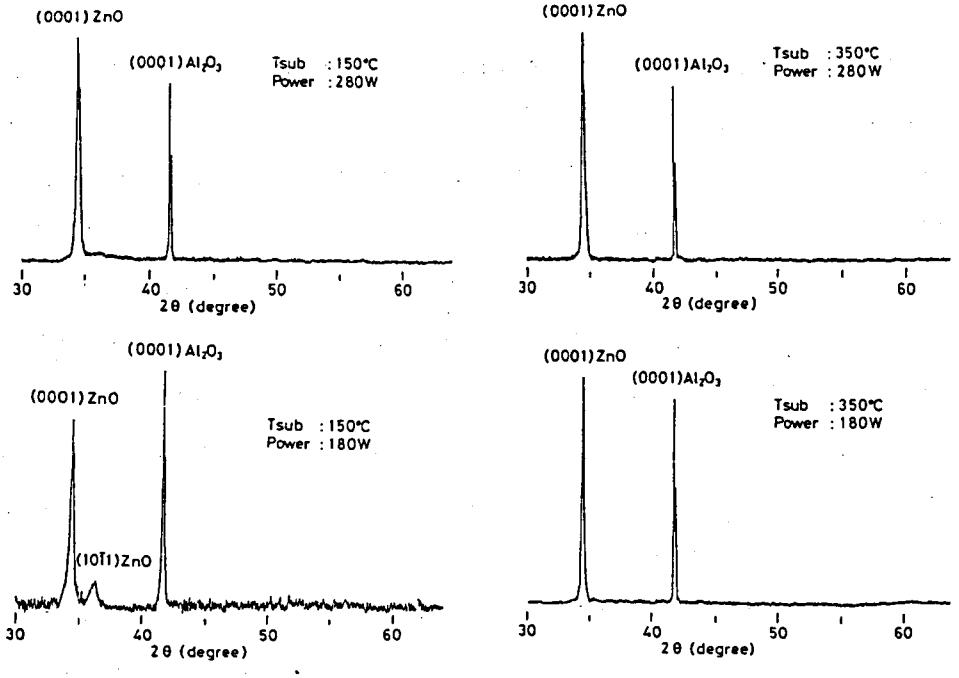

Fig.5.25. X-ray diffraction patterns of ZnO films on (0001) sapphire substrate.

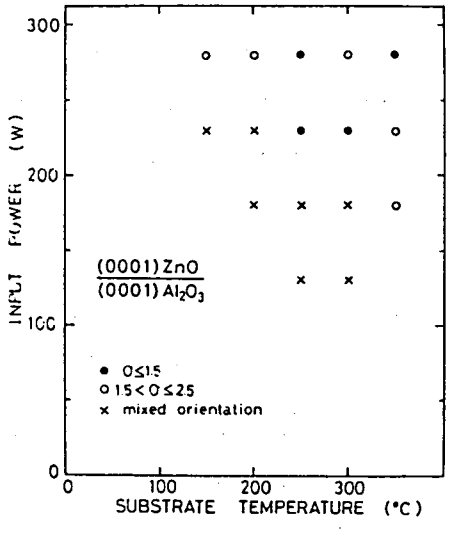

Fig.5.26. Film quality chart of ZnO films on (0001) sapphire substrate.

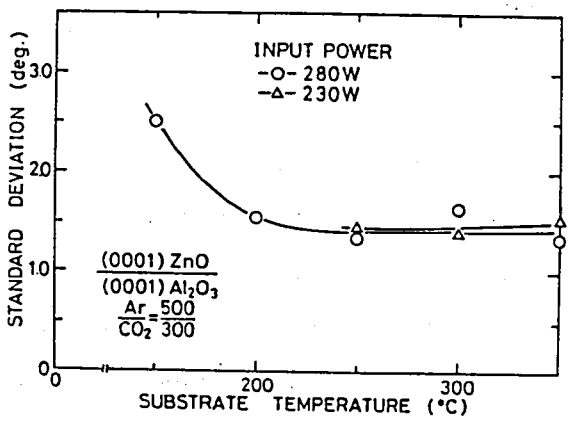

(a)

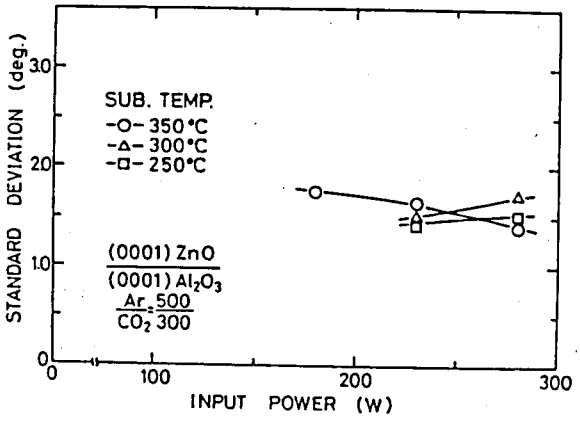

(b)

Fig.5.27. The dependence of standard deviation on (a) substrate temperature, (b) rf input power.

der Pauw method. Ohmic contacts were made by evaporating indium. These films showed n-type conductivity, and typical values at room temperature of resistivities , electron Hall mobilities and carrier concentration are $\rho = 10^{-3}$-10 Ωcm, $\mu = 0.5$-60$cm^2/v{\cdot}sec$ and $n = 10^{18}$-$10^{19} cm^{-3}$, respectively. ZnO films were grown on glass substrate at different substrate temperatures to investigate the influence of substrate temperature on electrical properties. The growth condition is that Ar flow rate is 400sccm through bubbler containing DEZ and CO_2 flow rate is 200sccm. The bubbler is kept at 20°C.

The structural nature of films measured above was studied by the x-ray diffraction method, which is shown in Fig. 5.28. As mentioned in Sec.5-3-1, whereas the ZnO films grown at lower substrate temperature exhibit the peaks from (00·2) and (10·1) plane etc., films grown at higher than 250°C exhibit a strong orientation of the c-axis (00·2) perpendicular to the substrate. X-ray peak intensity also increases as the substrate temperature increases. The standard deviation angle changes with increasing substrate temperature as shown in Fig.5.29.

Figure 5.30 shows the dependence of resistivity, mobility and carrier concentration of these films on substrate temperature. Resistivity decreases sharply with increasing substrate temperature, whereas carrier concentration increases up to about 260°C and a further increase of substrate temperature results in a decrease. From electrical and x-ray measurements, it is known that the dependence of mobility on substsrate temperature is similar to that of standard deviation. This fact means that the

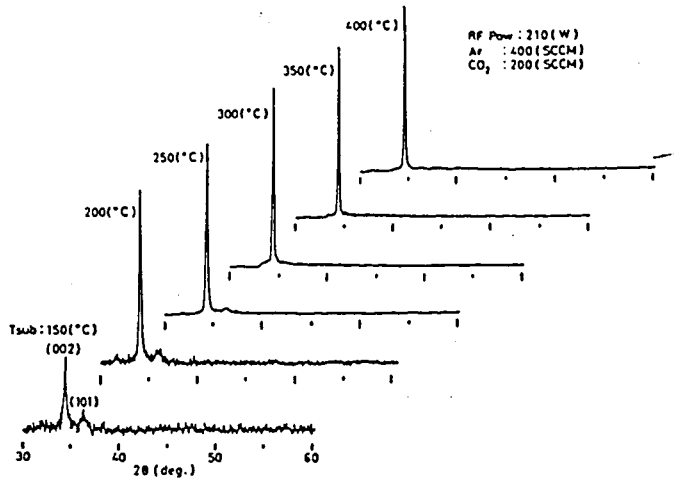

Fig.5.28. X-ray diffraction patterns of ZnO films on glass at 150 -400°C.

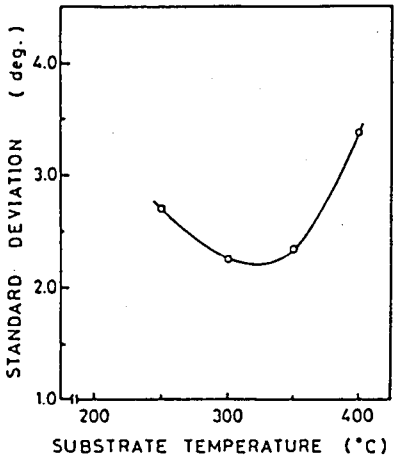

Fig.5.29. The dependence of standard deviation on substrate temperature.

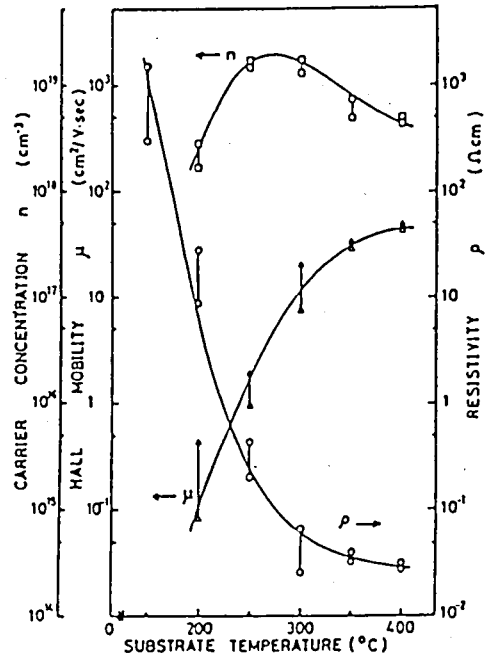

Fig.5.30. The dependence of electrical properties of ZnO films on substrate temperature.

increase in mobility can be attribute to an improvement of crystallinity. The change of carrier concentration is related to the stoichiometry or diffusion of impurities, for example alkali ions, from substrate.

The dependence of electrical properties on rf input power level was also investigated. The orientation of films grown at different rf input power is shown in Fig.5.31. Films obtained at low rf input power shows diffraction peaks from (100), (002) and (101) plane and films grown at higher than 150W show c-axis orientation. The standard deviation measurement, in Fig.5.32., shows that the degree of c-axis orientation decreases up to 210W and at higher than 210W increases with increasing rf power. This degrade of standard deviation angle is presumably due to the damage from plasma discharge. The change of electrical properties with rf input power shows in Fig.5.33. Resistivity decreases with increasing rf input power. Hall mobility of films grown at 300°C increases up to 200W and is saturated. However, that of films grown at 250°C increases rapidly over 200W. The saturation of mobility of films obtained at 300°C is related to degrade of standard deviation. The rapid increase of mobility of films obtained at 250°C is due to the disappearance of (101) peak over 210W. Carrier concentration increases gradualy and decreases when films grew at 250°C. This decrease of carrier concentration is due to the change of stoichiometric or impurities from electrode and substrate by damage of plasma dishcarge.

The electrical properties are also dependent on the mole ratio of CO_2 to DEZ. The conversion of conducstivity type was

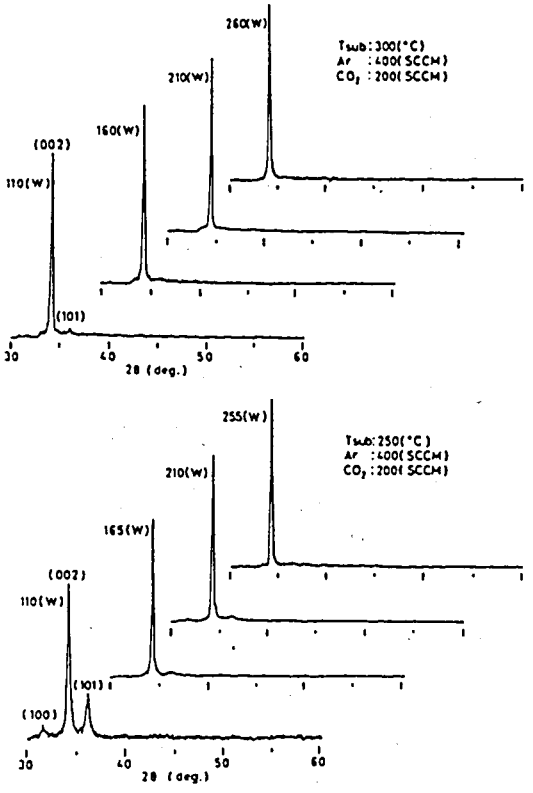

Fig.5.31. X-ray diffraction patterns of ZnO films at different substrate temperatures and rf input power levels.

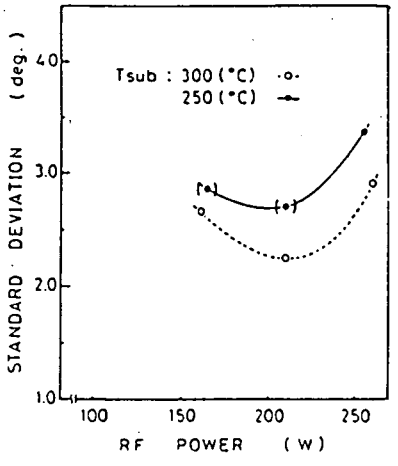

Fig.5.32. Standard deviation angle versus rf input power.

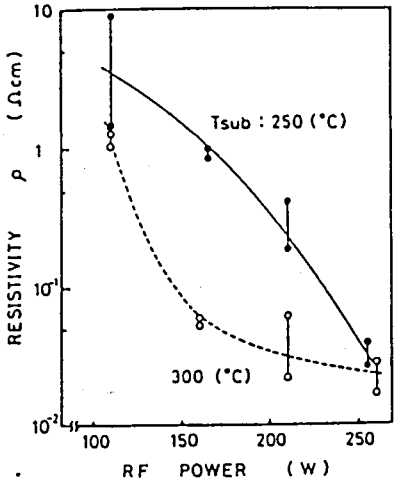

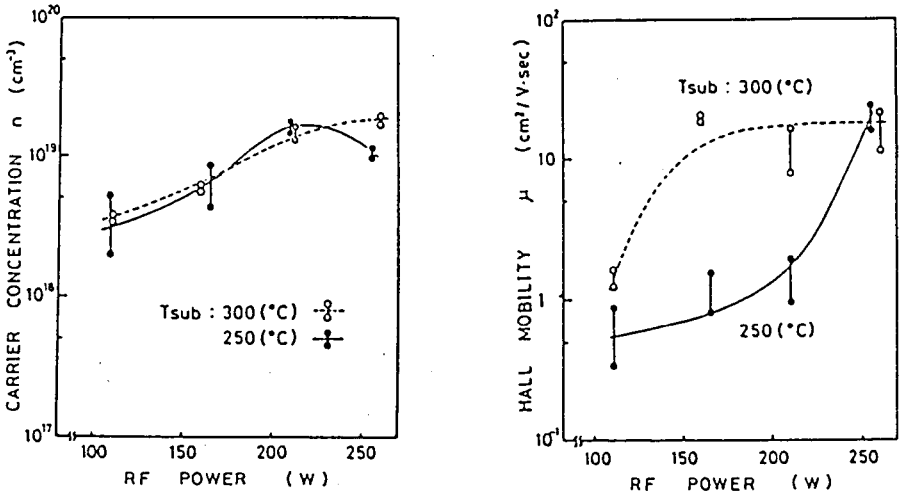

Fig.5.33. The change of electrical properties with rf input power.

not seen in the mole ratio range between 6 to 200. The dependence of electrical cahracteristics on the mole ratio of CO_2 to DEZ is shown in Fig.5.34. Hall mobility increases with increasing the mole ratio and reaches a maximum around 30-50 of mole ratio. This change of mobility means the change of crystallinity of film. Carrier concentration also reaches a maximum around 100 of mole ratio and decreases at larger mole ratio. At larger mole ratio above 100 the film components have better stoichiometry. Therefore, the variation of the film resistivity with mole ratio of CO_2 to DEZ is caused by the competition between crystalinity and degree of stoichiometry of the films.

The electrical properties of epitaxial films on sapphire substrate were also measured. The crystalinity is strongly dependent on substrate temperature, as described in section 5-3-6. Figure 5.35 shows the dependence of standard deviation angle of x-ray rocking curve on substrate temperature. The standard deviation angle, which shows the degree of c-axis orientation, decreases as the substrate temperature increases. This standard deviation measurements mean that films grown at higher substrate tempearture have better crystalline quality. The dependence of resistivity on substrate temperature is shown in Fig.5.36. Resistivity decreases with increasing substrate temperature and the dependence of resistivity on substrate temperature corresponds ot that of standarad deviation angle on substrte temperature. This tendency is also observed in the electrical characteristics of c-axis oriented films on glass substrate as mentioned above.

The influence of electrical properties of films grown on

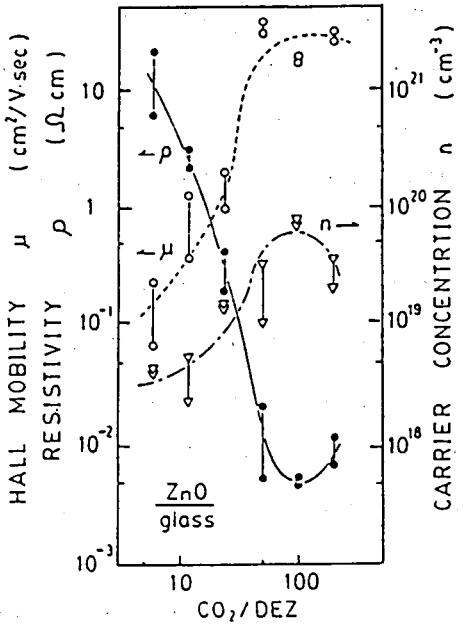

Fig.5.34. The dependence of electrical properties on the ratio of CO_2 to DEZ.

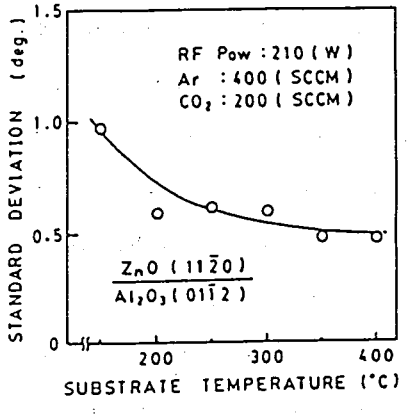

Fig.5.35. The dependence of standard deviation angle on substrate temperature.

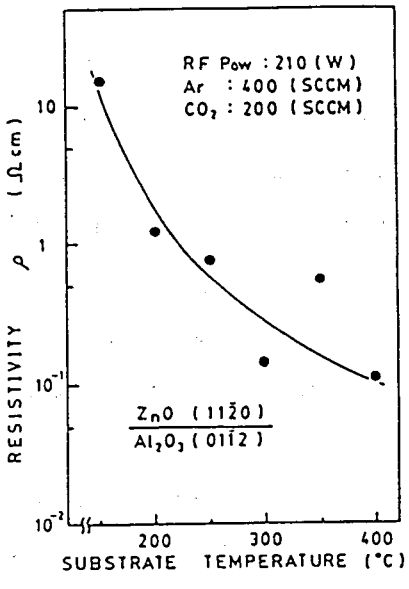

Fig.5.36. The dependence of resistivity on substrate temperature.

ceramic substrate on substrate temperature was also investigated. The film quality is strongly affected by substrate temperature as described in Section 5-3-4. The standard deviation decreases up to 200°C and increases as the substrate temperature increases as shown in Fig.5.37. The electrical characteristics of films by Hall measurement is shown in Fig.5.38. Mobility of films shows a maximum value at a substrate temperature of 200°C and the dependence of mobility on substrate temperature corresponds to that of standard deviation, which indicate the change of film quality. Carrier concentration decreases with increasing substrate temperature, possibly because of the better stoichiometry of films or diffusion of alkali ions from the substrate or both.

The surface component of ZnO films by PE-MO-CVD was analyzed by a Auger electron spectroscopy. Auger analysis of film grown on glass substrate, as shown in Fig.5.39., shows zinc and oxygen peaks and shows no evidence of the presence of carbon from source alkyl-metal compound (DEZ) and other major impurities in the films.

5-5. Optical Properties

The optical transmission spectrum was measured in the wavelength range from 300 to 800nm by a double beam photospectrometer (SHIMADZU, MPS-50L). The typical transmission spectra of film grown on glass substrate is shown in Fig.5.40. This sample was 800nm in thickness. Figure 5.40 shows film has the sharp absorption edge at 380nm and average transmittance of over 80% in the visible region.

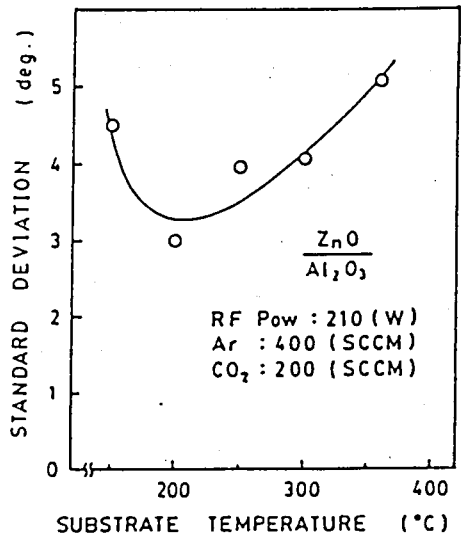

Fig.5.37. The dependence of standerd deviation angle on substrate temperature.

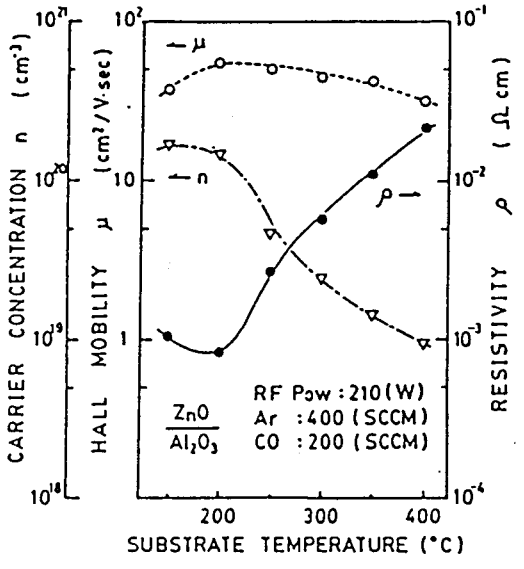

Fig.5.38. The dependence of electrical properties on substrate temperature.

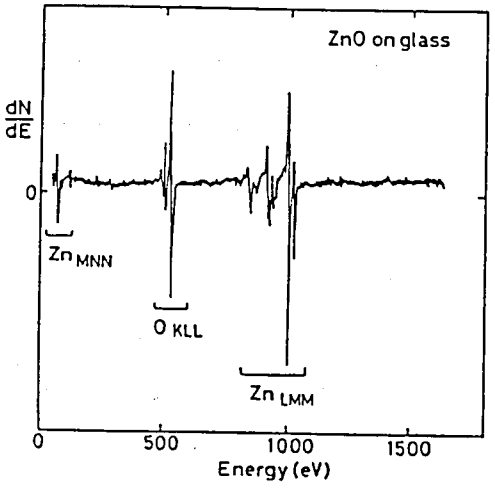

Fig.5.39. Auger spectrum of a ZnO film by PE-MO-CVD.

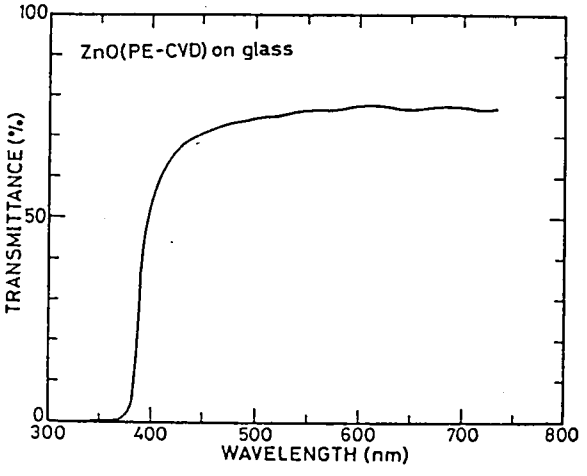

Fig.5.40. Optical transmission spectrum of a ZnO film.

Photoluminescence characteristic of films on sapphire substrate was also measured. The samples were excited with the 3650Å line of a high pressure mercury lamp. Fig.5.41 shows PL spectrums of ZnO films prepared by PE-MO-CVD, CVD and sputtering. In films grown by PE-MO-CVD, broad photoluminescence spectrum with the peak about 6400Å is observed, though CVD films exhibit green photoluminescence. The photoluminescence intensity of plasma-deposited film and sputtered film is smaller than that of CVD film. The dependence of photoluminescence spectrum on temperature, as shown in Fig.5.42 , shows no significant change of spectrum at low temperature. The temperature dependence of emission intensity was also measured. From Fig.5.43., it is seen that the peak intensity decreases slowly with increases in temperature up to 180^{o}C and a further increase results in a sharp decrease in emission intensity. The slope at high temperature region in Fig.5.43 corresponds to an activation energy of thermal quenching of 0.12eV.

5-6. Application Devices

5-6-1. Fabrication of Transducers

ZnO films prepared by PE-MO-CVD exhibit low resistivity as mentioned above and this property is not good for piezoelectric applications. The resistivity of greater than $10^{6}\Omega$cm is necessary for these applications. It is well known that lithium is used as p-type dopant for ZnO. Therefore an application to transducer was demonstrated by using lithium doped high resistivity ZnO.

At first stage, titanium electrode was deposited on fused

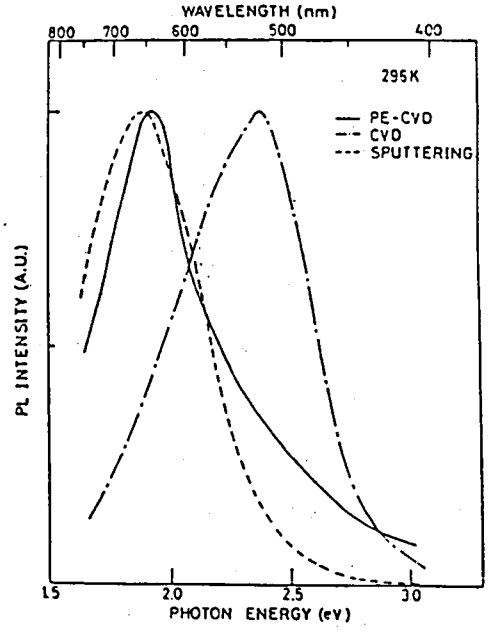

Fig.5.41. Photoluminescence spectrum of ZnO thin films by PE-MO-CVD, CVD and sputtering.

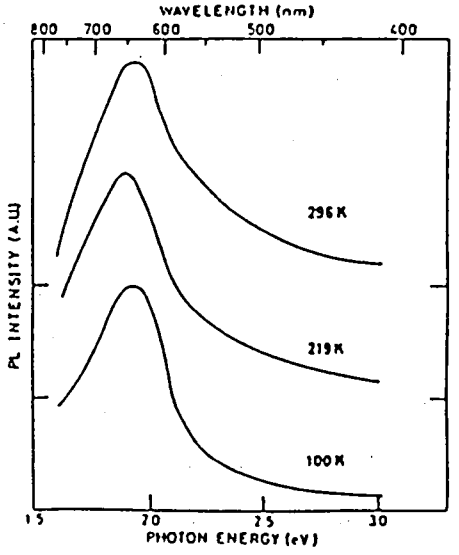

Fig.5.42. Temperature dependence of PL spectrum.

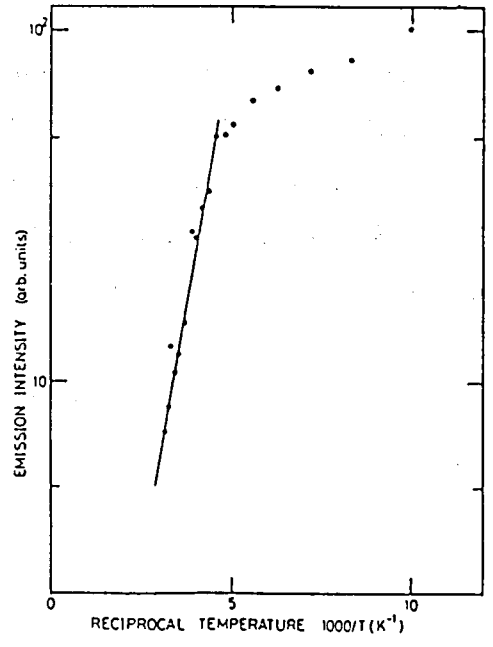

Fig.5.43. Temperature dependence of PL peak intensity.

quartz rod by the electron beam evaporation method because of its good adhesion to fused quartz. Au electrode as ohmic contact was deposited on titanium by the ordianry evaporation technique. In this structure the adhesion between Au and Ti was strong. After evaporating electrode, ZnO film was deposited at a substrate temperature of 300°C for 23 hours. And then lithium which acts as acceptor was diffused to increase resistivity by coating the films with LiOH alcoholic solution and heating them in air at 500°C for 10 hours. At last stage, the Au upper electrode was evaporated on ZnO film after diffusing treatment. The piezoelectrical characteristics of plasma-deposited film were measured by the pulse-echo method as shown in Fig.5.44. By using this method the attenuation and velocity of ultrasonic waves in solid can be measured. In this pulse-echo method, if we assume 1) the parallel plane wave propagates into sample in the range of echo used. 2) the reflection is perfect at both ends of the sample. 3) both ends of the sample have flat parallel faces, from the decay of pulse echo measured, absorption coefficient and sound velocity u of fused quartz is calculated. If the change of the peak value of pulse echo is given by following expressions

$$a = a_o e^{\beta t}$$

where a_o is pulse height of first reflected waves and β is absorption coefficient per unit time, absorption coefficient α is given by

$$\alpha = \beta / u$$

Then sound velocity is written by

$$u = 2l/T$$

where l is thickness of substrate and T is period of echo. Figure 5.45 shows the multiple reflections echo pattern which is observed at a repetition frequency of 35MHz.

The multiple reflection echos at 35MHz have high order values of 107MHz, 175MHz and 245MHz. For this reason the fundamental pulse frequency of this transducer is 35MHz. The velocity of transverse wave in fused quartz u of 5880 m/sec and absorption coefficiency of 3.76×10^{-2}dB/cm are determined from equations mentioned above. These values are similar to those reported in ref.57.

5-6-2. Fabrication of Heterojunction Solar Cells

Several transparent conductive oxide semiconductors, such as ITO and SnO_2 have been used to form heterojunction solar cells. ZnO has a band gap (Eg=3.3eV) large enough to be transparent to most of the useful solar spectrum as mentioned in section 5-5. In PE-MO-CVD, it can be prepared with a high transparency and a sufficiently low resistivity to prevent series resistivity losses in a heterojunction with ZnO as window layer.

CdTe is a promising material for high efficiency solar cells because it is a direct band gap semiconductor with nearly optimum band gap (Eg=1.44eV), and it has a high absorption coefficient over a major portion of the solar spectrum. For these reasons, using plasma deposited film we fabricated n-ZnO/p-CdTe heterojunction solar cells. An ideal ZnO/CdTe heterojunction band diagaram constructed following Anderson's model, for CdTe doping of $10^{17}cm^{-3}$, the depletion layer width is about 0.1 μm.

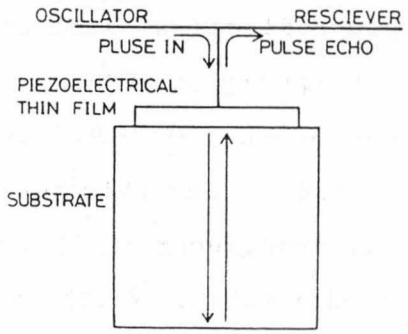

Fig. 5.44. Pulse-echo method.

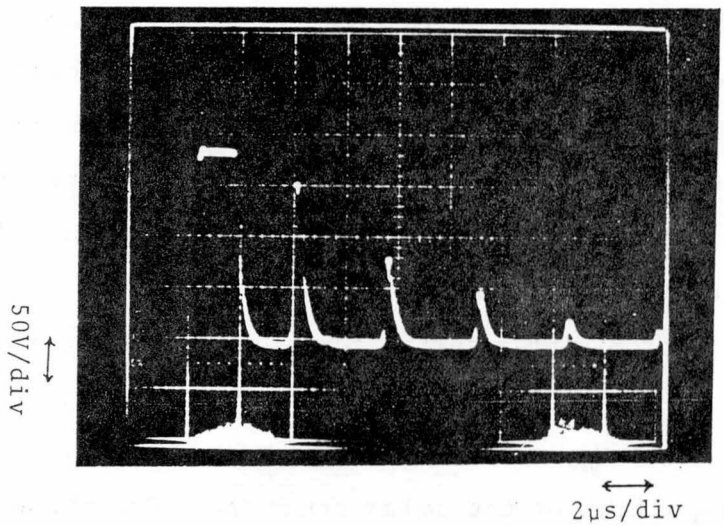

Fig.5.45. The multiple reflection echo pattern.

The p-type CdTe single crystal used in this study was grown by the Bridgeman method from a phosphrous doped source melt. A ingot of CdTe single crystal was cut into (110) wafers with about 1.5mm thickness, and then they were lapped and polished to mirror smooth. Finally polished (110) surfaces of samples were etched chemically for about seven minutes in Br methanol solution (1%). The growth condition of ZnO is shown in the Table of 5-3.

In order to reduce the density of interface states and resistivity, the postdeposition annealing was carried out at 450°C for five minutes in hydrogen. Indium was evaporated on the ZnO as an ohmic contact. An ohmic contact of CdTe was made by electrodeless plating with use of HAuCl [58].

The electrical characteristics of n-ZnO films and the p-CdTe substsrates were measured. The typical dark and illuminated J-V characteristics of the best cell is shown in Fig.5.46. The illumination is 100mW/cm^2(AM1) simulated light. The best cell showed an open-circuit voltage Voc of 514mV, a short-circuit current-density Jsc of 21.3mA/cm^2, a fill factor F.F. of 0.4 and a conversion efficiency of 4.4%. A series of cells was prepared under same conditions, with the results summerized in Table 5-4. In our n-ZnO/p-CdTe heterostructure solar cell, considerable improvement in conversion efficiency is expected by reducing the effect of the interface state, which can be achieved by determining optimum conditions of deposition of ZnO and of postdeposition annealing, and by decreasing electrode resistance.

5-7. Crystal Growth Using Reaction between Diethylzinc and N_2O

Table 5-3. The growth condition of ZnO by PE-MO-CVD.

Gas Flow	Ar	500 ml/min.
	CO_2	300 ml/min.
DEZ Bub. Temp.		15.5 °C
Sub. Temp.		250 °C
Input Power		230 W
Gas Pressure		1.5 Torr
Time		30 min.

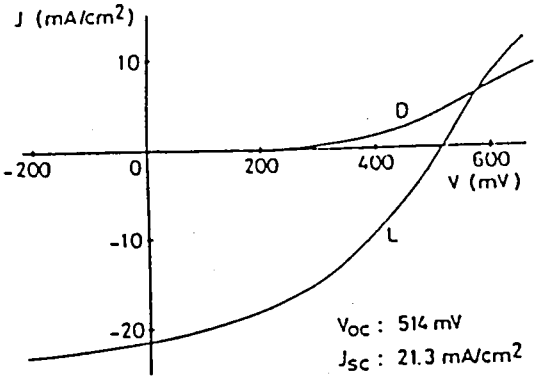

Fig.5.46. The dark and illuminated I-V characteristic of the best cell.

Table 5-4. Results on solar cells.

NO.	Anneal Temp. [°C]	Voc [mV]	Jsc [mA/cm²]	η [%]
S-1	450	337	13.2	1.4
S-2	450	514	21.3	4.4
S-3	450	390	14.3	2.3

5-7-1. Experimental Procedure

N_2O was also used as an oxidizing gas in the present work. The apparatus used, which is nearly same one mentioned above section, is shown in Fig.5.47. N_2O are fairly safe gases, however, in the use of N_2O there is a possibility of producing NO_x, which is one of the most dangerous gases in plasma discharge. Therefore, the exhaust was released to air through a scrubber, as shwon in Fig.5.47. The growth condition employed in the present case was that 500sccm of Ar flow through the DEZ bubbler and 100sccm of N_2O flow directly into the reaction chamber. A stainless steel bubbler containing DEZ was maintained at 20^oC.

In the present study, corning 7059 glass and $(01\bar{1}2)$ and (0001) plane sapphire were used as substrates. The structural nature of the deposited films also was examined by x-ray diffraction, reflection high energy electron diffraction (RHEED) an scanning electron microscopy (SEM).

5-7-2. Films Grown on Glass

In Fig.5.48, is shown the growth rate of the ZnO film grown on a glass substrate in using N_2O as a function of the inverse substrate temperature over the range from 150^oC to 400^oC. The film deposition rate in this case obeys the Arrhenius' equation. The activation energy of the reaction estimated by the data given in Fig.5.48 is 3.4KJ/mol smaller than that when CO_2 is used, 7.6KJ/mol. The value obtained by our work is much smaller than that in MO-CVD, 27K/mol, reported in ref.33. This fact supports

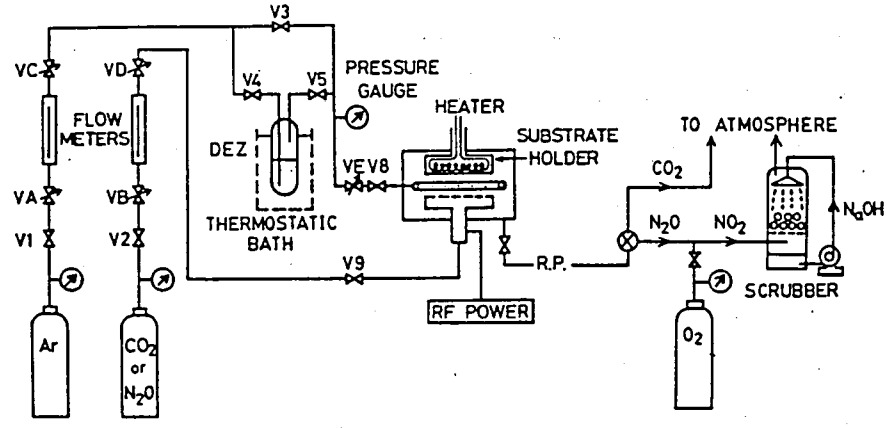

Fig.5.47. Shematic diagram of the PE-MO-CVD system.

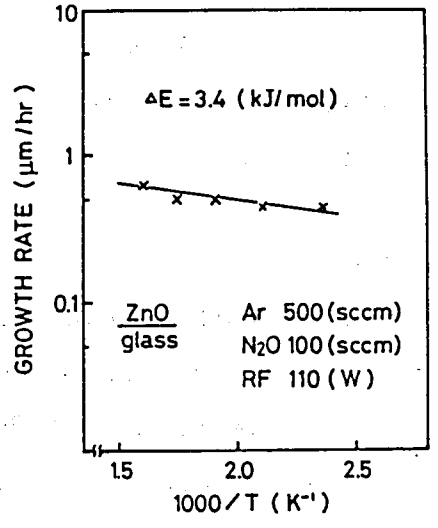

Fig.5.48. Variation of the growth rate of ZnO films as a function of inverse substrate temperature.

that the thermal energy from a substrate required in the reaction in PE-MO-CVD is less than that in MO-CVD and that the use of PE-MO-CVD technique allows the crystal growth at lower substrate temperatures.

Utilizing the reaction between DEZ and N_2O, c-axis oriented ZnO films were grown on a glass substrate at substrate temperatures of 150-350°C and rf input power levels of 60-260W, which were lower than those in the case of using CO_2. The film evaluation by the standard deviation from the x-ray rocking curve is shown in Fig.5.49. When the rf input power was not applied, nothing was deposited even if the substrate temperature was 300°C. However, at a substrate temperature of 350°C very thin grayish films were deposited unevently and weak x-ray diffraction peaks from (00·2), (10·0) and (10·1) planes of ZnO were observed. When the substrate temperature was 400°C, very weak peaks from ZnO (10·0), (00·2) and (10·1) planes, and Zn on the chamber wall and inlet nozzle were also observed. From these observations, we can see that the reaction between DEZ and N_2O for producing ZnO is caused by the energy of the plasma discahrge, not by the thermal energy of the substrate at temperatures below 400°C.

As shown in Fig.5.49 , c-axis oriented film grew even at a substrate temperature of 150°C and an rf input power of 60W, where the reaction between DEZ and N_2O for producing ZnO took place more easily than that between DEZ and CO_2. These facts indicate that the difference in readiness of the reaction may be due to the difference in bond dissociation energy of N_2O and CO_2, although the dissociation processes as well as active species

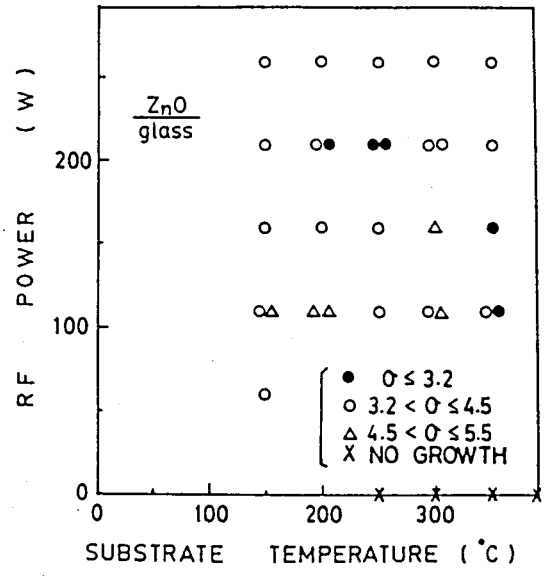

Fig.5.49. Film quality chart of ZnO films on glass using the reaction of DEZ with N_2O.

involved remain still unknown at the present stage of the work.

5-7-3. Epitaxial Growth

When $(01\bar{1}2)$ sapphire was used as a substrate, ZnO epitaxial layers grew at a substrate temperature of 250°C. The RHEED pattern exhibits distinct spots, as shown in Fig.5.50. It is noted that the different spot pattern could be observed periodically when the direction of the incident electron beam was changed. The comparison of the evaluation by the standard deviation in the cases of N_2O and CO_2 is given in Fig.5.51. The good quality films on sapphire substrartes are obtained at lower rf input power in using N_2O compared with using CO_2.

5-8. Conclusion

Highly c-axis oriented ZnO films were grown on glass substrates and epitaxial ZnO films were grown on sapphire substrates at substrate temperatures of 150-350°C by the PE-MO-CVD method, using DEZ and CO_2 (or O_2) as source materials. The crystallographic properties of the deposited films were highly dependent on the rf input power, substrate temperature and gas flow rate. By the PE-MO-CVD technique highly c-axis oriented ZnO films also were grown on Si, SiO_2, ceramic and polyimide substrates at relativly low substrate temperatures: 350, 300, 200 and 350°C, respectivley, using DEZ and CO_2 as source materials. By the use of DEZ and NO_2 highly c-axis oriented and epitaxial ZnO films were grown on glass and sapphire substrates at 150 and 250°C,

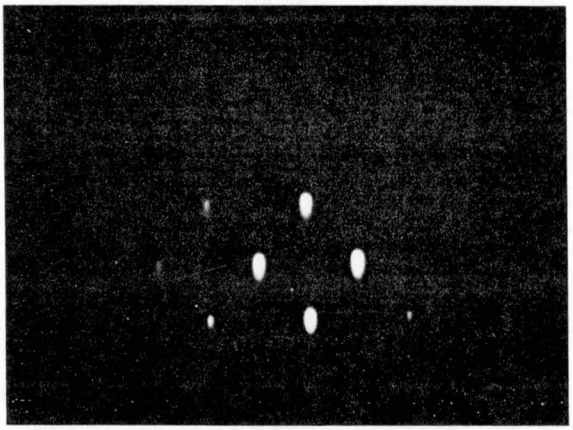

Fig.5.50. RHEED pattern of a ZnO film grown at 250°C.

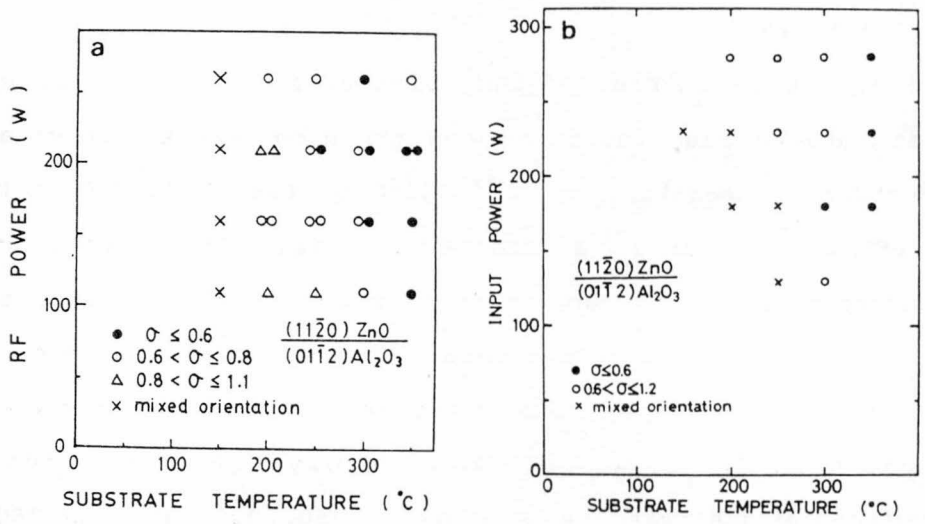

Fig.5.51. Film quality chart of ZnO films using the reaction of DEZ with (a) N_2O, (b) CO_2.

respectively. ZnO films were obtained at lower substrate temperatures and lower rf input power levels in NO_2 than in CO_2. The plasma deposited films had low resistivities of 10^{-3}-10Ωcm, Hall mobilities of 0.5-50cm^2/V·sec and carrier concentrations of 10^{18}-$10^{19}cm^{-3}$. The electrical characteristics of the ZnO films were strongly dependent on the substrate temperature the rf input power and the mole ratio of CO_2 or N_2O to DEZ. A piezoelectric transducer and heterojunction solar cells (n-ZnO/p-Si and n-ZnO/p-CdTe) were constracted.

References

[1] H.M.Manasevit, Appl.Phys.Letters 12(1968)156.

[2] H.M.Manasevit and W.I.Simpson, J.Cryst.Growth 116(1969)1725.

[3] H.M.Manasevit and W.I.Simpson, J.Electrochem.Soc. 118(1971)644.

[4] H.M.Manasevit, J.Electrochem.Soc. 118(1971)647.

[5] H.M.Manasevit,F.M.Erdmann and W.I.Simpson, J.Electrochem. Soc. 118(1971)1864.

[6] H.M.Manasevit, J.Cryst.Growth 13/14(1972)306.

[7] R.D.Dupuis and P.D.Dapkus, Appl.Phys.Letters 31(1977)466.

[8] R.D.Dupuis, Appl.Phys.Letters 35(1979)311.

[9] R.D.Dupuis and P.D.Dapkus,Appl.Phys.Letters 33(1978)68.

[10] R.D.Dupuis, P.D.Dapkus, N.Holonyak Jr., E.A.Rezek and R.Chin, Appl.Phys.Letters 32(1978)295.

[11] N.Holonyac Jr.,R.M.Kolbas,W.D.Laidig, B.A.Vojak, R.D.Dupuis

and P.D.Dapkus, Appl.Phys.Letters 33(1978)737.

[12] R.D.Dupuis, P.D.Dapkus, R.D.Yingling and L.A.Moudy, Appl.Phys.Letters 31(1977)201.

[13] R.A.Milano, T.H.Windhorn, E.R.Anderson, G.E.Stillman, R.D.Dupuis and P.D.Dapkus, Appl.Phys.Letters 34(1979)562.

[14] E.J.Thrush, P.R.Selway and G.D.Henshall, Electron.Letters 15(1979)562.

[15] H.Veenvliet, C.V.Opdorp, R.D.Tijburg and J.P.Andre, IEEE.J.Quantum.Electron. QE-15(1979)762.

[16] E.J.Thrush and J.E.A.Whiteaway, Electron.Letters 15(1979)666.

[17] D.R.Scifres, W.Streifer and R.D.Burham, IEEE.J.Quantum. Electron. QE-17(1981)2310.

[18] R.D.Dupuis and P.D.Dapkus, Appl.Phys.Letters 31(1979)839.

[19] Y.Mori and N.Watanabe, Electron.Letters 16(1980)284.

[20] E.E.Wagner, G.Hom and G.B.Stringfellow, J.Electron.Mater. 10(1981)239.

[21] Y.Mori, H.Sato, M.Ikeda, O.Matsuda, K.Kaneko and N.Watanabe, Appl.Phys.Letters 40(1982)293.

[22] N.J.Nelson, K.K.Johnson, R.L.Moon, H.A.Plas and L.W.James, Appl.Phys.Letters 33(1978)26.

[23] R.R.Saxena, C.B.Cooper III, M.J.Ludowise, S.Hikido, V.M.Sand and P.G.Borden, J.Cryst.Growth 55(1981)58.

[24] E.Fabre, A.Briere and J.P.Andre, Abs.'78 Spring Meeting of Electrochem.Soc. (1978)388.

[25] J.W.Burgess, R.Davis, B.T.Debney and R.Nicklin, ibid. p.398.

[26] J.P.Andre, M.Boulou, P.Guitterd and E.Roaux, Inst.Phys. Conf.Ser. No.56(1981)413.

[27] J.P.Andre, P.Guittard, J.Harris and C.Piaget, J.Cryst.Growth 55(1981)235.

[28] H.M.Manasevit and W.I.Simpson,J.Electrochem.Soc. 118(1971) 644.

[29] C.K.Lau, S.K.Tiku and K.M.Lakin, J.Electrochem.Soc. 127(1980) 1843.

[30] S.K.Ghandhi, R.J.Field and J.R.Shealy, Appl.Phys.Letters 37(1980)449.

[31] J.R.Shealy, B.J.Baliga, R.J.Field and S.K.Ghandhi, J.Electrochemical.Soc. 128(1981)558.

[32] A.P.Roth and D.F.Williams, J.Electrochemical.Soc. 128(1981) 2684.

[33] A.P.Roth and D.F.Williams, J.Appl.Phys. 52(1981)6685.

[34] P.J.Wright, R.J.M.Griffith and B.Cockayne, J.Cryst.Growth 66 (1984)26.

[35] P.Souletie, S.Bethke, B.W.Wessels and H.Pan, J.Cryst.Growth 86(1988)248.

[36] P.J.Wright and B.Cockayne, J.Cryst.Growth 59(1982)148.

[37] S.Fujita, Y.Tomomura and A.Sasaki, Jpn.J.Appl.Phys. 22(1983) L583.

[38] P.J.Wright, R.J.M.Griffith and B.Cockayne, J.Cryst.Growth 66 (1984)26.

[39] P.Blanconnier, M.Cordet, P.Henoc and A.M.Jean-Louis, Thin Solid Films 55(1978)375.

[40] P.Blanconnier, J.F.Hogrel, A.M.Jean-Louis and B.Sermage, J.Appl.Phys. 52(1981)6895.

[41] W.Stutis, Appl.Phys.Letters 33(1978)656.

[42] W.Stutius, J.Cryst.Growth 59(1982)1.

[43] P.I.Kuznetzov, V.V.Shemet, I.N.Odin and A.V.Novoseleva, Dokl.Akad.Nauk.SSSR. 248(1979)879.

[44] P.I.Kuznetzov, V.V.SShemet, I.N.Odin and A.V.Novoseleva, Izv.Akad.Nauk.SSSR,Neuragen.Mater. 17(1981)791.

[45] S.K.Ghandhi and I.Bhat, Appl.Phys.Letters 45(1984)678.

[46] W.E.Hoke, P.J.Lemonias and R.Traczewski, Appl.Phys.Letters 44(1984)1046.

[47] H.Booyens and J.H.Basson, Phys.Status Solidi(a) 85(1984)449.

[48] J.H.Basson and H.Booyens, Phys.Status Solidi(a) 80(1983)663.

[49] T.W.James and R.E.Stoller, Appl.Phys.Letters 44(1984)56.

[50] M.R.Czerniak and B.C.Eastan, J.Cryst.Growth 68(1984)128.

[51] S.J.C.Irvine, J.Tunnicliffe and J.B.Mullin, J.Cryst.Growth 65(1983)479.

[52] R.W.Kirk, in: Techiniques and Applications of Plasma Chemistry, Eds.J.R.Hallahan and A.T.Bell(Wiley, New York, 1974)Chap.9.

[53] A.R.Reinberg, U.S.Patent 3,753,733(1973).

[54] A.R.Reinberg, Abs.'74 Spring Meeting of Electrochemical Soc.

[55] R.S.Rosler, Solid State Technol. 20(1977)63.

[56] F.Takeda, T.Shiosaki and A.Kawabata, Appl.Phys.Letters 43(1983)51.

[57] T.Iida, in: Tables of Physical Constants (Asakura, Tokyo, 1974)p.81.

[58] de Nobel, Philips Res.Repts. 14(1959)361.

CHAPTER VI. GROWTH AND PROPERTIES OF ZnO THIN FILMS BY THE MICROWAVE PLASMA EXCITATION METHOD

6-1. Introduction

Low temperature formation and microfabrication techniques for fabrication semiconductor devices and integrated circuit using plasma and ion technology have been developed. Plasma CVD(chemical vapor deposition), specially, has been used extensively for producing dielectric films and amorphous silicon films. In plasma deposition technique, the decomposition of source materials to form films is principally assisted by the action of the glow discharge and many activated species excited by electron with high energy exist.

Recently the microwave plasma technology as a new method for chemical dry etching and deposition of poly-crystalline silicon, silicon dioxide and silicon nitride in LSI fabrication process has aroused considerable attention [1-5]. The microwave excitation technique has several advantages over the conventional RF(13.56 MHz) discharge method. For examples; 1) The microwave excitation method can produce active species with a long life time, 2) Therefore the etching and deposition region can be separated from the dischage region, 3) The plasma radiation damage(optical and particle radiation flux) to the samples can be eliminate. Microwave excitation method, as mentioned above, has the advantageous features, however little study of this method to the deposition of the III-V and II-VI compounds semiconductors have been found.

In order to obtain high quality ZnO thin film at low substrate temperatures for applications such as surface acoustic wave (SAW) devices, optical waveguided devices, sollar cell devices and transparent electrodes, we have developed the plasma-enhanced metalorganic chemical vapor deposition(PE-MOCVD) technique [6-8]. The plasma CVD system used was equipped with a capacitive coupling discharge system and parallel faced electrodes. The substrates were mounted on the electrode and were exposed by plasma discharge. Therefore, the effect of the plasma radiation damage on film formation was not minor. The observed degradation of film quality resulted from the deposition at higher RF power density was caused by the plasma damage. Then, the authors developed a technique to obtain high quality ZnO film using microwave plasmas.

In this chapter we are the first to describe experiment detailes of the low temperature growth of c-axis oriented and epitaxial ZnO thin films using the microwave excitation technique and an application for optical waveguide.

6-2. Experimental Procedure

The experimental system used is shown in Fig.6.1. This system consisted of a microwave generator, wave guides, a resonant reactor cavity, a quartz reactor tube(30cm in diameter and 125cm in length), a gas supplying system and a evacuation system. A microwave generator was capable of delivering up to 1.5kW. It was possible to adjust the position of the susceptor from 10 to 60cm from the cavity. The substrates on the susceptor were heated

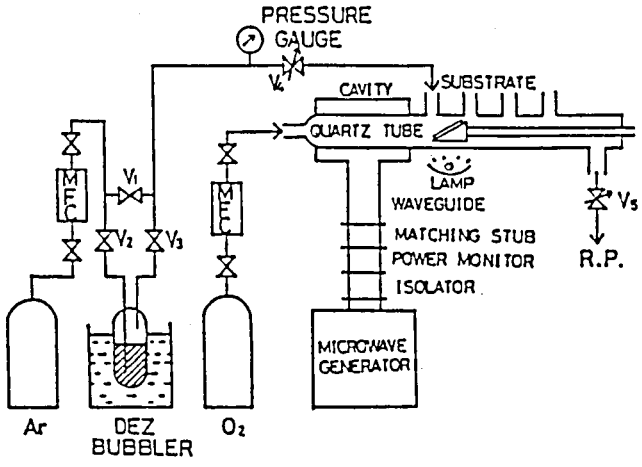

Fig.6.1. Schematic diagram of the microwave plasma excitation system.

by an infrared lamp.

In this growth system, diethylzinc(DEZ, $Zn(C_2H_5)_2$) reacted with microwave excited oxygen or dinitrogen monooxide to produce ZnO. An O_2 or N_2O gas was injected upstream of the discharge zone and DEZ was introduced into reactor from other inlet as shown in Fig.6.1. The flow rates of gases are controlled by mass flow controllers. In the present experiment, the gas flow rates of Ar through the DEZ bubbler, and O_2 and N_2O were 20-30, 414 and 300 sccm, respectively. The reaction tube was evacuated by a rotary pump(500 l/min) and the reaction pressure was controlled by a throttle valve joined with the rotary pump. The reaction pressure was about 1 Torr during the growth run. In the present study, Corning 7059 glass and sapphire were used as substrates.

Optical emission spectrum from the oxygen microwave plasmas were analyzed by a monochrometer(25 cm) in the 300-800 nm spectral range. The structual nature of the deposited films was examined by an X-ray diffraction, reflection high energy electron diffraction(RHEED) and secondry electron microscope(SEM). The electrical and optical properties were also measured.

6-3. Results and Discussion

In the early stages of our experiment, DEZ was passed through the microwave radiation field, where a discharge was generated, to obtain Zn films. However, the injection of DEZ into the plasma region led to very unstable discharge and plasma discharge was not maintained for a long time. In this experi-

ment, the deposition of black materials, which was found to be a carbon by an Auger analysis, was observed on the inner wall of quartz tube only in discharge region and did not obtain Zn films on a substrate. Therefore, in our study, DEZ reacted with the microwave excitated O_2 or N_2O to produce ZnO.

The optical emission spectrum from the oxygen plasma was measured to investigated the growth process. Many peaks from excited atomic oxygen, and molecular oxygen ions were observed as shown in Fig.6.2. Spectroscopic examination revealed that the reactive oxygen radicals played very important role of the growth process [9,10].

6-3-1. Effect of Substrate Temperature

The deposition rate of ZnO films on a glass substrate as a function of reciprocal substrate temperature is shown in Fig.6.3.. In this experiment, the substrates were placed at a distance of 20cm from discharge region. The variation of the deposition rate of films by the plasma excitation technique is small, however that of films obtained by thermal MOCVD increases as the substrate temperature increases. The caluculated activation energy of the reaction using MOCVD in the temperature range of 100-400^{o}C is larger than that when the microwave excited oxygen is used, as shown in Fig.6.3. This supports that the energy required in the reaction in the microwave plasma enhanced method is less than that in thermal MOCVD and that the microwave plasma enhancement technique allows crystal growth at lower substrate temperatures.

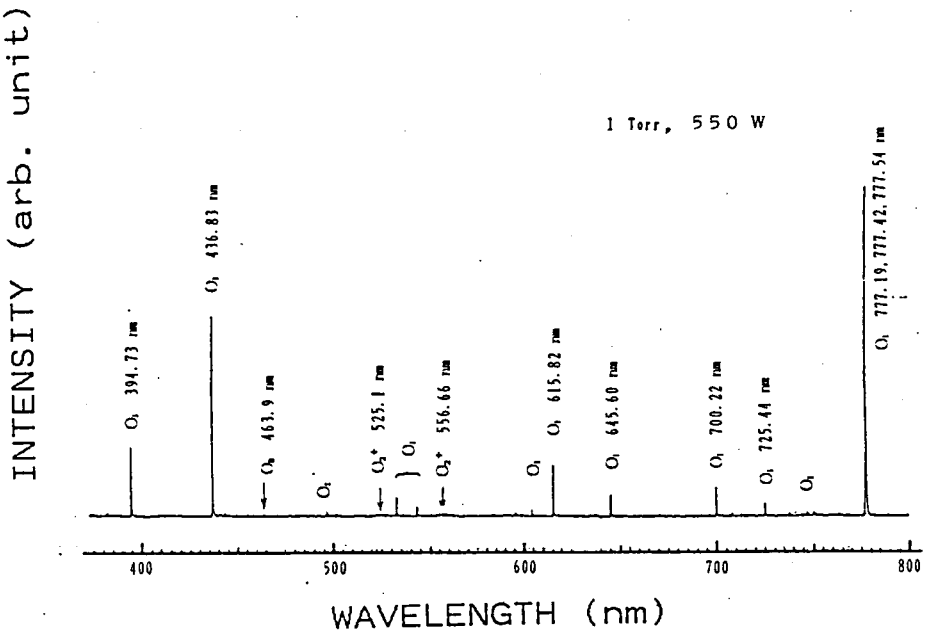

Fig.6.2. Optical emission spectrum from the oxygen plasma.

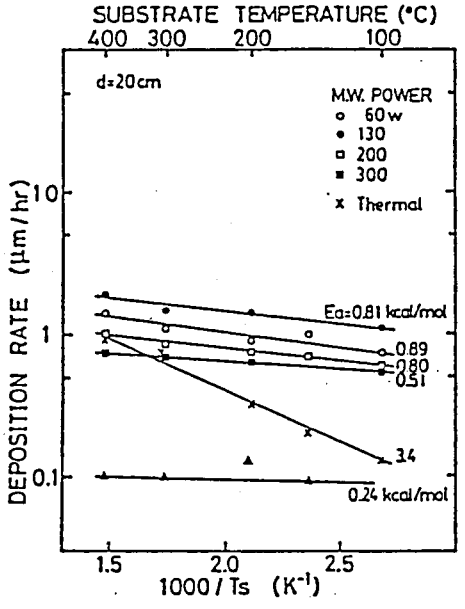

Fig.6.3. Deposition rate of ZnO films on a glass substrate as a function of reciprocal substrate temperature.

In our experiment, the deposition of ZnO was observed when the substrates were placed at a distance of 50cm from the discharge region. This means that the activated species with a long life time (reactive oxygen radicals) existed and reacted with DEZ. The maximum deposition rate was obtained at a microwave input power of 130W regardless of substrate temperature and the position of the susceptor. Increasing the power to the discharge will increase the probability of completely dissociating O_2 molecule generating oxygen radicals or energetic metastable. Therefore the effect of microwave input power on the deposition rate may be related to the change in the number of activated species by changing electron density with power and to the mutual reaction with the activated species. However the details have not been well understood in this stage.

In this system c-axis oriented ZnO films have been grown successfully on a glass substrate at substrate temperatures of higher than 200^{o}C. Figure 6.4 shows the X-ray diffraction patterns of films obtained at 200^{o}C by the plasma excitation method and thermal MOCVD. Only c-plane reflection peaks were observed in both films. The film evaluation by the peak intensity and the half width of an x-ray diffraction patterns, and the standerd deviation angle(σ) of the X-ray rocking curve for the (0002) peak indicated that the films obtained by the plasma excited method showed better crystalline quality than when they were grown by thermal MOCVD. The substrate temperature and microwave input power dependence of σ value of films is shown in Fig.6.5. This film quality chart means that more highly c-axis

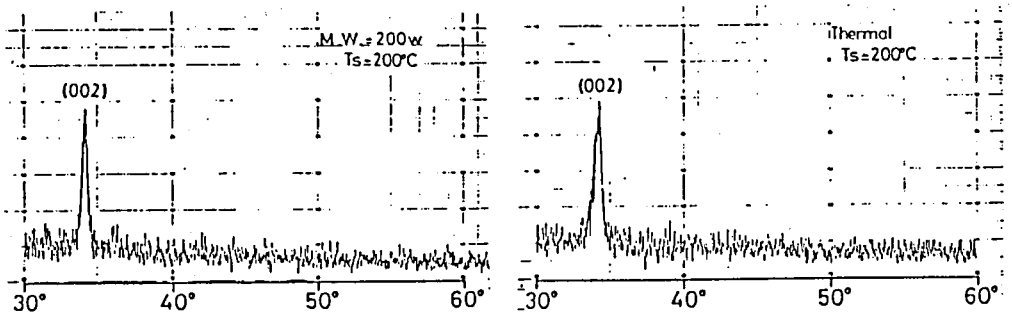

Fig.6.4. X-ray diffraction patterns of ZnO thin films on glass substrates at 200°C by : (a) the plasma excitation method, (b) thermal MOCVD.

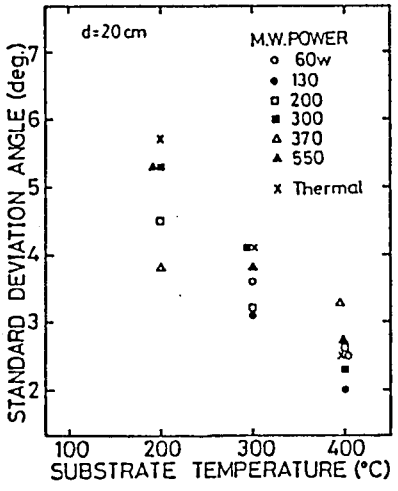

Fig.6.5. Dependence of standard deviation angle on substrate temperature.

oriented films were obtained by the microwave excitation plasma method at same substrate temperatures.

The electrical resistivity of the grown films was measured. Figure 6.6 shows the variation of resistivity as a function of substrate temperature. Resistivity decreases as the temperature increases up to the substrate temperature of 300°C and increases at higher than 300°C, which may be caused by the competition between crystallization and degree of nonstoichiometry of the films. Resistivity of films grown by thermal MOCVD showed higher than that of films by microwave excited MOCVD. The improvement in c-axis orientation of film obtained by microwave excited MOCVD is one of the most effective causes in the decrease of resistivity.

The optical transmittance of the films was measured using a double-beam spectrophotometer (SHIMADZU: MPS-2000). ZnO films obtained at various substrate temperatures by microwave excited method shows excellent transmittance as indicated in Fig.6.7, and the average transmittance is found to be about 80%. Even though the deposition parameters were same, the transmission spectrum of the films obtained by thermal MOCVD showed lower transparency and interference effect was not observed. It is found that our microwave excited MOCVD method has proved to be an excellent method to obtain highly transparent ZnO films for various applications.

6-3-2. Effect of Gas Flow

The dependence of deposition rate on the DEZ and O_2 flow was

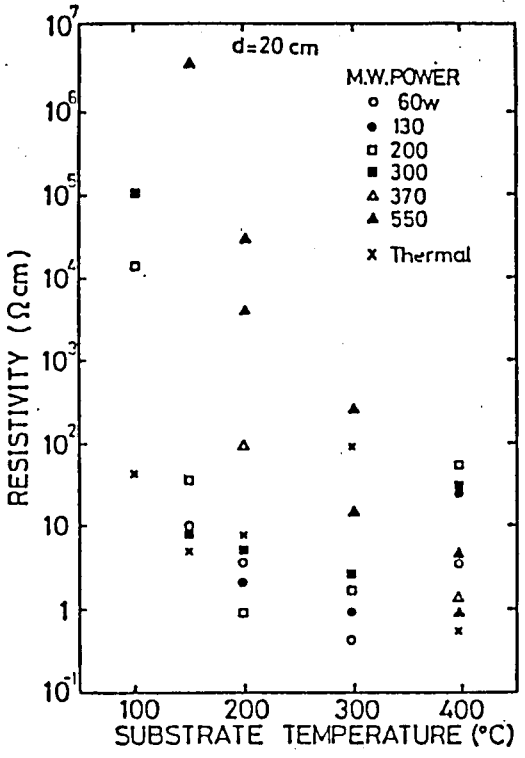

Fig.6.6. Dependence of resistivity on substrate temperature.

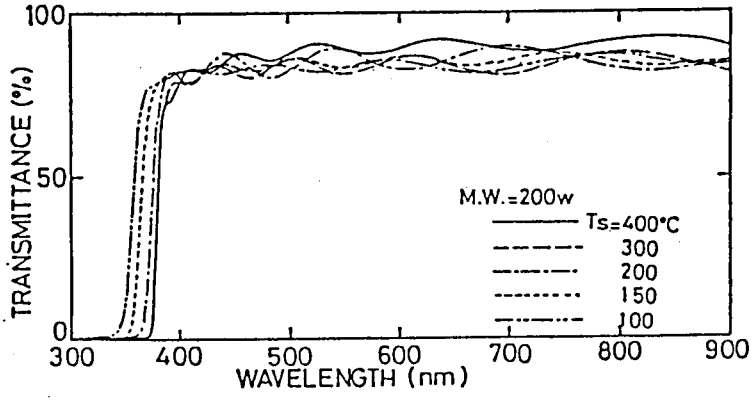

Fig.6.7. Optical transmittance spectra for ZnO thin films.

also investigated. Figure 6.8 shows the deposition rate as a function of DEZ concentration. The increase in deposition rate with increasing DEZ concentration for O_2 flow of 1.85×10^{-2} mol/min was observed. A similar result was also reported in the growth of ZnSe and InAs when VI and V group source materials were supplied sufficiently. Contrary to the DEZ flow, the deposition rate decreased as the O_2 flow increased, when the DEZ flow was kept to 2.5×10^{-5} mol/min, as shown in Fig.6.9. The excess O_2 resulted in a reduction in a deposition rate, which may be caused by some complexes.

6-3-3. Effect of Reaction Pressure

The effect of total reaction pressure on deposition rate was measured, which is shown in Fig.6.10. The depositon rate increases with increasing pressure due to the increase of gas concentration caused by the decrease in gas velocity. The deposition rate decreases rapidly as a reactor pressure increases over 2 Torr, which is caused by some premature reactions including homogenious recombination of the atomic species due to the high concentration of gas sources. The increase in pressure also causes a decrease in electron temperature, which leads to a decrease in the energy transfer between the electrons in the plasma and the O_2 molecules.

The orientation of the grown films was changed with increasing total reaction pressure. When the films were deposited at 1 Torr and 400°C, only c-plane reflection peaks were observed. However, (00·2) and (10·1) peaks appeared when films were deposited

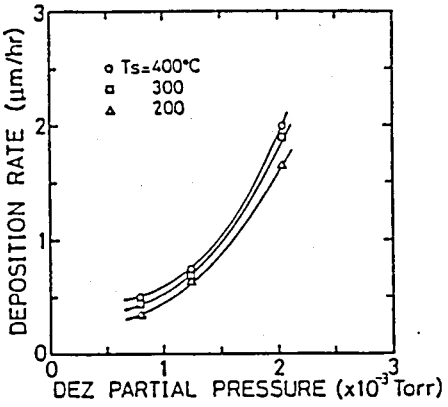

Fig.6.8. Dependence of deposition rate on the DEZ partial pressure.

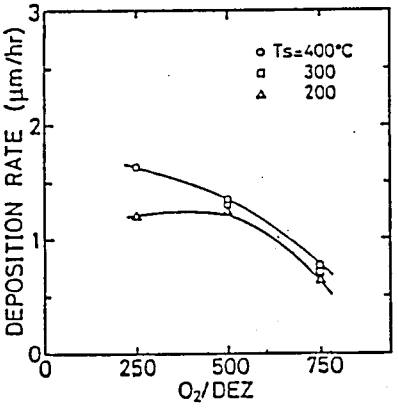

Fig.6.9. Dependence of deposition rate on the O_2 flow rate.

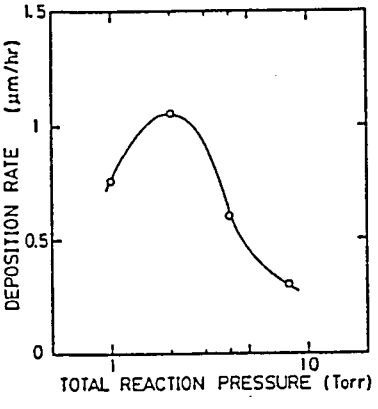

Fig.6.10. Dependence of deposition rate on reaction pressure.

at higher than 2 Torr. The gas phase reaction and the surface reaction were effected by the reaction pressure. Thus the orientation depended on gas pressure as mentioned above.

The electrical resistivity of grown films a pressures of 1-8 Torr showed 1-10^3Ωcm and exhibited a minimum at a pressure of 2 Torr. This variation of resistivity is similar to the reaction pressure dependence of the grain size measured by SEM observation. Therefore this resistivity variation may be related to the change in the Hall mobility which is limited by scattering at grain boundaries.

6-3-4. Doping Effect

ZnO thin films with high resistivity have been used for applications to SAW devices and integrated optics. Recently low resistive ZnO films have been attracting attention as transparent electrodes and window material of soller cells. Therefore, controlling the electrical resistivity of ZnO film is an important objective. In this study, the doping of Li and Al to ZnO was carried out.

LiOH was used as a dopant of Li. The small quartz vessel loaded with LiOH was put into the plasma discharge region. The doped ZnO films grown at 200°C showed the resistivity of 10^5-10^7 Ωcm, which is 10^4-10^6 higher than undoped films. This doping method resulted in difficulties in controlling the doping contents and in the reproducibility.

Trimethylauminium(TMA, $Al(CH_3)_3$) was also introduced into a reactor as a dopant of Al. The flow rate of Ar through a TMA

bubbler was 15sccm. The temperature dependence of resistivity and an effect of Al doping are shown in Fig.6.11. The non-doped films had resistivities of $10\text{-}10^{-1}$ Ωcm, however the Al doped films showed lower resistivities of $10^{-1}\text{-}10^{-3}$ Ωcm. The resistivity of film could be controlled easily from 10^{-1} to 10^{-3} Ωcm by changing TMA flow rate and controllability was fairly good.

6-3-5. N_2O as an Oxidizing Gas

N_2O was also used as an oxidizing gas in the present study. The growth condition employed in the present case was that 20-30 sccm of Ar flow through the DEZ bubbler and 30 sccm of N_2O flow. ZnO films were obtained by using the reaction between DEZ and microwave excited N_2O.

The substrate temperature dependence of the deposition rate is shown in Fig.6.12 , and it can be seen that the films obtained by this microwave method have higher deposition rate than that of thermal MOCVD film.

In this system, c-axis oriented films have been grown on glass substrate at a substrate temperature of 150°C, which is lower than that when O_2 was used. When films were prepared by thermal MOCVD at lower than 200°C, the X-ray diffraction peaks from (10·0), (00·2), (10·1) planes of ZnO were observed and c-axis oriented films have not been grown.

Films obtained by our method showed the better crystallinity than that of films by MOCVD as mentioned above, however they had higher resistivity. The resistivity of films prepared at 150-400°C by the plasma excitation method was of 10^{-1} to 10^{7} Ωcm. On

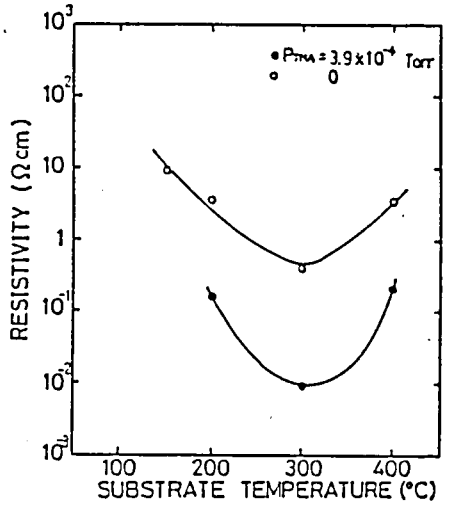

Fig.6.11. Resistivity versus substrate temperature and Al doping effect.

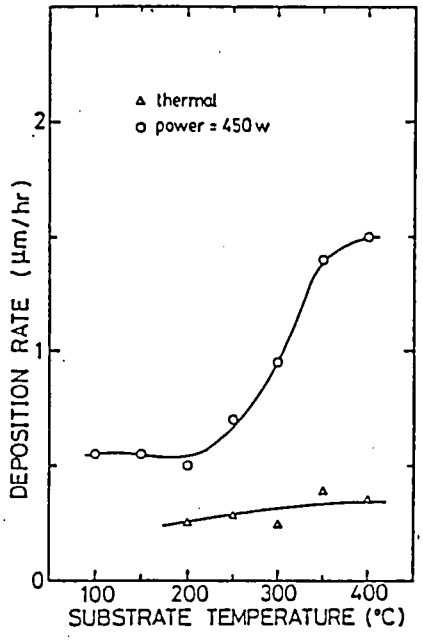

Fig.6.12. Variation of deposition rate as a function of substrate temperature.

the other hand, the thermal MOCVD films showed the resistivity of 10^{-3}-10^{1} Ωcm. This can be easily understood by considering the films by the plasma method have better stoichiometric but the effect of nitrogen doping as acceptor is not definite.

6-3-6. Epitaxial Growth

Epitaxial growth of ZnO films on sapphire substrates has been carried out. In this experiment, $(01\bar{1}2)$ and (0001) sapphire were used as substrates and O_2 gas was used as an oxidizing gas. The growth condition were the same as mentioned in section 6-2. The dependence of the crystalline structure on the substrate temperature was examined by an X-ray diffraction and the RHEED method. Films didn't grow epitaxially at substrate temperatures of lower than 400°C. Films grown on $(01\bar{1}2)$ sapphire at 400°C showed a only ZnO $(11\bar{2}0)$ plane peak and the separation of $CuK_{\alpha 1}$ and $CuK_{\alpha 2}$ trace was also observed. The RHEED pattern of the film grown at 400°C, as shown in Fig.6.13 , has the spots. These indicate that the film is single crystalline. When (0001) sapphire was used as a substrate, (0001) ZnO layers grew higher than 400°C and the RHEED pattern exhibits distinct spot as shown in Fig.6.14. When films were grown by thermal MOCVD, the epitaxial films could not obtained at 400°C.

Films grown an $(01\bar{1}2)$ and (0001) sapphire by the microwave plasma technique generally showed the average transmittance of higher than 80%, which was higher than that of thermal MOCVD films as shown in Fig.6.15.. The reflactive index(n_e), which was measured by the m line method, of the $(11\bar{2}0)$ epitaxial film

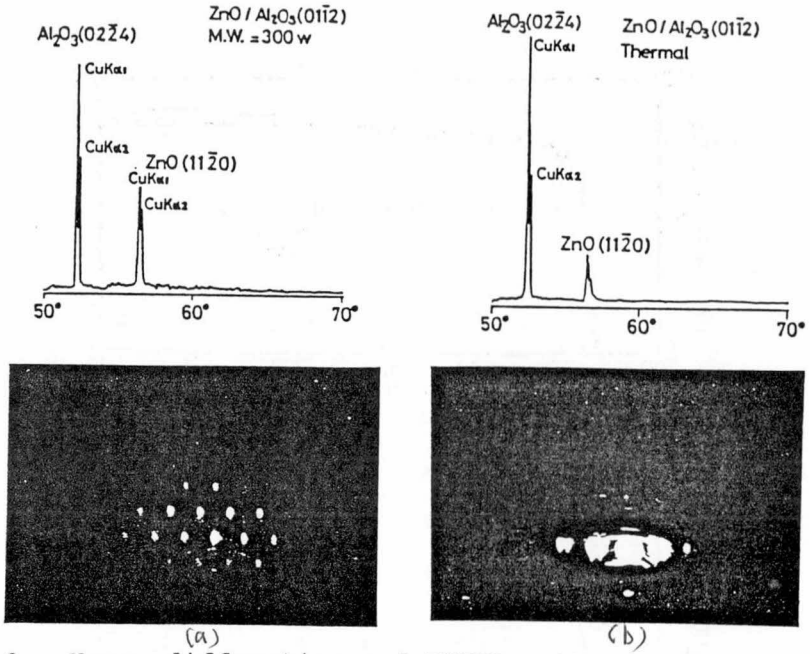

Fig.6.13. X-ray diffraction and RHEED patterns of ZnO thin films grown on (01$\bar{1}$2) sapphire at 400°C by; (a) the microwave plasma excitation method, (b) the thermal MOCVD method.

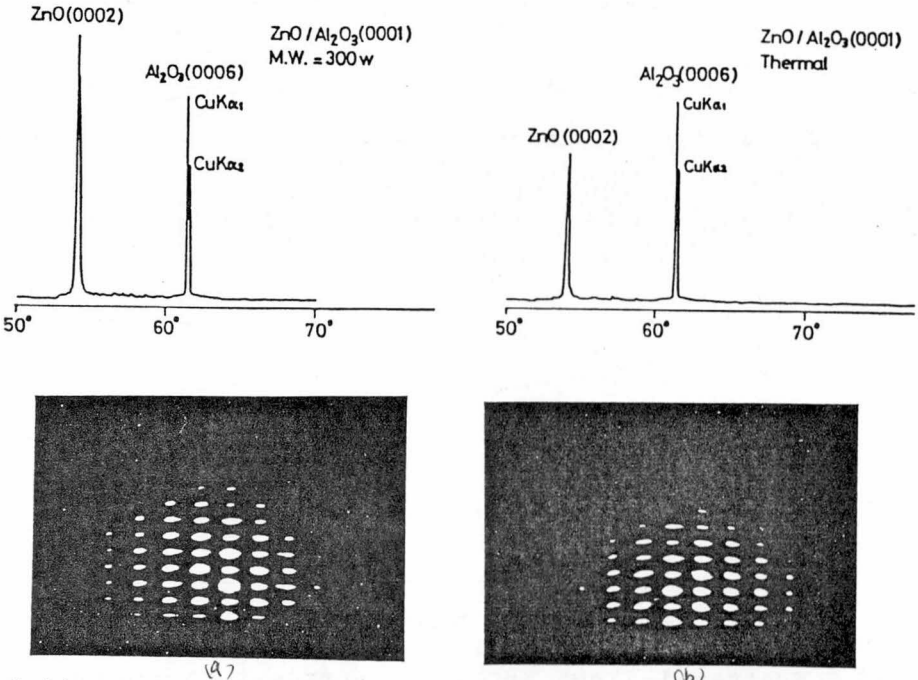

Fig.6.14. X-ray diffraction and RHEED patterns of ZnO thin films grown on (0001) sapphire at 400°C by; (a) the microwave plasma excitation method, (b) the thermal MOCVD method.

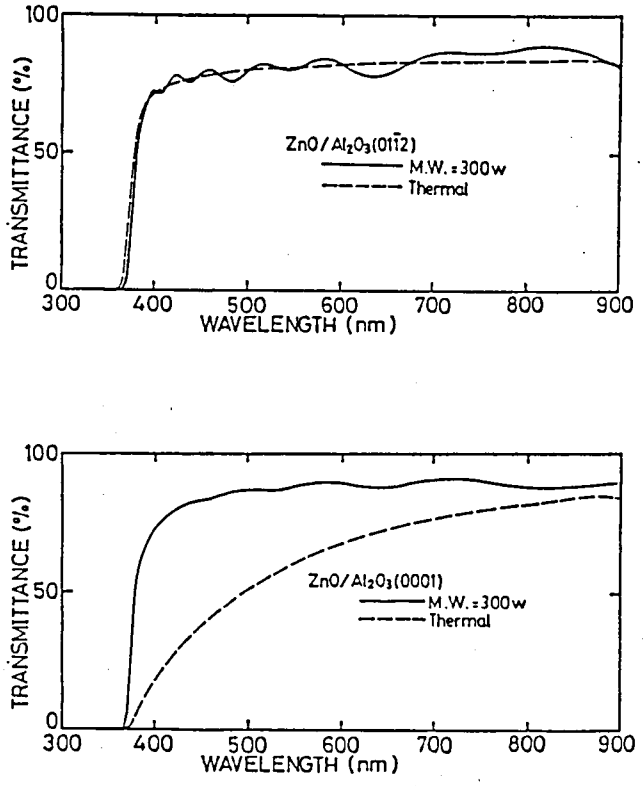

Fig.6.15. Optical transmittance spectra for ZnO thin films grown on sapphire substrate at 400°C.

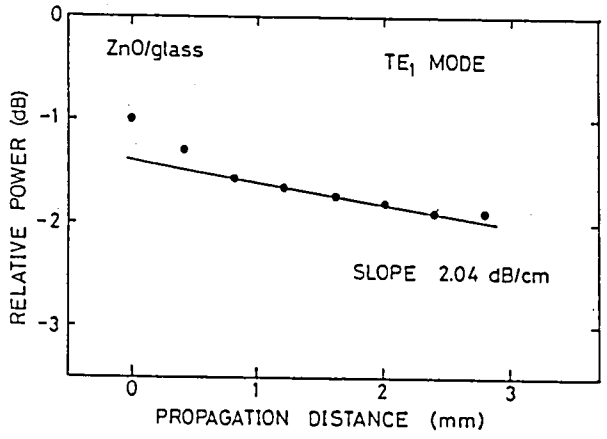

Fig.6.16. Scattered light intensity versus propagation distance on ZnO film for TE_1 mode.

deposited at 400°C and 300W was 1.997. This value was nealy same of the bulk crystal's(n_e=1.993).

6-3-7. Application to Optical Waveguide

It is well known that ZnO is one of the suitable materials for application to optical waveguided devices because of its large piezoelectricity, high transparency, large diffractive indices, and good acoust-optic and electro-optic coefficient. Therefore thin films of ZnO with low optical waveguided losses have potential applications as various integrated optical devices. In waveguided devices, the guided wave propagation loss is very important factor. The attenuation includes the scattering loss at film surface and interfacial region, and the bulk loss. The light propagation losses were measured by the scattering detection method at the He-Ne laser wavelength(6328Å) and experimental details may be found elsewhere. Most of films obtained showed waveguide attenuation of about 10dB/cm for the TE_0 mode. The best result obtained was the minimum propagation loss of 2.04dB/cm for the TE_1 mode as shown in Fig.6.16. It was founded that the propergation losses of films grown by our method was lower than them grown by thermal MOCVD. The MOCVD films, generally, had short light propagation distances due to high scattering losses. This means that ZnO films grown by the microwave plasma excitation method have smooth surfaces and high crystallinity.

6-4. Conclusion

The growth of c-axis oriented and epitaxial ZnO films have been achieved using DEZ, and microwave oxygen or dinitrogen monooxide plasmas. The effect of the growth conditions (substrate temperature, microwave input power, reaction pressure, plasma-substrate distance and gas flow rate) on the deposition rate, crystallinity, and electrical and optical properties of ZnO films on glass and sapphire substrates have been investigated. C-axis oriented and epitaxial ZnO films were grown successfully at substrate temperatures of 150°C and 400°C, respectively. In this method, the film formation was observed on substrates placed at a maximum distance of 50cm from plasma region, which means that the active oxygen species(excited oxygen atoms) with a long life time played an important roles in the growth process and, therefore, the plasma radiation damage was fairly minor. As deposited films showed the resistivity of 10^{-1}-10^{4} Ωcm and the the resistivity could be controlled from 10^{-3} to 10^{7} Ωcm by the doping of Al and Li. The average transmittance of films was found to be 80% and refractive index (n_e) of epitaxial film was 1.997. A comparison of film characteristics using the microwave excitation technique and the thermal MOCVD technique showd that our technique utilizing microwave plasmas was an excellent method to obtain high quality ZnO films with good surface flatness and high transparency at low substrate temperature. The best result obtained for optical waveguided device application was a optical propagation loss of 2.0dB/cm in the TE_1 mode.

References

[1] M.Shibagaki, Y.Horiike, T.Yamazaki and M.Kashiwagi, Proc. of Electrochem. Soc. Fall Meeting 152(1977)416.

[2] Y.Horiike and M.Shibagaki, Proc. of the 7th Conference on Solid State Devices,Tokyo,1975, Jpn.J.Appl.Phys. Suppl.15 (1976)13.

[3] M.Shibagaki, Y.Horiike and T.Yamazaki, Proc. of the 9th Conference on Solid State Devices,Tokyo,1977, Jpn.J.Appl.Phys. Suppl.17-1(1978)215.

[4] I.Kato, S.Wakana and S.Hara, Jpn.J.Appl.Phys. 20(1983)L40.

[5] B.Robinson, P.D.Noh and P.Madakson, Proc. of 8th International Symposium on Plasma Chemistry (1985)1111.

[6] M.Shimizu, T.Yamamoto, T.Shiosaki and A.Kawabata, Proc. of 2nd Symposium on Ultrasonic Electronics,Tokyo,1981, Jpn.J.Appl.Phys. Suppl.21-3(1982)63.

[7] M.Shimizu, T.Horii, T.Shiosaki and A.Kawabata, Thin Solid Films 96(1982)149.

[8] M.Shimizu, Y.Matsueda, T.Shiosaki and A.Kawabata, J.Cryst.Growth 71(1985)209.

[9] S.Dzioba, G.Este and H.M.Naguib, J.Electrochem.Soc. 129(1982)2537.

[10] K.Miyake, S.Kimura, T.Warabisako, H.Sunami and T.Tokuyama, Proc. of Int'l Ion Engineering Congress-ISIAT'83 & IPAT'83, Kyoto, (1983)915.

CHAPTER VII. LOW TEMPERATURE GROWTH OF ZnO FILM BY PHOTO-MOCVD

7-1. Photo-MOCVD of ZnO Thin Films

7-1-1. Introduction

Many fabrication techniques for growing ZnO film with good crystalline quality have been developed. In order to obtain highly c-axis oriented and epitaxial ZnO films, we have developed thin film fabrication techniques such as rf planar magnetron sputtering [1-3], chemical vapor deposition (CVD) [4-7] and plasma-enhanced metalorganic chemical vapor deposition [8-10], as mentioned before. The plasma deposition method does have some disadvantages such as film surface bombardment by energetic particles, deviation of stoichiometry and a low growth rate. However, the CVD ($ZnO-H_2-O_2-H_2O$) system developed by our group has given single crystal ZnO films and the selective area growth of the ZnO film was successful [5-7]. One problem with the CVD system is thermal damage to both the substrate surface and the complex device on the substrate, caused by the high substrate temperature (800-1000^{o}C) required in this method. Therefore the development of a new technique for obtaining highly c-axis oriented and epitaxial ZnO thin films, and selective film growth technique of ZnO at low substrate temperatures, is required.

In recent years the photochemical vapor deposition (photo-CVD) technique has received much attention in the research field of amorphous materials , metal films and compound semiconductors, because of its low processing temperature , little bombardment by energetic particles, low contamination and selective film growth.

However, it has not been very long since research on the photo-MOCVD of III-V and II-VI compound semiconductors was started. Especially in II-VI semiconductors, the reaction mechanism of thermal decomposition and photochemical processes using metalorganic compounds are very complicated and remain unknown. In the work on film preparation of ZnO by laser-induced CVD, some reports were published by R. Solanki and coworkers[11,12]. In their study, high deposition rates were obtained using an excimer laser; however, the effects of light irradiation on crystalline and electrical properties were not clarified in detail.

In this section, we report on the low substrate temperature photodeposition and properties of Zn and ZnO films obtained by utilizing the reaction between diethylzinc[DEZ:$Zn(C_2H_5)_2$] and oxygen or nitrogen dioxide, when exposed to a mercury lamp or xenon-mercury lamp. Some effects of ultraviolet light irradiation on the growth process are also described.

7-1-2. Experimental Procedure

The photo-MOCVD system used in this work is shown in Fig.7.1. In this system, the source alkylmetal compound DEZ reacts with O_2 or NO_2 as an oxidizing gas to produce ZnO. The light source used is a 500W high pressure mercury lamp or a 500W xenon-mercury lamp. An ultraviolet transmitting filter is placed between the light source and the incident quartz window of the reaction chamber in order to study the wavelength dependence for photodeposition. Only ultraviolet light is introduced through this filter, thus preventing an increase of the substrate tem-

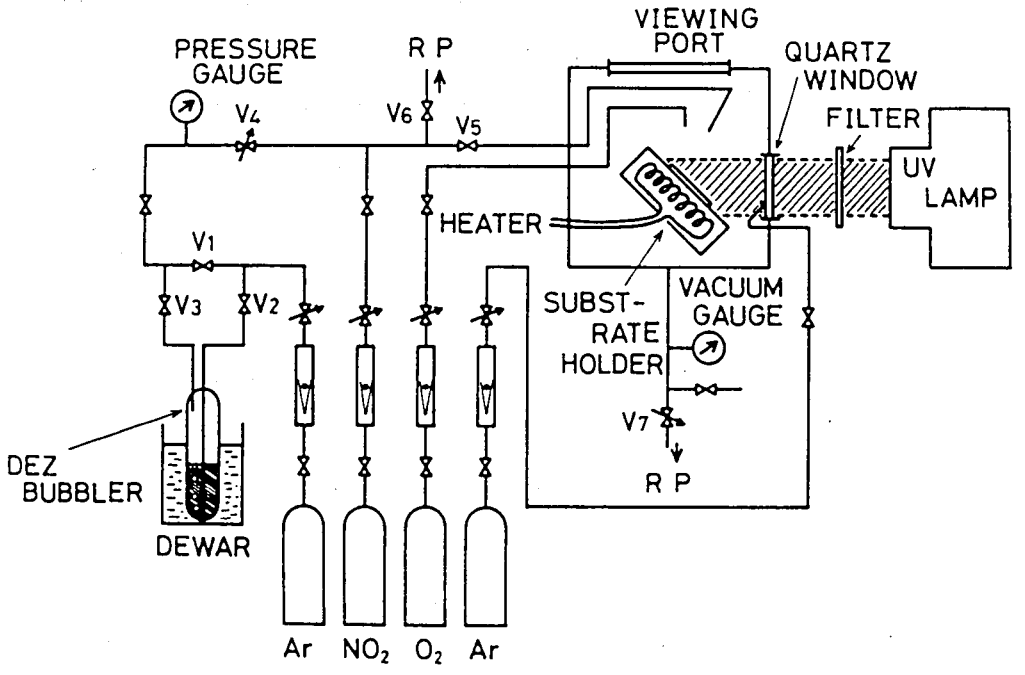

Fig.7.1. Schematic diagram of photo-MOCVD system.

perature by exposing the substrate to infrared irradiation. The chamber used measures 15cm in diameter and 20cm in height, and has a purge system designed to prevent ZnO deposition on the window. The gas flow system is assembled using 1/4 inch stainless tubing, stainless steel valves, flow meters and a stainless steel bubbler for DEZ which is in temperature controlled bath. The reaction chamber is evacuated by a normal rotary pump (500 l/min), and the pressure is about 1 Torr during the growth run. Corning 7059 glass was used as a substrate.

7-1-3. Photodeposition of Zn Films

The photo decomposition of DEZ was carried out at an earlier stage of our study. Zn films of a grayish color were deposited at substrate temperatures of 250-350^{o}C. When the substrate was exposed to the ultraviolet light from a high pressure mercury lamp, at room temperature Zn films formed on the substrate. The thickness of films obtained increased as the short wavelength limit of the light source was decreased from 300nm to 220nm using the ultraviolet transmitting filters. No film at all was deposited when the filter reached the transmittance limit wavelength of 300nm. The above mentioned wavelength results show that the photodissociation wavelength of DEZ is below 300nm which coincides with the 280nm figure reported by H.W. Thompson et al. [13-15]. When a large amount of DEZ was introduced into the reactor and maintained at room temperature without heating the substrate, a thick Zn film with a mirrorlike surface was deposited only on the light irradiation region(i.e. selective film growth).

7-1-4. Photodeposition of ZnO Films using the Reaction between Diethylzinc and O_2

The photodeposition of ZnO was also achieved using a xenon-mercury lamp. Using two kinds of wavelength regions, i.e. 220-410nm and 320-410nm, the reaction between DEZ and oxygen was used to obtain ZnO films. The dependence of the deposition rate on the substrate temperature is shown in Fig.7.2. When no light irradiation was used, the deposition rate was lower than when it was present. Shortening the wavelength emitted by the light irradiation had an effect on increasing the deposition rate up to a substrate temperature of 350°C. This photo irradiation effect on deposition rate suggests that the photodissociation of DEZ (220-410nm) and the contribution of the red-shifted tail in the absorption spectrum to some gas-phase photodissociation of DEZ(320-410nm) are important. The red shift in the absorption of DEZ adosorbed on substrate surface is also an important factor [16]. More complete dissociation of DEZ (and NO_2) by UV irradiation and the role of UV light on enhancing the mobility of the adsorbed species also demand consideration in both wavelength regions. The activation energy of the reaction using photo-MOCVD(220-410nm) is 8.7(kJ/mol) calculated from using an Arrhenius equation,lower than that when the films were grown using MOCVD,14.5(kJ/mol). This shows that UV light irradiation assists the growth rate of ZnO thin films. Although the detailed reaction mechanism in the photochemical process between DEZ and oxidant is presently unknown, the growth rate and the crystallinity are influenced by the photochemical reaction in the gas

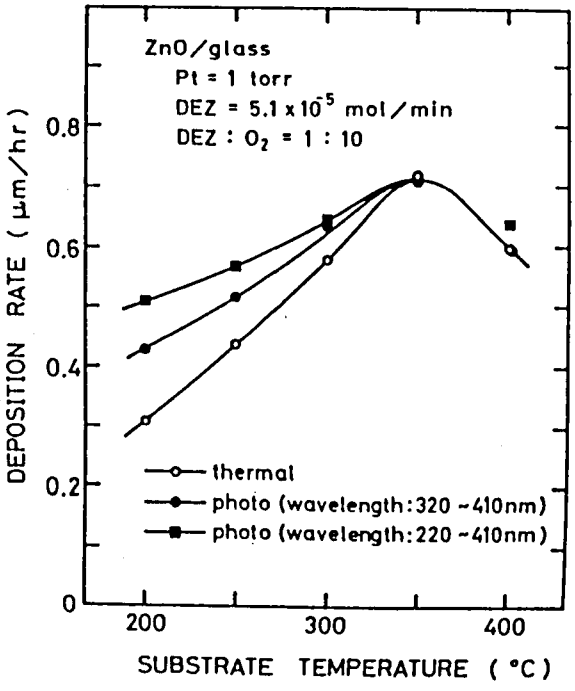

Fig.7.2. Variation of the deposition rate as a function of substrate temperature and effect of the UV light irradiation on the deposition rate. DEZ=5.1 x 10^{-5}mol/min, O_2=5.1 x 10^{-4}mol/min, Pt=1Torr, P=0.4mW/cm^2 (320-410nm) and 0.7mW/cm^2 (220-410nm).

phase and/or the surface reaction. In our experiment, the rise in surface temperature of the substrate from the UV light in the UV wavelength region used is negligible as the light power is low (0.4-3.4mW/cm^2). The difference of the deposition rate, with or without a light irradiation, decreases as the substrate temperature increases. The decrease of the deposition rate above 350^{o}C may be attributed to reevaporation and change in the sticking coefficient.

C-axis oriented ZnO films were grown successfully at a substrate temperature of 250^{o}C under light irradiation of 220-410nm,as shown in Fig.7.3. However, film grown under 320-410nm irradiation showed a strong x-ray peak from (002) planes, as well as weak peaks from (100), (101) and (110) planes. Without irradiation, films obtained at 250^{o}C showed weak peaks from (100), (002), (101) and (110) planes,as shown in Fig.7.3 , and c-axis oriented films could be grown at a substrate temperature of more than 300^{o}C regardless of whether or not light irradiation occurred. When ZnO films are grown on glass substrates,the growth obeys Bravais's rule and films grown generally show c-axis orientation,as is well known [17,18]. Our experimental results mentioned above (as shown in Fig.7.3) reveal that UV irradiation allows crystal growth at lower substrate temperatures, and photon energy assists the reaction in the vapor phase, and also surface reactions such as adsorption, desorption, and acceleration of surface migration and photo induced carrier excitation effect.

7-1-5. Photodeposition of ZnO Films using the Reaction between

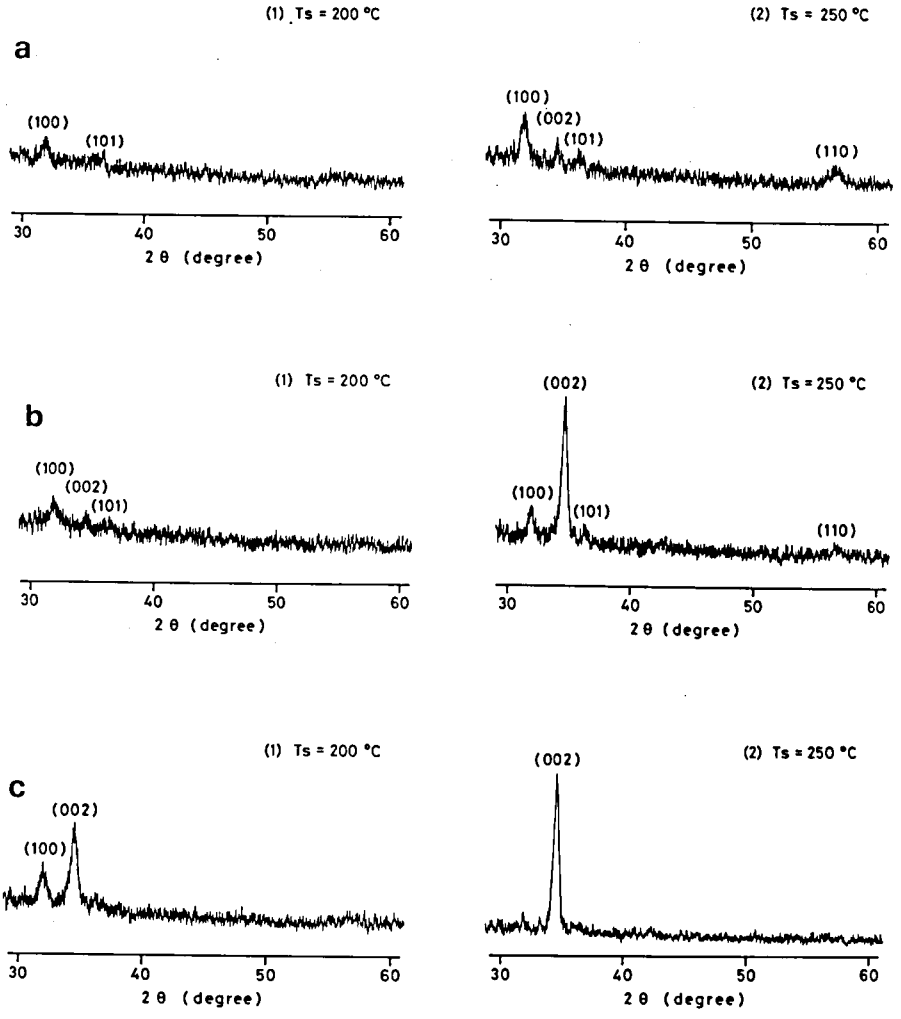

Fig.7.3. X-ray diffraction patterns of ZnO films grown by: (a) MOCVD; (b) photo-MOCVD (320-410nm; 0.4mW/cm^2); (c) photo-MOCVD (220-410nm, 0.7mW/cm^2).

Diethylzinc and NO_2

Photodeposition using the reaction between DEZ and NO_2 (dissociated under 398nm)[19-21] was also carried out. In contrast to the rapid reaction between DEZ and O_2, DEZ hardly react with NO_2 directly at substrate temperature lower than 150°C. The light source used was a high pressure mercury lamp. Figure 7.4 shows the dependence of the deposition rate on the substrate temperature. The deposition rate of films grown by photo-MOCVD proved to be higher than that of films grown by thermal-MOCVD. This means that the wavelength of the light source used coincide with the dissociation wavelength of DEZ and NO_2, and also the UV light has an effect on the surface reactions.

The X-ray diffraction patterns of films grown by MOCVD and photo-MOCVD,utilizing the reaction of DEZ with NO_2, at a substrate temperature of 150°C are shown in Fig.7.5. From this figure it can be seen that the X-ray intensity from a photo-deposited film is stronger than that from a film without light irradiation, although the film thickness of both samples are nearly the same. The standard deviation angle which indicates the degree of c-axis orientation of films obtained by photo-MOCVD at 150°C is about 6°. Photodeposition films showed a lower standard deviation angle than those of films grown under no photo irradiation as in the case of using DEZ and O_2.

The dependence of resistivity on substrate temperature (150-450°C) was also examined,as shown in Fig.7.6. The lowest resistivity of the ZnO films was observed at a substrate temperature of about 300°C. The decrease in resistivity as the temperature

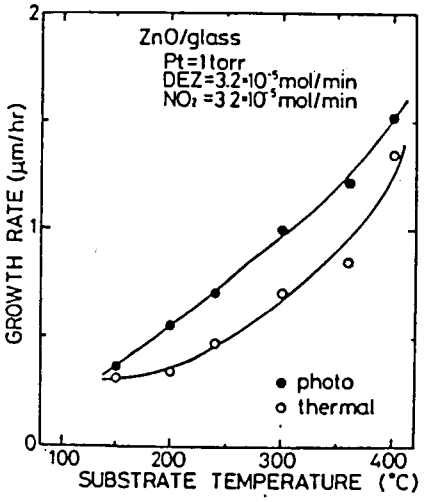

Fig.7.4. Variation of the deposition rate as a function of substrate temperature and effect of the UV light irradiation on the deposition rate. DEZ=3.2 x 10^{-5}mol/min, NO_2=3.2 x 10^{-4}mol/min, Pt=1Torr, P=2.2mW/cm^2 (250-410nm).

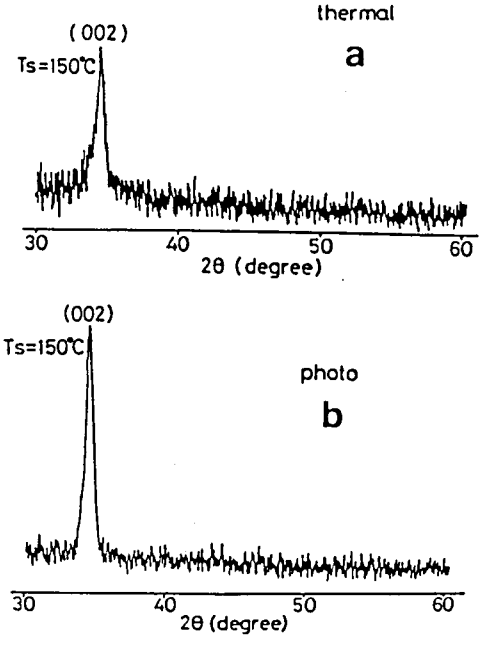

Fig.7.5. X-ray diffraction patterns of ZnO films at a substrate temperature of 150°C by: (a) MOCVD; (b) photo-MOCVD (250-410nm; 2.2mW/cn^2). DEZ=1.4 x 10^{-5}mol/min, NO_2=3.0 x 10^{-5}mol/min, Pt=1Torr.

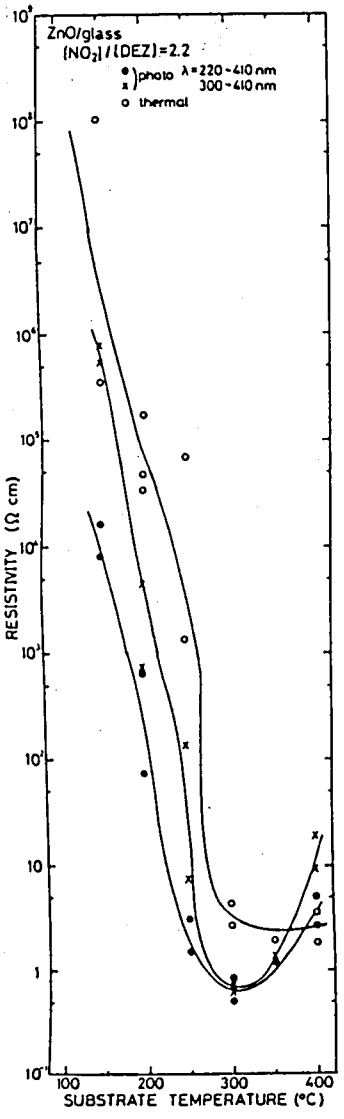

Fig.7.6. Dependence of the resistivity as a function of substrate tempearture and effect of the UV light irradiation on resistivity. DEZ=1.4 x 10^{-5}mol/min, NO_2=3.0 x 10^{-5}mol/min, Pt=1Torr, P=0.7mW/cm^2 (220-410nm) and 0.42mW/cm^2 (300-410nm).

increased from 150 to 300°C can be related to the increase in the Hall mobility caused by an improvement in the crystallinity of the films. The variation of the film resistivity above 300°C may be caused by decreasing the carrier concentration. Photodeposited films had resistivities of $1\text{-}10^4$ Ωcm while films grown under no light irradiation showed resistivities of $10\text{-}10^7$ Ωcm. Photodeposited films showed lower resistivities than those of non-photodeposited films at the same substrate temperatures. The lower resistivities of photodeposited films may be attributed to the better crystallinity, as mentioned above.

7-2. Effects of UV Light Irradiation on the Growth of ZnO Films

7-2-1. Introduction

Photoprocessing , such as laser-induced CVD and laser etching, has proved to be an excellent technology in the production of VLSI and other devices [22]. The photochemical deposition of metals, insulators, amorphous materials and semiconductors using laser technology has been attracting considerable attention because of the need for processes free from ion damage and which occur at low processing temperature. The photo-CVD process also has the advantages of micro fabrication with fine resolution, the ability of doping in local areas, and the possibility of controlling the photochemical process by changing the light wavelength [23]. However, the mechanisms of photopyrolytic deposition are very complicated, and the influence of photon energy on crystal growth is still largely unknown.

Recentry, the photo-CVD technique for the deposition of ZnO

thin films has been employed by R.Solanki,et al. [11,12]. In their work, laser photodissociation of organometallic DMZ (dimethylzinc), and NO_2 and N_2O has been performed to obtain ZnO films with high deposition rates. However, the effects of photochemical reactions in the gas phase and on the surface on film growth characteristics (growth rate, crystallinity, surface morphology, and electrical properties) still remain unknown.

In our group, c-axis oriented ZnO films for applications to SAW devices and optical waveguide devices, using DEZ (diethylzinc), and O_2 and NO_2 as source materials, have been successfully grown at a low substrate temperature (150^{o}C) by using the photo-MOCVD technique with either a Hg or a Xe-Hg lamp [24]. In our experiments, the observed effects of UV light irradiation during the growth run included an increase in the deposition rate, an improvement in c-axis orientation and a decrease in electrical resistivity. Therefore, in ref.24,we suggested that these effects were caused by gas phase and/or surface reactions. However, the different effects between gas phase and surface reactions on the growth of ZnO film have not been clarified.

In this section, photochemical reactions in the gas phase were separated from surface reactions by using an excimer laser as a light source, and the effects of these reactions on the growth of ZnO film are described.

7-2-2. Experimental Procedure

The experimental arrangement is shown schematically in Fig.7.7. The ZnO layers were grown using DEZ($Zn(C_2H_5)_2$) and NO_2

as source materials. The flow rates of gaseous species were regulated by mass flow controllers (STEC Inc. SEC-300). The chamber measures 15cm in diameter and 20cm in height, and has a Ar purge system designed to prevent ZnO deposition on the fused quartz window. The reaction chamber was evacuated by a rotary pump (500 l/min) and the reactor pressure was controlled by a throttle valve. In the present experiment, the flow rates of DEZ and NO_2 were 1.3×10^{-5} (mol/min) and 3.0×10^{-5}(mol/min) ([VI]/[II]=2.3), respectively. The reactor pressure was 1 Torr during the growth run. An excimer laser (Hamamatsu Photonics Co.,Ltd. C2540) operating at 248nm(KrF), with a repetition rate of 30Hz and average power of 0.8W was used as a light source to study the gas phase and surface reactions. DEZ and NO_2(which has larger absorption cross sections than N_2O) have optical absorption bands in the ultraviolet region [13-15,17-21], and are photodissociated at 248nm.

In our photo-MOCVD, in order to investigate the effects of the gas phase and surface reactions by UV light on the growth of ZnO, incident laser beams were directed in two distinct ways. In order to study the photo-CVD process in the gas phase, the laser beam was directed parallel to the substrate by changing the angle of susceptor to the light source. The parallel incident laser beam passed about 1mm above the substrate in order to cause deposition. To change photon density this laser beam was introduced in three ways as follows; 1) without a lens, 2) with a cylindrical lens(f=15cm), 3) with a convex lens(f=15cm). The samples were also situated on the front side of the susceptor at

an angle of 45° to the incident laser light in order to study the effects of surface reactions on growth. Corning 7059 glass and fused quartz were used as substrates. The glass substrate does not transmit KrF laser light, while the quartz substrate is transparent to it. The structural nature of the films was examined by X-ray diffraction, reflection electron diffraction and scanning electron microscopy. Film thickness was measured with a mechanical micro stylus profile meter (Taylor-Hobson Co., Talysurf 4) and by in-situ monitoring of reflectance using a He-Ne laser system.

7-2-3. Gas Phase Reaction

The parallel incident laser light with a rectangular beam of 10 x 22 mm^2 passed above the substrate and caused deposition in the three ways mentioned above. The growth rate of films obtained with and without light irradiation was compared. Figure 7.8 shows the change in growth rate as a function of substrate temperature. The growth rate was affected by the UV light irradiation as well as the photon density of the incident laser light beam. When the laser light was introduced without a lens or with a cylindrical lens, no increase over the thermal growth rate was observed. However, an 25-50% enhancement in growth rate was obtained when the laser beam was focused with a convex lens. When a laser beam is focused into a spot in a gas phase, highly excited gaseous species are formed. Therefore our result suggests that the high excitation of DEZ and/or NO_2 accelerates the reaction to produce the activated species and adsorbed species

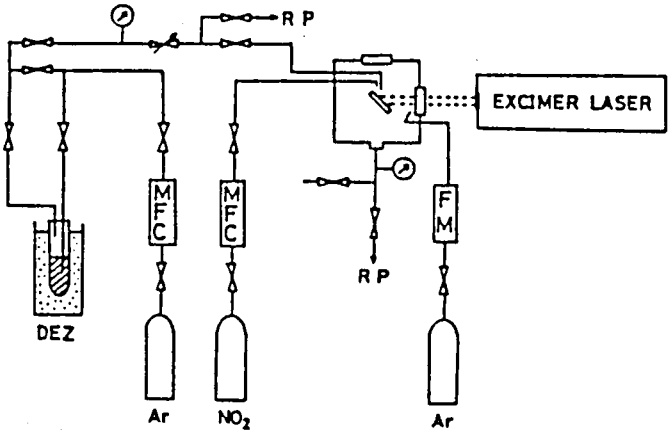

Fgi.7.7. Experimental arrangement for photo-MOCVD system.

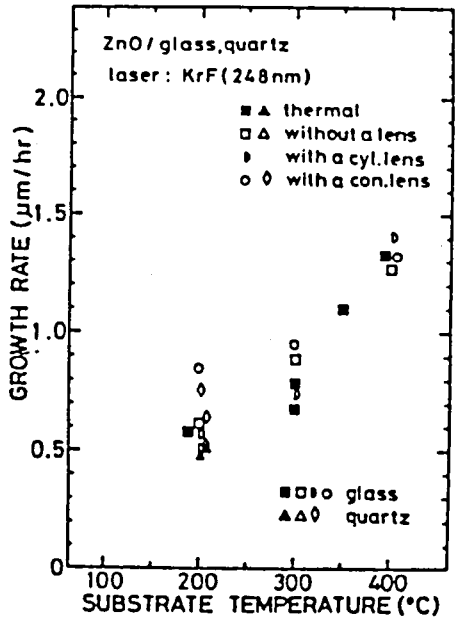

Fig.7.8. Effect of UV laser light irradiation on the growth rate of ZnO films when laser beams passed above the substrate.

responsible for ZnO growth.

The crystalline properties of ZnO films were evaluated by an X-ray diffraction technique and a reflection high energy electron diffraction (RHEED) technique. X-ray diffraction patterns of films grown at higher than 200°C showed only a (002) peak (c-axis planes parallel to the substrate surface). The X-ray diffraction patterns of ZnO films obtained on glass substrates with and without laser light irradiation at a substrate temperature of 200°C showed little difference in crystallinity as shown in Fig.7.9. From this figure it can be seen that the X-ray intensity and the line width of the (002) diffraction peak are almost same. The values of the line width of the (002) diffractions are between 0.7° and 0.75°. The RHEED patterns of the same samples measured above also showed a typical pattern of c-axis oriented ZnO film. These X-ray diffraction and RHEED observation indicates that the crystallinity of the films is not substantially altered by the introduction of light or various photon density. The crystallinity of films on quartz substrates was also unchanged regardless of laser light irradiation.

Surface morphology of the films was observed by a scanning electron microscope (SEM). Using this technique the surface differences of the films observed was insignificant.

Electrical resistivities of ZnO films were measured. The films had resistivities of 10^0-10^6 Ωcm and resistivities were strongly dependent on the substrate temperature as shown in Fig.7.10. The variation of the film resistivity with substrate temperature is caused by the competition between crystallization

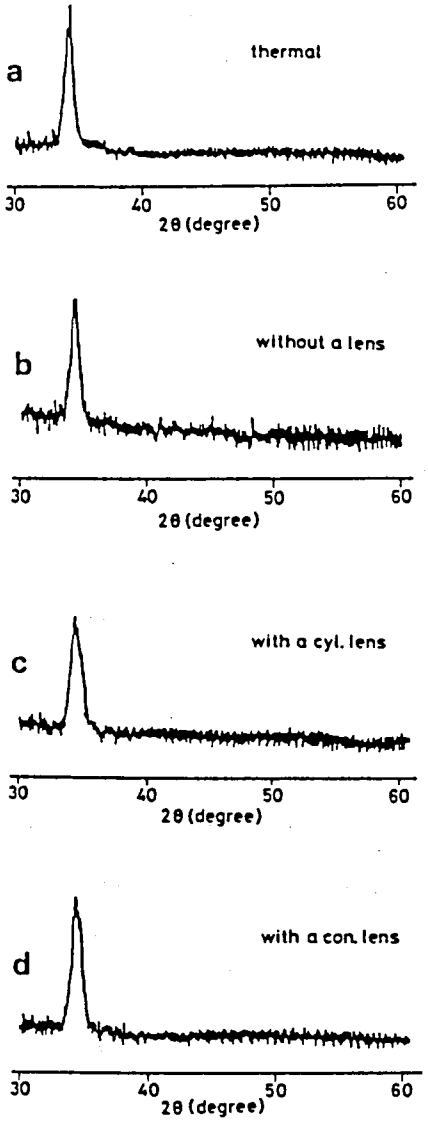

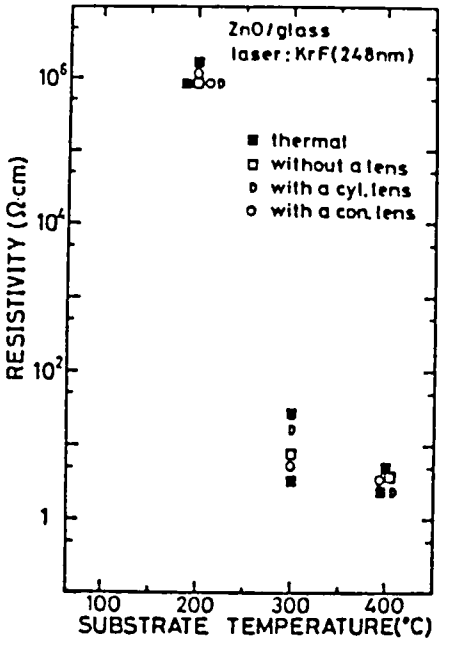

Fig.7.10. Effect of UV laser light irradiation on the resistivity of ZnO films when laser beams passed above the substrates.

Fig.7.9. X-ray diffraction patterns of ZnO films grown at 200°C by: (a) MOCVD; (b) photo-MOCVD (without a lens); (c) photo-MOCVD (with a cylindrical lens); (d) photo-MOCVD (with a convex lens). In photo-MOCVD, laser beams passed above the substrates.

and degree of nonstoichiometry of the films. Resistivities of the films showed nearly the same values regardless of the different kind of irradiation. This means that the electrical characteristics are not dependent on the laser light irradiation in a gas phase, and suggest that the surface reaction rather than the gas phase reaction plays an important role in determining electrical characteristics and growth rate (see under "7-2-4. Surface reaction").

7-2-4. Surface Reaction

In this experiment the substrate surface was set at an incline of 45^{o} to the incident laser beam as shown in Fig.7.7., so that surface as well as the gas phase reactions occurr upon irradiation. However, the more effective reaction of the two is clarified by comparing the results of section '7-2-4.' with '7-2-3.'. In order to prevent the surface temperature from rising, the average laser power used was under 0.8W and the laser beam was introduced without a lens. Figure 7.11 shows the growth rate as a function of substrate temperature. Photo-deposited films on glass and quartz substrates had higher growth rates than those obtained without laser light irradiation at the same substrate temperatures. This increase in the growth rate may be caused by the photodissociation of adsorbed species on the substrate surface and photo-induced carrier excitation effects [25]. The growth rate also increased as the incident laser power was increased, when the substrate temperature was kept at 200^{o}C. This power dependence on growth rate suggests that the enhance-

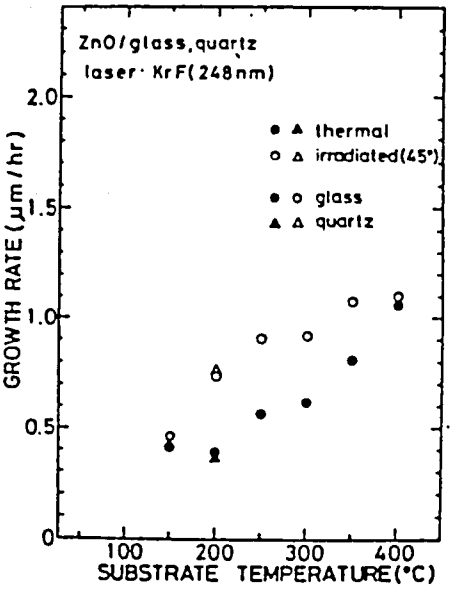

Fig.7.11. Effect of UV laser light irradiation on the growth rate of ZnO films when substrates were directly irradiated by laser beams.

ment of the surface reaction depends on laser power.

C-axis oriented ZnO films were grown on glass substrates by photo-CVD at substrate temperatures higher than 150°C. Figure 7.12 shows the typical X-ray diffraction patterns of the films grown with and without laser light irradiation. The films grown without photo irradiation at 150°C and 200°C were polycrystalline, and showed the weak and broad (002) peak (the line width were 0.9° and 0.6°, respectively.). On the other hand, the X-ray diffraction patterns of the films obtained by photo-CVD at 150°C and 200°C showed the strong and sharp (002) peak (the line width were 0.55° and 0.35°), and a great improvement in c-axis orientation was observed, as shown in Fig.7.12.. The RHEED patterns of these films also showed an improvement in c-axis orientation compared with those of films grown under no laser light irradiation. This improvement in c-axis orientation of films was also observed when fused quartz was used as a substrate. The better quality films could be explained by more complete dissociation of DEZ and NO_2, and the role of UV light on enhancing mobility of adsorbed species.

SEM observations showed that laser light irradiation also did not produce a great improvement in surface morphology in most cases and showed the enlargement of grains.

Figure 7.13 shows electrical resistivities of ZnO films as a function of substrate temperature. It is noted that the resistivity is decreased by increasing the substrate temperature. ZnO films grown by photo-MOCVD have lower resistivities (10^{-1}-10^{0} Ω cm) than those obtained without photo irradiation. The im-

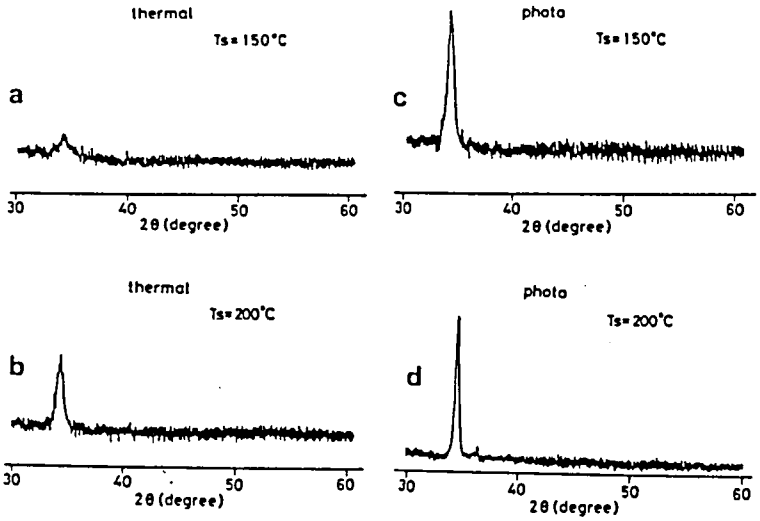

Fig.7.12. X-ray diffraction patterns of ZnO films grown by: (a) MOCVD (150°C); (b) MOCVD (200°C); (c) photo-MOCVD (150°C); (d) photo-MOCVD (200°C). In photo-MOCVD, the substrates were directly irradiated by laser beams.

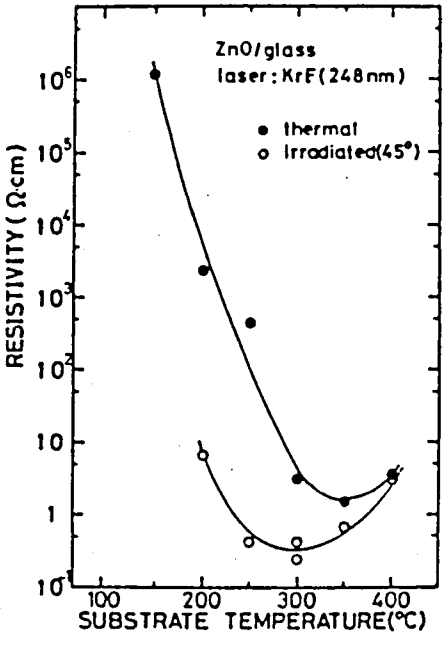

Fig.7.13. Effect of UV laser light irradiation on the resistivity of ZnO films when the substrates were directly irradiated.

provement in c-axis orientation of film with photo irradiation is one of the most effective causes in the decrease of film resistivity.

As mentioned above, the different characteristics of films grown using photochemical reactions in the gas phase and at the surface were observed. The improvement in crystallinity of ZnO films on sapphire substrates for obtaining single crystalline films was also observed only when the substrates were irradiated directly. These results show that the surface photochemical reactions caused by UV light irradiation play a very important role in adsorption, desorption, the photo induced carrier excitation effect on both the deposited ZnO layers and on the substrate [25], and acceleration of surface migration. The details of photochemical reactions which occur at the sample surface still remain unknown because they are very complicated, and difficult to observe in situ. At this stage, we have observed the effects of laser light irradiation on the initial adsorbed DEZ and NO_2 species which, in turn, affected the succeeding photo-CVD process. Therefore, we think that the effects of UV light irradiation on the adsorbed species is one of the important factors in photo-CVD.

For chemical interaction on light absorbing substrates, the substrate heating effect by direct laser irradiation is an important factor in determining the surface reaction rates. In our experiment, the solution of the heat conduction equation shows that an estimation of the surface temperature rise caused by a laser beam should be lower than about $30^{\circ}C$ [26]. It has been

shown that the same photo irradiation effects can be observed when UV lamps with low irradiation power are used as a light source [24]. Therefore the UV photoirradiation effects mentioned in this paper are light-induced and not thermal.

7-3. Conclusion

In summary, metallic Zn films and c-axis oriented ZnO films have been successfully grown, the former at room temperature and the latter at a substrate temperature of 150^{o}C, respectively, by photo-MOCVD. In our deposition technique, the UV light has effects on growth rate, crystallinity and resistivity because of its important role in the gas phase reaction and the surface reaction. The light source was a mercury lamp or xenon-mercury lamp. Consequently, a complex light source system, such as an excimer laser, is not always necessary to obtain ZnO films.

Photo-MOCVD experiments were also performed, using DEZ and NO_2 as source materials and an excimer laser as a light source, to investigate the effect of UV light on the gas phase and surface reactions responsible for the growth of ZnO. The incident laser beam was directed in two distinct ways. When the laser light was induced above the substrate, photochemical reactions which occurred in the gas phase affected the growth rate of films but the crystallinity was not affected. When the substrate was irradiated directly by a laser light beam, changes in the growth rate, the c-axis orientation, and the electrical resistivity of ZnO films were observed. In this experiment, c-axis oriented ZnO films have been grown successfully on glass sub-

strates at a substrate temperature of 150°C. These experimental results indicate that surface reactions induced by photon energy, such as photoadsorption, photodesorption, photoinduced carrier excitation effect and photocatalytic reaction, play an important role in affecting the growth of ZnO films. These detailed surface reactions are now under investigation.

References

[1] T.Shiosaki, S.Ohnishi, Y.Murakami and A.Kawabata, J.Crystal Growth 45(1978)346.

[2] T.Shiosaki, in: Proc.1978 IEEE Ultrasonics Symp.,1978,p.100.

[3] T.Yamamoto, T.Shiosaki and A.Kawabata, J.Appl.Phys. 51(1980)3113.

[4] S.Ohnishi, Y.Hirokawa, T.Shiosaki and A.Kawabata, Japan.J.Appl.Phys. 17(1978)773.

[5] T.Shiosaki, S.Ohnishi and A.Kawabata, J.Appl.Phys. 50(1979)3113.

[6] M.Shimizu, Y.Murakami, S.Wada, T.Shiosaki and A.Kawabata,in: Proc.2nd Meeting on Ferroelectric Materials and TheirApplications, 1979, p.185.

[7] M.Shimizu, T.Shiosaki and A.Kawabata, J.Crystal Growth 57(1982)94.

[8] T.Shiosaki, T.Yamamoto, M.Yagi and A.Kawabata, Appl.Phys. Letters 39(1981)399.

[9] M.Shimizu, T.Horii, T.Shiosaki and A.Kawabata, Thin Solid

Films 96(1982)149.

[10] M.Shimizu, Y.Matsueda, T.Shiosaki and A.Kawabata, J.Crystal Growth 71(1985)209.

[11] R.Solanki and G.J.Collins, Appl.Phys.Letters 42(1983)662.

[12] P.K.Boyer, C.A.Moor, R.Solanki, W.K.Ritchie, G.A.Roche and G.J.Collins,in: Laser Diagonostics and Photochemical Processing for Semiconductor Devices, Eds. R.M.Osgood, S.R. J.Brueck and H.R.Schlossberg (Elsevier, Amsterdam, 1983).

[13] H.W.Thompson, J.Chem.Soc. 2(1934)790.

[14] H.W.Thompson, Proc.R.Soc.London A150(1935)603.

[15] H.W.Thompson and J.W.Linnett, Proc.Roy.Soc.(London) A156(1936)108.

[16] D.J.Ehrlich and R.M.Osgood,Jr., Chem.Phys.Letters. 79(1981)381.

[17] P.Hartman, Physicsand Chemistry ofthe Organic Solids (Interscience, New York, 1963).

[18] S.Hayakawa and K.Wasa, Thin Film Technology(Kyoritsu, Tokyo, 1982)(in Japanese).

[19] T.C.Hall, Jr. and F.E.Blacet, J.Chem.Phys. 20(1952)1745.

[20] I.T.N.Jones and K.D.Bayes, J.Chem.Phys. 59(1973)4836.

[21] H.S.Johnston and R.Graham, Can.J.Chem. 52(1974)1415.

[22] D.J.Ehrlich, R.M.Osgood,Jr. and T.F.Deutsch, IEEE. J. Quantum Electron. QE-16(1980)1233.

[23] D.J.Ehrlich and J.Y.Tsao, J.Vac.Technol. B1(1983)969.

[24] M.Shimizu, H.Kamei, M.Tanizawa, T.Shiosaki and A.Kawabata, J.Crystal Growth 89(1988)365.

[25] H.Yokoyama, Appl.Phys.Letters 49(1986)1345.

[26] D.M.Kim, D.L.Kwong, R.R.Shah and D.L.Crosthwait, J.Appl.Phys. 52(1981)4995.

CHAPTER VIII. CONCLUSIONS

In this study, the growth of ZnO thin films by various techniques and their characteristics were investigated. The applications of the obtained ZnO films, such as optical waveguides, piezoelectric transducers and solar cells, were also investigated. The following results were obtained.

(1) A historical background of this study and the purpose of the study were described. (CHAPTER I.)

(2) Singlecrystal ZnO films with smooth surfaces have been grown on sapphire substrates by a CVD ($ZnO-H_2-O_2-H_2O$) system. The $(11\bar{2}0)$and (0001) ZnO have been grown epitaxially on $(01\bar{1}2)$ and (0001) sapphire substrates. In this CVD method, at the first step of the film growth, an intermediate thin layer was deposited by a sputtering system. At succeeding process, a $ZnO-H_2-H_2O-O_2$ chemical reaction syatem was carried out. The intermediate sputter-deposited ZnO layer played an important role of providing a high density of nuclei in succeeding CVD process. This layer also acts as a buffer layer which reduce the difference of thermal expansion coefficient at lattice constant between ZnO and sapphire. The successful selective crystal growth was made by using this CVD technique.

The as-grown films showed a n-type conduction and had resistivities of 10^{-2}-10^{-1} Ωcm, Hall mobilities of 40-120 $cm^2/Vsec$ and carrier concentrations of 10^{17}-10^{18} cm^{-3}. The temperature dependence of these electrical properties was very weak. This suggest that the obtained ZnO films are degenerated or have some

shallow doners. The dependence of electrical properties on film thickness also showed the existence of highly conductive layer at the interface between ZnO and sapphire. Films with average transmittance above 80% in visible region were obtained. The electrical and optical characteristics were strongly dependent on the growth rate and substrate temperature. (CHAPTER II.)

(3) The low losses epitaxial ZnO optical waveguides were fabricated by the CVD metod. The minimum attenuation loss obtained was 0.87 dB/cm for TE_0 mode at 6328Å. The ridge type optical waveguides with about 2.5 μm width were also fabricated by the selective area growth technique in our CVD. The ridge type waveguide showed the attenuation loss of 40.3 dB/cm. (CHAPTER III.)

(4) A higly c-axis oriented ZnO thin film with a high optical transparency was grown at a high growth rate of 90 μm/hr on a silicon substrate by a ZnO-H_2-O_2-H_2O CVD system. Thin ZnO films were reproducibly obtained on silicon substrates only when an intermediately sputterd thin ZnO layer was presented. In this CVD method, the intermediate thin ZnO layer provides a high density of nuclei and serves as a buffer layer in succeeding CVD process. A ZnO film was selectively chemical-vapor-deposited on the part of the silicon substrate with a very thin sputter-deposited ZnO layer, with no chemical vapor deposition on the bare silicon substrate itself. The low resistivity, combined with optical transparency at visible to infrared, surface flatness, and good adherence to the silicon substrate of the ZnO film suggest the feasibility of ZnO/Si heterojunction solar cells,

which have shown a rather poor conversion efficiency of 0.92% so far. (CHAPTER IV.)

(5) Plasma-enhanced metalorganic chemical vapor deposition, using diethylzinc as a source of Zn, has proved to be an excellent method to obtain ZnO films at low substrate teperatures. Highly c-axis oriented and epitaxial ZnO films have been grown on glass and sapphire substrates at substrate temperatures of 150-350^{o}C. In this method, ZnO films were obtained by reacting diethylzinc with CO_2 or O_2 gas. The crystallographic properties and surface morfology of the films were greatly affected by the rf input power level, the substrate temperature and the growth rate.

Thin ZnO films with a high degree of c-axis orientation has been grown on Si, SiO_2/Si, ceramic and polyimide substrates at substrates temperatures of 200-350^{o}C and rf input power of 150-260W, using CO_2 as an oxidizing gas. Utilizing the reaction of diethylzinc with NO_2, highly c-axis oriented films have been obtained on glass substrate at substrate temperatures of 150-350^{o}C and rf input power of 60-260W, and epitaxial films have been grown on sapphire substrates at higer than 250^{o}C and rf input power of more than 100W. A piezoelectric transducer with a fundamental frequency of 35MHz and heterojunction solar cells were obtained by using the plasms-deposited ZnO films. The maximum conversion efficiencies obtained with an n-ZnO/p-Si cell and n-ZnO/p-CdTe cell were 0.95% and 4.4%, respectively. (CHAPTER V.)

(6) For the first time, a low pressuer microwave discharge

process has been used to deposit c-axis oriented and epitaxial ZnO thin films. The growth of ZnO films were accomplished by using the reaction between diethylzinc, and microwave(2.45GHz) oxygen or dinitrogen monooxide plasmas at substrate temperatures of 150 and 400°C, respectively. In this method, ZnO films have been obtained at a maximum distance of 50cm from the microwave plasma region because of the fact that the active oxygen and dinitrogen monooxide species have a long life time. Therefore, film deposition can be free from plasma damage and the surface of the ZnO films obtained showed good flatness. The crystallographic, and electrical and optical properties of films were strongly dependent on the growth conditions. The control of resistivity was carried out by doping Li and Al. c-Axis oriented ZnO film showed the minimum optical waveguide loss of 2.0dB/cm for TE_1 mode at 6328Å. (CHAPTER VI.)

(7) Zn films and c-axis oriented ZnO films have been successfully grown, the former at room temperature and the latter at a substrate temperature of 150°C, respectively, by photo-MOCVD, using a mercury lamp and a xenon-mercury lamp as a light source, and DEZ as a source of Zn, and O_2 and NO_2 as an oxidizing gas. The effects of ultraviolet light irradiation on the growth of ZnO have been examined. An increase in the growth rate, an improvement in c-axis orientation and a decrease in the electrical resistivity of ZnO film were observed when the substrates were irradiated by an ultraviolet light during the growth run.

The effects of UV laser light irradiation on the growth of ZnO films by photo-MOCVD, using DEZ and NO_2 as source materials

and an excimer laser as a light source, have been investigated. When the laser beams were passed above the substrates, the film growth rate changed compared to growth without laser light. When the substrates were directly irradiated by the laser beam, the observed effects included an increase in the growth rate of the film, an improvement in c-axis orientation and a decrease in the electrical resistivity of the ZnO film. These results mean that surface reactions play a very important role in photo-MOCVD of ZnO. (CHAPTER VII.)

APPENDIX : MECHANICAL PROPERTIES OF FILM

1-1. Adhesion of ZnO Films to Substrates

1-1-1. Introduction

The strength and durability of a relatively fragile film is largely dependent on the adhesion between the film and substrate. Adhesion is the force of static friction between two bodies or the effects of this force. Since adhesion is related to the nature and the strength of the binding forces at interfaces between the two materials in contact with each other, a study of thin film is of both practical and fundamental interest.

Many attemps have been used to measure adhesive force. The typical methods for measuring adhesion are as follows;

1) scratch test [1-9]
2) pull test [10-11]
3) peel test ("scotch tape" test) [12-13]
4) others
   i) topple test [14]
   ii) abrasion test [15-16]
   iii) ultrasonic test [17]
   iV) centrifugal force test [18-20]

Among these methods mentioned above peel method (tape method) is simplest one. This method employs an adhesive tape to lift the film off the substrate and gives only qualitative results. Tensile tester (pull test), ultrasonic vibrations (ultrasonic test), and ultra centrifuge (centrifuge test) have been employed to apply the required force but with inconsistent results.

I our study the scratch tests suggested by Heavens was used

to measure adhesion between ZnO film and the substrates.

1-1-2. Experiemtal Procedure

In the scratch test, a smoothly rounded stylus which is drawn across the film surface is used. A vertical load applied to the stylus is gradually increased until a critical value is reached. The film is peeled from the substrate and a clear channel is left when a critical value is reached. The critical load, the scratch channel width and the cracking area along the scratch track of the film indicate the adhesion of the film.

The experimental apparatus used in this study was a micro-hardness tester (Taiyo Tester Co. Ltd. SM-2), which is shown in Fig.1.1. This commercial hardness tester has a scratch stylus similar to the Knoop hardness indentor with diamond tips. The loads of indentor can be changed from 3 grams for weakly adherent films to 500grams for strongly adherent films, and the stage on which sample is set can be moved from a velocity of 0.1mm/sec to 0.36mm/sec. The scratched traces of the films are observed by a microscope.

1-1-3. Results and Discussion

In the scratch test technique, the extent of peeling of film by indentor indicates the amount of adhesion to be studied. The load of indentor was changed from 5g to 50g, and the stage on which sample was set was moved parallel to the tip of indentor at a velocity of 0.2mm/sec. The scratch traces were inspected by a microscope, as shown in Fig.1.2. This figure shows a typical

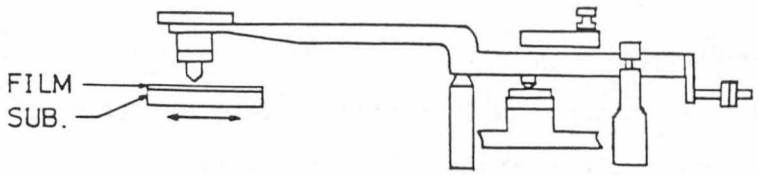

Fig.1.1. Schematic diagram of a microhardness tester.

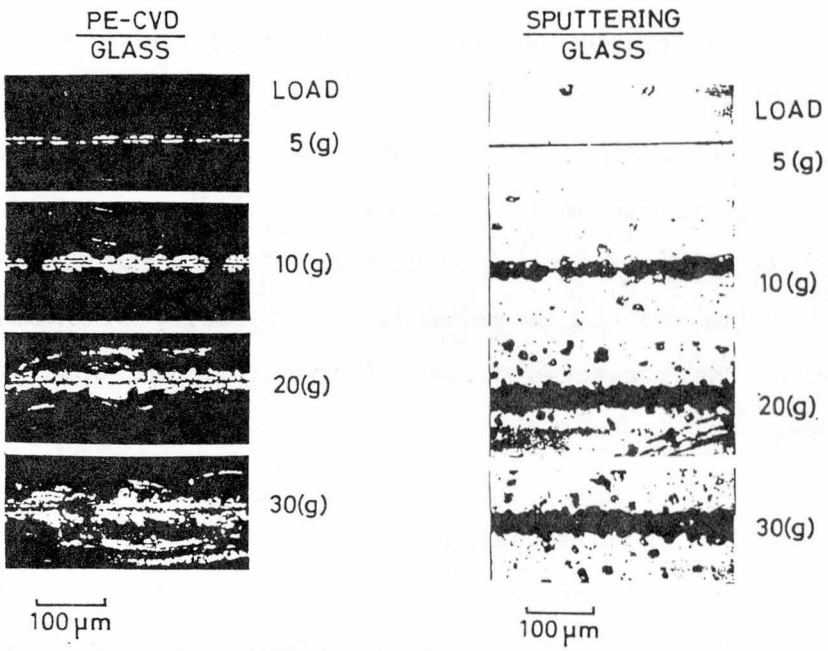

Fig.1.2. Optical micrographs of a scratch test illustrating the effect of the indentation load and the film preparation methods.

scratch test of adhesion of ZnO film depoisited on glass substrate by the sputtering and PE-MO-CVD methods. The scratch track width increased as the test load was increased. The peeling width and area along the scratch track of the film grown by the sputtering method was somewhat smaller than that of the film grown by the PE-MO-CVD method. This indicates that the adhesion of plasma-deposited ZnO film to glass substrates is somewhat weaker than that of sputtered ZnO film. The optical micrographs of scratch tests of ZnO film on sapphire $(01\bar{1}2)$ substrate by the sputtering, PE-MO-CVD and CVD method is shown in Fig.1.3. ZnO films illustrated in this figure are epitaxially grown on sapphire substrate. In this case the scratch track width also increased with increasing the test load, and so much difference of the track width of the film deposited by each method could not be found, which means that epitaxially grown films obtained by different deposition technique as mentioned above have nearly same adhesion to sapphire $(01\bar{1}2)$ substrate. The adhesion test of the films to the glass substrate and sapphire substrate, as shown in Fig.1.4., clarifys that the adhesion between epitaxial films and sapphire substrate is stronger than that between ċ-axis oriented films and glass substrate.

The adhesion between ZnO films and other substrates was also examined. The typical scratched traces are shown in Fig.1.5. The width and area of peeling increased with increasing load. The peeling area of the films on glass and (111)Si substrates was larger than that on SiO_2/(100)Si and polyimide films at the same load. In the case of polyimide substrate, the scratch width

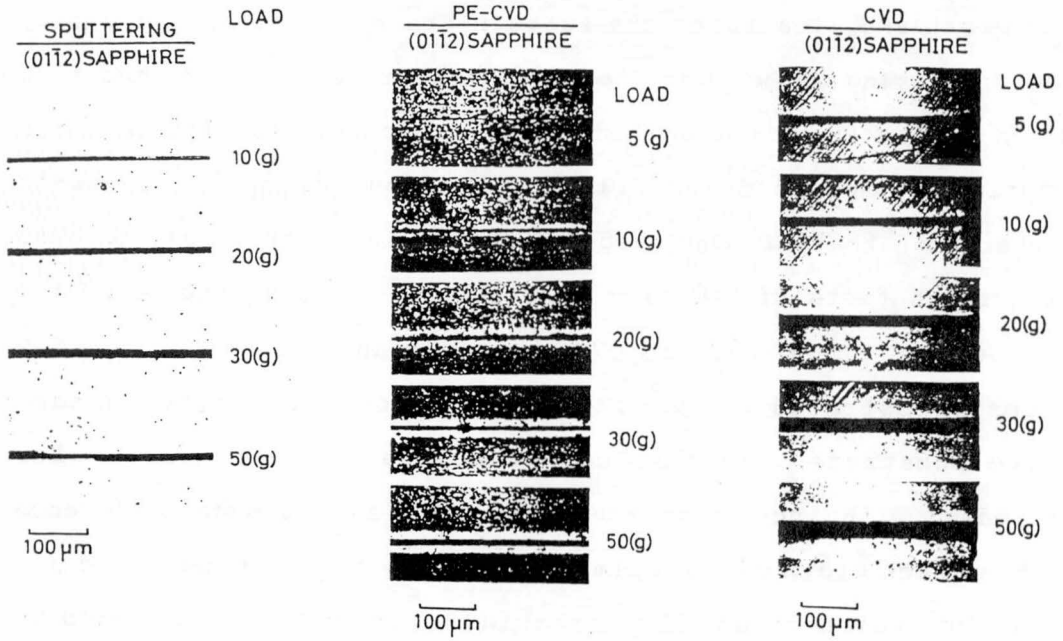

Fig.1.3. Optical micrographs of scratch tests illustrating the effect of the indentation load and the film preparation methods.

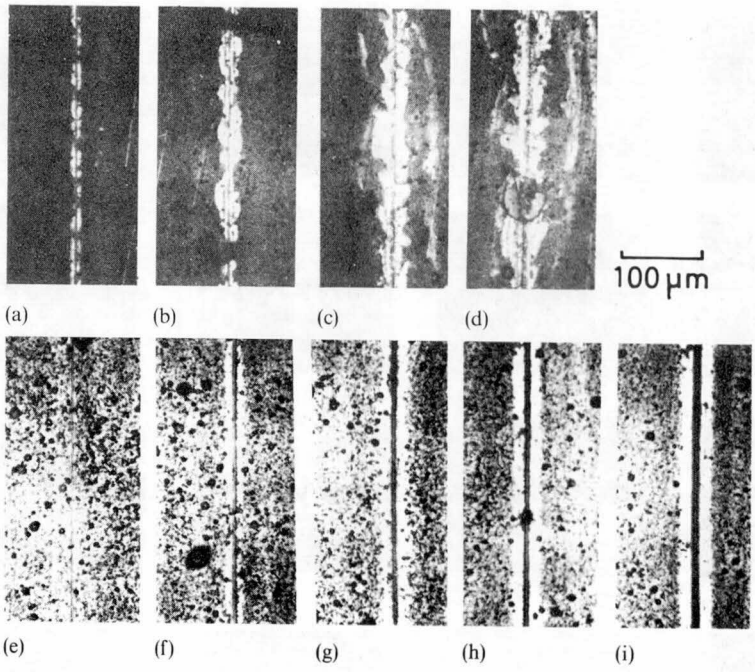

Fig.1.4. Optical micrographs of scratch test illustrating the effect of the indentation load and the substrate: (a)-(d) highly c-axis oriented ZnO film on a glass substrate; (e)-(i) ZnO ($11\bar{2}0$) film on a sapphire (0112) substrate at the following loads: (a), (e) 5gf; (b), (f) 10gf; (c), (g) 20gf; (d), (h) 30gf; (i) 50gf.

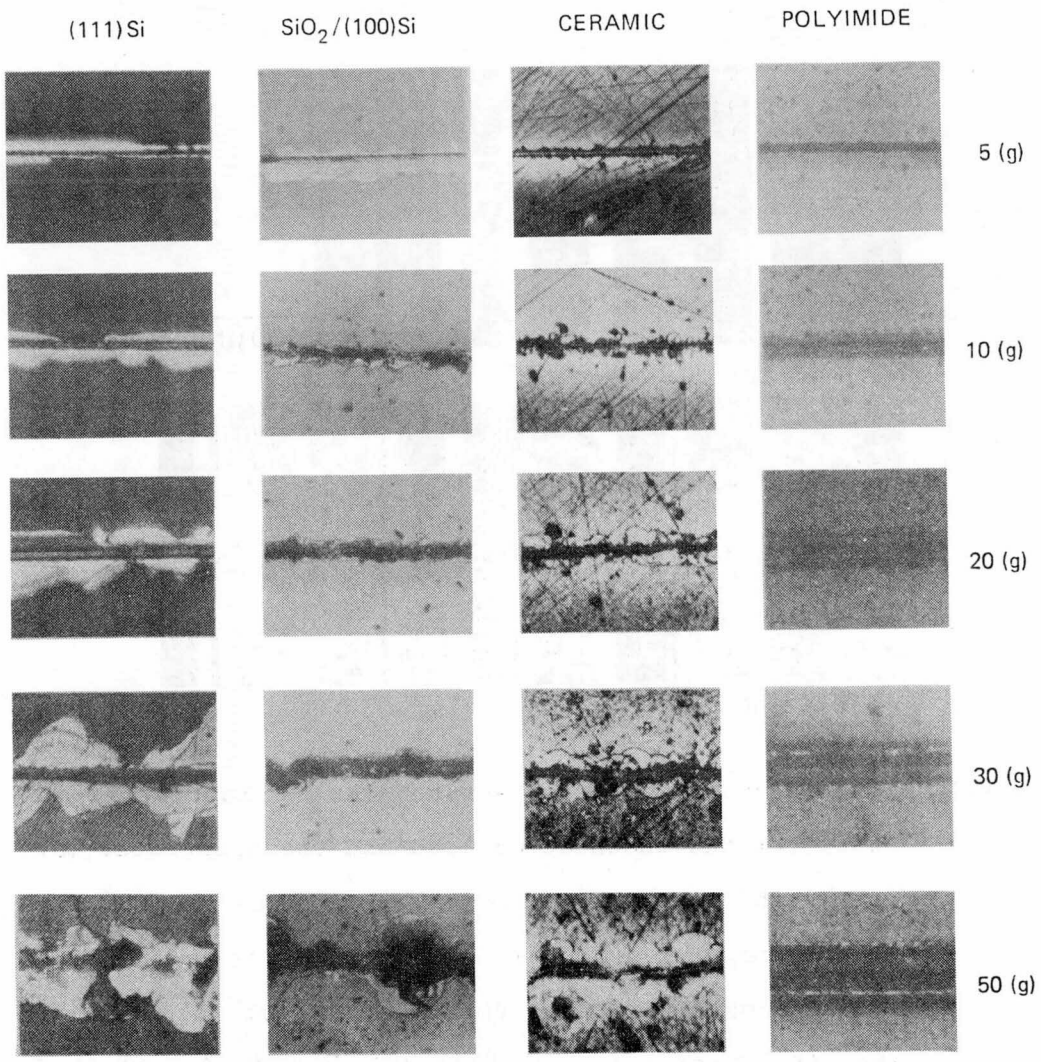

Fig.1.5. Optical micrographs of scratch tests illustrating the effect of the indentation load and the substrate.

increased with increasing load, although no peeling of the ZnO film was observed. Polyimide substrates with thick ZnO deposition curled up owing to difference between ZnO and polyimide of the expansion coefficience, but the films did not peel off the substrates. These facts show that the adhesion between the ZnO film and the polyimide substrate is considerably stronger than that between the film and other substrates.

Figure 1.6 shows the results of the adhesion test for ZnO films grown by PE-MO-CVD and also by sputtering to polyimide substrates. The sputtering system used was an rf planar magnetron sputtering system. The peeling and cracking area along the scratch track of the film grown by the sputtering was somewhat larger than that of the film by PE-MO-CVD.

1-2. Microhardness of ZnO Films

1-2-1. Introduction

Whatever the application of thin films may be their mechanical stability are also essential qualities. The hardness is a kind of mechanical properties of film and is defined as a resistance of a metal or other material to indentation, scratching, abrasion, or cutting. Some methods are used to determine the relative hardness of a metal, mineral, or other material according to one of several scales, such as Brinell, Mohs, or Shore. The hardness test using light test loads is called microhardness test. The relative hardness of materials is determined by the Knoop indentation test and Vikcers hardness test [20]. The Knoop test has higher sensitivity than the Vickers test in measuring

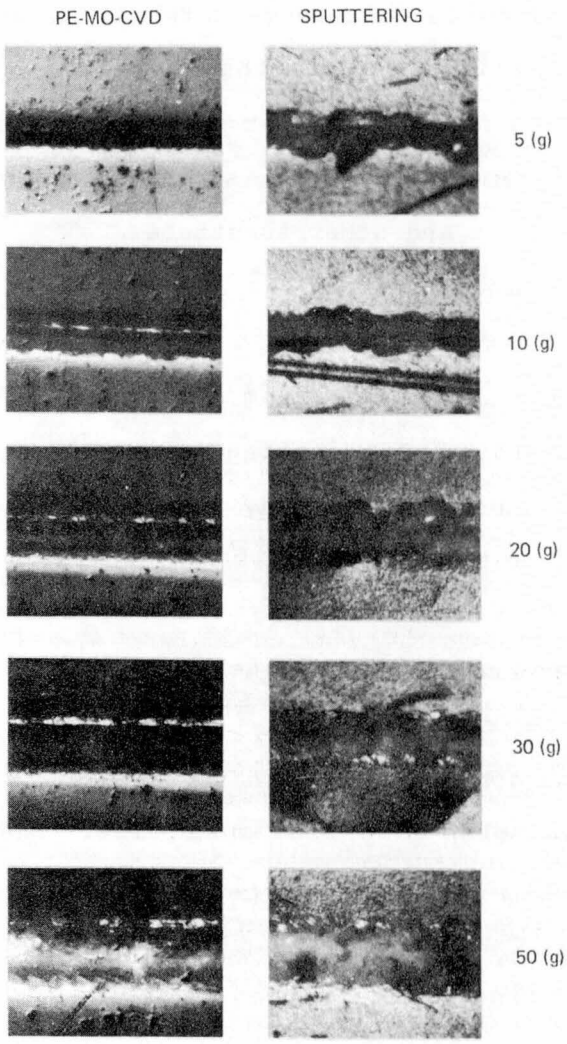

Fig.1.6. Optical micrographs of scratch tests illustrating the effect of film fabrication.

the film hardness, and is suitable for microhardness test of thin film. In this study the relative microhardness of a ZnO film was determined by the Knoop indentation test.

1-2-2. Experimental Procedure

In microhardness test, a microhardness tester (Taiyo Tester Co. Ltd. SM-2) was also used. A diamond pyramid indenter which has a rhombic base with diagonals in a 1:7 ratio and included apical angles of 130° and $172^{\circ}30'$ is forced under variable loads into the surface of a test specimen. The relative microhardness is determined by the depth to which the Knoop indenter penetrates.

The Knoop hardness is given by

$$H_K = F/0.070281^2$$

where F is a load and l is a diagonal (see Fig.1.7).

1-2-3. Results and Discussion

The Knoop hardness of films obtained by CVD, PE-MO-CVD and sputtering was measured. The Knoop hardness (H_K) is given in Table 1-1. This haradness value of each sample is averaged one over five times. It is clear that the Knoop hardness of film prepared by CVD is smallest. Films grown on $(01\bar{1}2)$ sapphire substrate show smaller hardness value than that of films grown on glass substrate. This facts means that the hardness of films depends on growth plane.

1-3. Conclusion

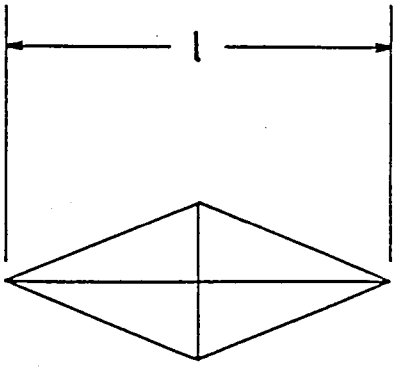

Fig.1.7. The knoop hardness test.

Table 1-1. Results of the knoop hardness test.

	HARDNESS TEST			
Sample		H_k	Load (g)	Depth (μm)
CVD	(Sapphire)	306.7	5	0.5
PE-CVD	(Sapphire)	519.5	15	0.6
PE-CVD	(Glass)	514.4	15	0.7
Sputter	(Sapphire)	718.9	15	0.6
Sputter	(Glass)	523.1	15	0.7

The adhesion of highly c-axis oriented and epitaxial ZnO films grown by sputtering, CVD and PE-MO-CVD to glass, sapphire, Si, SiO_2/Si, ceramic and polyimide substrates was measured. This adhesion test was performed by the scratch test technique. The adhesion of ZnO films to sapphire and polyimide substrates was stronger than that to glass and Si substrates. The adhesion of thin films obtaine by PE-MO-CVD to polyimide substrates is fairly good, not inferior to that when the sputtering method, is applied. The Knoop hardness of ZnO film was also measured, and it was found that the hardness of the CVD film was smaller than that of the PE-MO-CVD and sputtered films.

References

[1] T.Kuroda, T.Noda, R.Ueda, Oyo Butsuri 17(1948)331.

[2] O.S.Heavens, J.Phys.Radium 11(1950)355.

[3] S.Baleson, Vacuum 2(1952)365.

[4] P.Benjamin and C.Weaver, Proc.Roy.Soc. A254(1960)163.

[5] P.Benjamin and C.Weaver, Proc.Roy.Soc. A254(1960)177.

[6] P.Benjamin and C.Weaver, Proc.Roy.Soc. A261(1961)516.

[7] P.Benjamin and C.Weaver, Proc.Roy Soc. A274(1963)267.

[8] M.M.Karnowsky and W.B.Estill, Rev.Sci.Instrum. 35(1964)1324.

[9] J.R.Frederick and K.C.Ludema, J.Appl.Phys. 35(1964)256.

[10] R.B.Belser and W.H.Hicklin, Rev.Sci.Instrum. 27(1956)293.

[11] R.Jacobsson and B.Kruse, Thin Solid Films 15(1973)71.

[12] J.Strong, Rev.Sci.Instrum. 6(1935)97.

[13] B.N.Chapman, in: Aspects of Adhesion, Ed.D.J.Alner (Univ. London Press,London,1971).

[14] D.W.Butler, J.Phys. E3(1970)979.

[15] M.G.Townsley, Rev.Sci.Instrum. 16(1945)143.

[16] F.Scossberger and D.Franson, Vaccum 9(1959)28.

[17] S.T.Moses and R.K.Witt, Ind.Eng.Chem 41(1949)2334.

[18] J.W.Beams, J.L.Young and J.W.Moor, J.Appl.Phys. 17(1946)886.

[19] J.W.Beams, J.B.Frezeal and W.L.Bart, Phys.Rev.100(1955)1657.

[20] J.W.Beams, in: Structure and Properties of Thin Films, Eds. C.A.Neugebauer, J.W.Newkivk and D.A.Vermilea, (Willy,New York,1959)p.183.

[21] Thin Film Handbook, Ed. Japan Society for the Promotion of Science 131st Committee, (Ohm.Co.,Tokyo,1983)p.349.

LIST OF PUBLICATIONS AND REPORTS

I. List of Publications

1) "Fabrication Technique of Ridge Waveguides by CVD Selective Crystal Growth of ZnO Thin Films",
M.Shimizu, Y.Murakami, S.Wada, T.Shioski and A.Kawabata: Proc. 2nd Meeting of Ferroelectric Materials and Their Applications (1979) pp.185-188.

2) "Plasma-Enhanced Metalorganic Chemical Vapor Deposition of c-Axis Oriented and Epitaxial Films of ZnO at Low Substrate Temperatures",
T.Shiosaki, T.Yamamoto, M.Yagi, M.Shimizu and A.Kawabata:
Proc. IEEE 1981 International Ultrasonics Symposium (IEEE New York, 1981) pp.498-501.

3) "Growth of c-Axis Oriented ZnO Thin Films with High Deposition Rate on Silicon by CVD Method",
M.Shimizu, T.Shiosaki and A.Kawabata:
J.Cryst.Growth 57(1982) pp.94-100.

4) "Preparation of Highly c-Axis Oriented ZnO Thin Films by Plasm-Enhanced Metalorganic Chemical Vapor Deposition",
M.Shimizu, T.Yamamoto, T.Shiosaki and A.Kawabata:
Proc. of 2nd Symposium on Ultrasonic Electronics, Tokyo 1981, Jpn.J.Appl.Phys. 21, Suppl.21-3 (1982) pp.63-65.

5) "Preparation of ZnO Thin Films by Plasma-Enhanced Organometalic Chemical Vapor Deposition",
M.Shimizu, T.Horii, T.Shiosaki and A.Kawabata:

Thin Solid Films 96(1982) pp.149-154.

6) "Growth of ZnO Films by the Plasma-Enhanced Metalorganic Chemical Vapor Deposition Technique",
M.Shimizu, Y.Matsueda, T.Shiosaki and A.Kawabata:
J.Cryst.Growth 71(1985) pp.209-219.

7) "Low Temperature Growth of ZnO Films by Photo-MOCVD",
M.Shimizu, H.Kamei, M.Tanizawa, T.Shiosaki and A.Kawabata:
J.Cryst.Growth 89(1988) pp.365-370.

8) "Effects of UV Light Irradiation on the Growth of ZnO Films",
M.Shimizu, A.Monnma, T.Shiosaki, A.Kawabata and Y.Yamamoto:
J.Cryst.Growth 94(1989)pp.895-900.

9) "Photo-MOCVD of ZnO Epitaxial Films",
M.Shimizu, T.Katayama, T Shiosaki and A.Kawabata:
to be published in J.Cryst.Growth

10) "Laser-Induced MOCVD of ZnO Thin Film",
M.Shimizu, T.Katayama, Y.Tanaka, T.Shiosaki and A.Kawabata:
to be submitted to J.Cryst.Growth

II. International Conference

1) "Plasma-Enhanced Metal Organic Chemical Vapor Deposition of c-Axis Oriented and Epitaxial Films of ZnO at Low Substrate Temperatures",
T.Shiosaki, T.Yamamoto, M.Yagi M.Shimizu and A.Kawabata:
IEEE 1981 International Ultrasonic Symposium, Chicago, Illinois, USA, October 14-16, 1981.

2) "Preparation of ZnO Thin Films by Plasma-Enhanced Organometallic Chemical Vapor Deposition", M.Shimizu, J.Horii, T.Shiosaki and A.Kawabata: Metallurgical Coatings International Conference, 1982, San Diego, California, USA, April 5-8, 1982.

III. List of Technical Reports

1) "Growth of ZnO Thin Films on Sapphire Substrates with Intermediately Sputter-Deposited ZnO Layers", M. Shimizu, Y. Murakami, T. Shiosaki and A. Kawabata, Extended Abstracts (The 39th Autumn Meeting, 1978); The Japan Society of Applied Physics p.40.

2) "Electrical Properties of Single-Crystaline ZnO ThinFilms" M. Shimizu, K. Sakai, Y. Murakami, T. Shiosaki and A. Kawabata, Extended Abstracts (The 26th Spring Meeting, 1979); The Japan Society of Applied Physics and Related Societies p.236.

3) "Fabrication of Ridge Optical Waveguides by Chemical Vapor Deposition", M. Shimizu, Y. Murakami, T. Shiosaki and A. Kawabata, Extended Abstracts of the 2nd Meeting on Ferroelectric Materials and Their Applications (1979) pp.55-56.

4) "Fabrication of ZnO Ridge Optical Waveguides", M. Shimizu, S. Wada, T. Shiosaki and A. Kawabata, Extended Abstracts (The 27th Spring Meeting, 1980); The Japan Society of Applied

Physics and Related Societies, p.222.

5) "Electrical and Optical Properties of ZnO SingleCrystalline Films", M. Shimizu, H. Kakuno, T. Shiosaki and A.Kawabata, ibid p.694.

6) "Diffusion Effects of Metal on the Properties ofSputtered ZnO Films for Optical Waveguide", S. Wada, Y. Hamana, M. Shimizu, T. Shiosaki and A. Kawabata, ibid, p.293.

7) "Photoluminescence Properties of ZnO Thin Films", M. Shimizu, S. Wada, T. Shiosaki and A. Kawabata, Extended Abstracts; The Physical Society of Japan (1980) p.99.

8) "Diffusion Effects of Se and S on the Properties ofZnO Single Crystal Films", M. Shimizu, S. Wada, T. Goto, T. Shiosaki and A. Kawabata, Extended Abstracts (The 41th Autumn Meeting, 1980); The Japan Society of Applied Physics, p.622.

9) "Growth of ZnO on Silicon Substrates by CVD", M.Shimizu, T. Shiosaki and A. Kawabata, ibid, p.624.

10) "Preparation of ZnO Thin Films by MO-CVD", M. Yagi, M. Shimizu, H. Nitta, T. Shiosaki and A. Kawabata, ibid p.625.

11) "Diffusion Effects of Se and S on the properties of ZnO Single Crystal Films (II)", M. Shimizu, H. Yada, T.Shiosaki and A. Kawabata, Extended Abstracts (The 28th Spring Meeting, 1981); The Japan Society of Applied Physics and Related Societies, p.671.

12) "Preparation of ZnO Thin Films by Plasma-Exhanced Metalorganic CVD (I)", M. Yagi, H. Nitta, M. Shimizu, H. Kakuno, T. Shiosaki and A. Kawabata, ibid, p.672.

13) "Preparation of ZnO Thin Films by Plasma-Enhanced

Metalorganic CVD (II)", M. Yagi, H. Nitta, M.Shimizu, H. Kakuno, T. Shiosaki and A. Kawabata, ibid, p.672.

14) "Preparation of ZnO Thin Films by Plasma-Enhanced Metalorganic CVD (III)", M. Shimizu, T. Yamamoto, T. Horii, T. Shiosaki and A. Kawabata, Extended Abstracts (The 42th Autumn Meeting, 1981); The Japan Society of Applied Physics, p.742.

15) "Fabrication of ZnO Thin Films by Plasma-Enhanced CVD", M. Shimizu, T. Yamamoto, T. Shiosaki and A. Kawabata, Extended Abstract of 2nd Symposium on Ultrasonics, Tokyo, 1981, pp.73-74.

16) "Preparation of ZnO Thin Films by Plasma-Enhanced Metalorganic CVD (IV)", M. Shimizu, T. Horii, T. Shiosakiand A. Kawabata, Extended Abstracts (The 29th Spring Meeting, 1982); The Japan Society of Applied Physics and Related Societies, p.768.

17) "I-V Characteristics of Thin Film ZnO-Bi_2O_3 Structure", H. Kakuno, M. Shimizu, T. Shiosaki and A. Kawabata, ibid, p.302.

18) "Preparation and Photoluminescence Studies of ZnO Thin Films" M.Shimizu, T.Horii, T.Shiosaki and A.Kawabata, The Institute of Electronics and Communication Engineering of Japan, CPM82-14(1982) pp.45-52.

19) "Preparation of ZnO Thin Films by Plasma-Enhanced Metalorganic CVD (V)", M. Shimizu, H. Sumida, T. Shiosaki and A. Kawabata, Extended Abstracts (The 30th Spring Meeting, 1983); The Japan Society of Applied Physics and Related Societies, p.634.

20) "Growth of ZnO Thin Films by MO-CVD and Effects of UV Light

Irradiation on the Growth", H. Kamei, M. Shimizu, T. Shiosaki and A. Kawabata, Extended Abstracts (The 44th Autumn Meeting, 1983); The Japan Society of Applied Physics, p.568.

21) "Preparation of ZnO Thin Films by Plasma-Enhanced Metalorganic CVD (VI)", M. Shimizu, Y. Matsueda, T. Shiosaki and A. Kawabata, Extended Abstracts (The 31th Spring Meeting, 1984); The Japan Society of Applied Physics and Related Societies, p.590.

22) "Growth of ZnO Thin Films by MOCVD and Effects of UV Light Irradiation on the Growth (II)", H. Kamei, T. Ishizumi, M. Shimizu, T. Shiosaki and A. Kawabata, ibid, p.591.

23) "Preparation of ZnO Thin Films by Plasma-Enhanced Metalorganic CVD (VII)", M. Shimizu, H. Nakahata, T. Shiosaki and A. Kawabata, Extended Abstracts (The 45th Autumn Meeting, 1984); The Japan Society of Applied Physics, p.599.

24) "Growth of ZnO Thin Films by MOCVD and Effects of UV Light Irradiation on the Growth (III)" M. Tanizawa, M. Shimizu, T. Shiosaki and A. Kawabata, ibid, p.599.

25) "Growth of ZnO Thin Films by MOCVD and Effects of UV Light Irradiation on the Growth (IV)", M. Tanizawa, A. Monma, M. Shimizu, T. Shiosaki and A. Kawabata, Extended Abstracts (The 32th Spring Meeting, 1985); The Japan Society of Applied Physics and Related Societies, p.682.

26) "Preparation of ZnO Thin Films by Microwave Plasma-Enhanced CVD", H. Nakahata, M. Shimizu, T. Shiosaki and A. Kawabata, ibid, p.683.

27) "Growth of ZnO Thin Films by MOCVD and Effects of UV Light

Irradiation on the Growth (V)", M. Shimizu, M. Tanizawa, A. Monma, T. Shiosaki and A. Kawabata, Extended Abstracts (The 46th Autumn Meeting, 1985); The Japan Society of Applied Physics, p.693.

28) "Preparation of ZnO Thin Films by Microwave Plasma-Enhanced CVD (II)", H. Nakahata, M. Shimizu, T. Shiosaki and A. Kawabata, ibid, p.693.

29) "Growth of ZnO Thin Films by Photo-CVD", A. Kawabata, T. Shiosaki and M. Shimizu, Extended Abstracts (The 33th Spring Meeting, 1986); The Japan Society of Applied Physics and Related Societies, p.456.

30) "Preparation of ZnO Thin Films by Microwave Plasma-Enhanced CVD (III)", H. Nakahata, A. Azuma, M. Shimizu, T. Shiosaki and A. Kawabata, ibid, p.777.

31) "Growth of ZnO Thin Films by MOCVD and Effects of UV Light Irradiation (VI)", A. Monma, Y. Yamamoto, M. Shimizu, T. Shiosaki and A. Kawabata, ibid, p.777.

32) "Growth of ZnO Thin Films by MOCVD and Effects of UV Light Irradiation on the Growth (VI)", A. Monma, M. Shimizu, T. Shiosaki and A. Kawabata, Extended Abstracts (The 47th Autumn Meeting, 1986); The Japan Society of Applied Physics, p.718.

33) "Preparation of ZnO Thin Films by Microwave Plasma-Enhanced CVD (IV)", M. Shimizu, H. Nakahata, A. Azuma, T. Shiosaki and A. Kawabata, ibid, p.719.

34) "Growth of ZnO Thin Films by MOCVD and Effects of UV Light Irradiation on the Growth (VII)", A. Monma, M. Shimizu, T.

Shiosaki and A. Kawabata, Extended Abstracts (The 34th Spring Meeting, 1987); The Japan Society of Applied Physics and Related Societies, p.111.

35) "Preparation of ZnO Thin Films by Microwave Plasma-Enhanced CVD (V)", T. Miki, A. Azuma, M. Shimizu, T. Shiosaki and A. Kawabata, ibid, p.111.

36) "Low Temperature Growth of ZnO Thin Films and Their Optical Properties", M. Shimizu, A. Azuma, T. Shiosaki and A. Kawabata, Extended Abstracts (The 48th Autumn Meeting, 1987); The Japan Society of Applied Physics, p.156.

37) "Growth of ZnO Films on Sapphire by Photo-MOCVD", T. Katayama, M. Shimizu, T. Shiosaki and A. Kawabata, Extended Abstracts (The 35th Spring Meeting, 1988); The Japan Society of Applied Physics and Related Societies, p.289.

38) "Growth of ZnO Films on Sapphire by Photo-MOCVD (II)", M. Shimizu, T. Katayama, T. Shiosaki and A. Kawabata, Extended Abstracts (The 49th Autumn Meeting, 1988); The Japan Society of Applied Physics, p.243.

39) "Growth of ZnO Film on Sapphire by Photo-MOCVD (III)", M. Shimizu, S. Tanaka, T. Shiosaki and A. Kawabata, Extended Abstracts (The 36th Spring Meeting, 1989); The Japan Society of Applied Physics and Related Societies, p.358.

40) "Preparation of ZnO Thin Films by Microwave Plasma-Enhanced CVD", M. Shimizu, T. Shiosaki and A. Kawabata, Abstract of Sputtering and Plasma Processes; Japan Technology Transfer Association (1989) Vol.4, No.2, pp.49-57.